HYSTERESIS IN TEXTILE BENDING

by

Dara Ardeshir Jilla
B. Text., University of Bombay
(1966)

Submitted in partial fulfillment
of the requirements for the degree of

Master of Science in Textile Technology

at the

Massachusetts Institute of Technology

June 1968

Archives
MASS. INST. TECH.
FEB 11 1969
LIBRARIES

Signature of Author _____

Department of Mechanical Engineering
Fibers and Polymers Division

Certified by _____

Thesis Supervisor

Accepted by _____

Chairman, Department Committee on Graduate Students

Abstract

A study has been conducted on the bending behavior of plain-weave nylon and cotton fabrics when bent on the bias. A special moment-curvature instrument was used to measure bending moment as a function of imposed curvature. Data obtained on this equipment were used to establish the bending parameters of the various materials under investigation. Specimens were taken at five various orientations between warp and filling directions and polar plots have been obtained for such quantities as elastic rigidity, frictional energy loss, residual elastic energy and bending recovery.

The energy loss due to frictional-restraints, such as inter-fiber friction, at bias bends was found to depend on fiber properties, fabric geometric structure, and effective curvature of the component yarns. For given fiber properties and fabric geometry, this energy loss was found to be a function of the effective curvature of component yarns, and for a dimensionally balanced fabric it was found to be constant at any orientation of bias bending. Also, it was observed that for given fiber properties and orientation of bias bending, this energy loss has been found to be linearly related to fabric structural tightness.

From the analysis of the mathematical model of frictional effect, it has been shown that the hysteresis loop of a bending-unbending cycle represents the sum of the actual energy loss in overcoming frictional restraints, and residual elastic energy. A definite relation has been observed between residual elastic energy and bending recovery. For a given fabric, as elastic rigidity varies with orientations of bias bends, the residual elastic energy also varies and as a result affects the recovery. Also, it was observed that for a given orientation of bias bend, as elastic rigidity increases with increasing structural tightness, residual elastic energy also increases.

Acknowledgements

I sincerely thank Professor Stanley Backer, my thesis supervisor, for suggesting the problem and for his encouragement and expert advice in all phases of the investigation. The author owes his gratitude to Professor Stanley Backer for receiving financial support during studies and research.

Thanks also go to the staff and students of the Fibers and Polymers Division for the advice and assistance given, and especially the untiring labors of Miss Dorothy Eastman in the typing of this thesis.

I also wish to thank Mr. Jan Krizik of IDR, Needham, for making available the moment-curvature instrument used in the investigation.

Table of Contents

Table of Contents

List of Symbols

U_T	Total energy input in loading (or bending) the mathematical model (or fabric) through a deflection (or curvature) K_i
$\overline{U}_F$	Total frictional work loss due to the frictional element (or relative fiber motion) during a loading-unloading (or bending-unbending) cycle
U_{FL}	Frictional work loss during loading (or bending)
U_{FU}	Frictional work loss during unloading (or unbending)
U_S	Fraction of U_T stored as elastic energy in the spring element (or fibers)
U_R	Energy recovered during unbending
V	Residual elastic energy of spring element (or fibers)
R	Bending recovery
k	Curvature
K_i	Imposed curvature
K_r	Residual Curvature
$(EI)_f$	Fiber bending rigidity
$(EI)_y$	Yarn bending rigidity
$(EI)_F$	Fabric bending rigidity
$(EI)_{yF}$	Bending rigidity of yarn as it lies in the fabric
$(GI_P)_{yF}$	Torsional rigidity of yarn as it lies in the fabric
$(M_B)_\alpha$	Bending couple applied to fabric for a specimen at orientation $\alpha°$ to filling direction
D_f	Fiber diameter
N_f	Number of fibers (or filaments) per yarn
μ	Fiber (or filament) coefficient of friction
c	Yarn crimp
r	Height to width ratio of yarn
N	Number of threads per inch

List of Symbols

p	Yarn spacing
α	Specimen orientation to filling direction
q	Ratio of length of restricted region to total yarn length between crowns
S_t	Total yarn length between crowns
S_p	Length of restricted region

NOTE;

Subscript $_1$ refers to warp threads
Subscript $_2$ refers to filling threads

Chapter I
INTRODUCTION

The mechanics of bending in textiles has been classically dealt with in the literature in two parts. The first studies the simple warpwise or fillingwise bending behavior for woven fabrics, and the second investigates the variation of bending behavior of woven fabrics when bent on the bias. Both of these investigations have studied the mechanics of bending with such influencing factors as fiber properties and structural geometry.

The investigation of the simple warpwise or fillingwise bending behavior has been classically dealt with in the literature by means of two limiting assumptions. The first case assumes complete freedom of interfiber motion and neglects completely any interfiber frictional restraints which arise as a result of relative fiber motion during bending. The second assumes no freedom of interfiber motion and considers bending behavior of fabric almost as a solid sheet material. However, the actual bending behavior of fabric falls between these two boundary conditions and shows intermediate cases of frictional interactions. It is the intermediate cases of interfiber frictional interactions that are responsible for the non-linearity in the bending behavior of fabrics. A number of investigations have been done on this subject by Bostwick, Behre and Kärrholm[1], Livesey and Owen[6], Popper[8], Zorowski and Chen[15], Grosberg[3], and Grosberg and Swani[4]. Popper[8] demonstrated that the mechanical behavior of multi-layer beams with friction between layers is, in many aspects, analagous to that of textile structures. He further established that such structures which display frictional interactions demonstrate three distinct characteristics, even if the individual elements are completely elastic. First, the friction system is stiffer than the zero friction system; second, there may be energy losses in bending which produce non-linear behavior; and third, imposed deformations are not completely recoverable.

On the general subject of anisotropy in bending behavior of woven fabrics bent on the bias, the literature seems to be lacking. Cooper[2] applied a simplified theoretical approach in investigating anisotropy in stiffness of woven fabrics by assuming linear

elasticity of fibers instead of complex visco-elastic properties. He further reported theoretical expressions that predict the stiffness of fabrics when bent on the bias. Skelton[10] derived a theoretical expression for the anisotropy of the crease-recovery of monofilament fabrics with orientation of the crease to the thread directions. Shinohara and Go[9] derived theoretical expressions predicting the crease recovery angle in any direction as a function of values in the warp and filling. Steele[11] investigated the interactions between yarn twist and the torsional component of the deformation of the individual yarn which develops as a result of bias bending of the fabric. He reported anisotropy in bending behavior as a result of this torsion-twist interaction.

On the investigation of the influence of the frictional restraints for bias bends of fabrics, again, the literature seems to be scanty. The study reported here will attempt to investigate further the Mathematical Model of Frictional Effect reported by Popper[8] for analyzing the bending behavior of textile structures. An analysis of the hysteresis loop of the moment-curvature relation has been carried out and an energy balance is given for the bending-unbending cycle. The concept of unrecovered residual elastic energy which the fabric possesses at the end of the bending-unbending cycle is presented. This may be taken as a measure of the bending recoverability of the fabric.

Further, in bias bends of fabrics, the warp and filling yarns experience curvatures different than that of the fabric. As a result, these yarns exhibit different energy losses due to frictional restraints that develop in relative fiber motion and (for asymmetric fabrics) relative motions of adjacent yarns. An attempt has been made to analyze these frictional restraints for bias bending, and expressions have been derived to predict the total frictional energy losses at any direction as a function of values measured for warp and filling bends.

In this experimental investigation an instrument designed and constructed by Popper[8] has been used to measure continuously the moment-curvature relation of textile materials. From this measurement, such quantities as elastic rigidity, energy loss in bending, unrecoverable residual elastic energy, and bending recovery have been used in describing bending behavior at low curvatures.

Chapter II
THEORETICAL PRINCIPLES

1. Flexural Rigidity of Woven Fabrics Bent on the Bias.

For simple warpwise or fillingwise bending of woven fabrics (Figure 2.1) it can be seen that when a pure moment is applied to the fabric, all elements of the bent yarn not touching a cross yarn are also under a pure moment, and change their curvature by an amount $(M_B)/(EI)$. Each element of yarn in the restricted region retains its original curvature. Following up this analysis, Popper[8] derived the expression for the rigidity of a yarn as it lies in fabric

$$(EI)_{yF_1} = (EI)_{y_1} \frac{1}{(1+C_1)(1-q)} \qquad (2.1)$$

The above equation predicts the rigidity of a yarn in a woven fabric. The structural variable in this equation is a factor involving crimp of the bent yarns and the spacing of the cross yarns. Also, it is clearly evident from the above equation that the rigidity of a yarn in a woven fabric is greater than that of the yarn before it was woven, due to the restrictions to curvature changes imposed by the cross yarns.

For the bias bending, each set of warp and filling yarns is under a bending moment, and also a twisting moment. Part of the bending transforms into torsional deformation and actual yarn strain induced by fabric bending is smaller than it appears. From geometry[2,10] it can be shown that the warp and the filling threads in a fabric bent to curvature K_i are under a curvature of $K_i \sin^2\alpha$ and $K_i \cos^2\alpha$, respectively, and a torsion is $K_i(\cos\alpha)(\sin\alpha)$. Cooper[2] derived the expression for the stiffness per unit width of a fabric in any direction as

$$\frac{(M_B)_\alpha}{K_i} = (EI)_{y_1} \cdot \sin^4\alpha \cdot N_1 + (EI)_{y_2} \cdot \cos^4\alpha \cdot N_2 + \\ + [(GI_p)_{yF_1} + (GI_p)_{yF_2}] \cdot \sin^2\alpha \cos^2\alpha \cdot N_1N_2 \qquad (2.2)$$

where $(GI_p)_{yF_1}$ and $(GI_p)_{yF_2}$ represent the effective torsional rigidities per yarn of the warp and filling assemblies as they

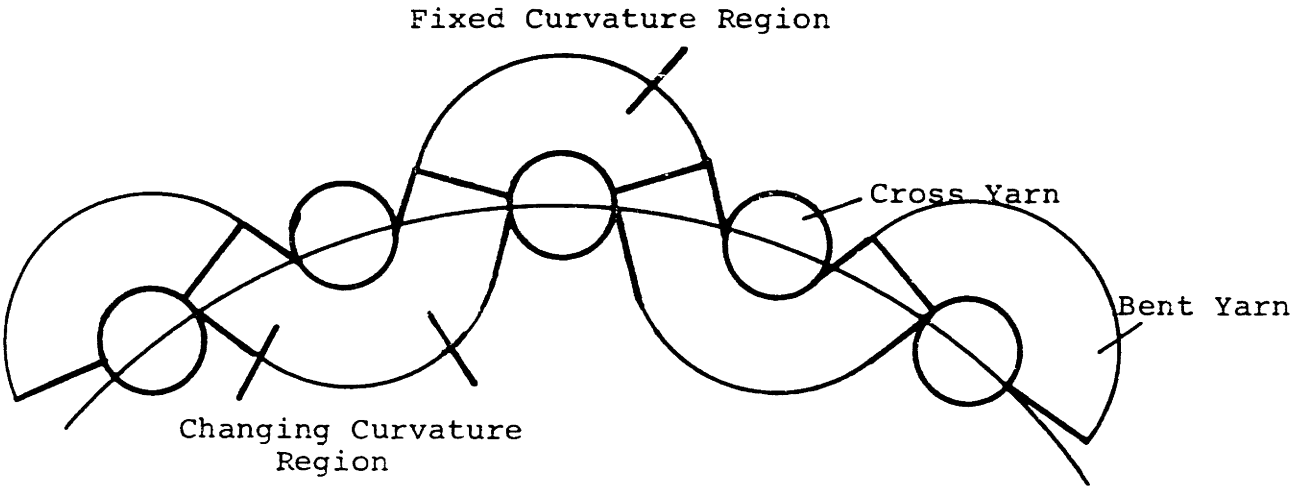

Figure 2-1a
Effect of Fabric Structure
on Rigidity

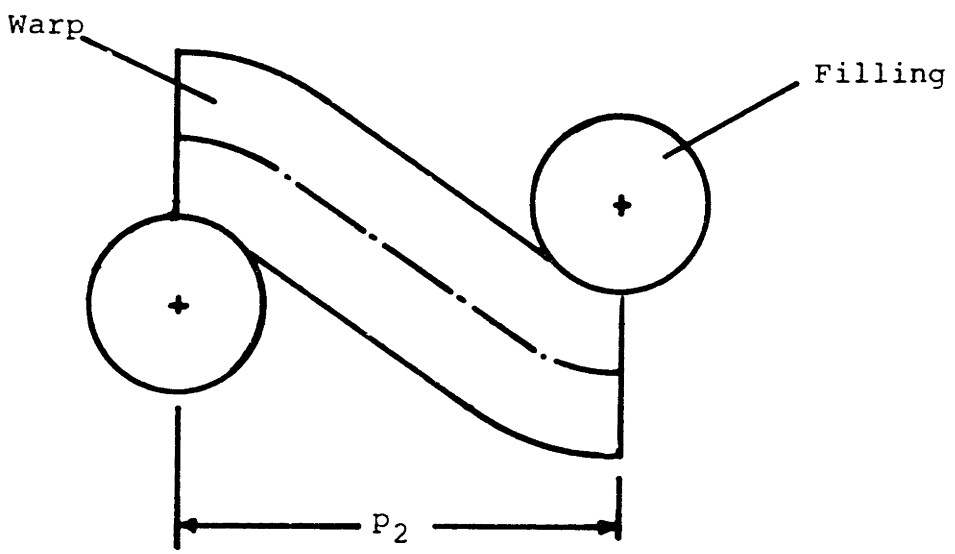

Figure 2-1b
Idealized Geometry of
Woven Fabric

exist in the fabric structure, and N_1 and N_2 are warp and filling threads per inch.

It is important to note that the above equation has been derived neglecting the structural interactions between yarns, namely, the crimp of the bent yarns and the spacing of the cross yarns. However, in many fabrics, such interactions have to be taken into account and the expression for the stiffness per unit width of a fabric at any orientation can be shown to be as

$$\frac{(M_B)_\alpha}{K_i} = (EI)_{yF_1} \cdot \sin^4\alpha \cdot N_1 + (EI)_{yF_2} \cdot \cos^4\alpha \cdot N_2 + \\ + [(GI_p)_{yF_1} + (GI_p)_{yF_2}] \cdot \sin^2\alpha \cos^2\alpha \cdot N_1N_2 \qquad (2.3)$$

where $(EI)_{yF_1}$ and $(EI)_{yF_2}$ represent the effective elastic rigidities per yarn of the warp and filling assemblies as they exist in the fabric structure.

Both the applicability of the equation (2.3) for predicting the stiffness of a woven fabric at various orientations and the agreement with the experimental results are presented in Chapter IV.

2. Friction Work Loss in Woven Fabrics Bent on the Bias.

The case of simple warpwise or filling bending is considered first. The more complex case of bias bending is treated next.

As a fabric is bent, the fibers slide by each other. This relative fiber motion is resisted by frictional forces which develop as a result of the internal pressure of the fabric. Several attempts have been made to compute this frictional restraint. From the theory of mechanical behavior in bending of a set of plates, Grosberg[3] and Olofsson[7] reported an expression for friction moment as

$$EI \cdot K_i = M_B - M_f \qquad (2.4)$$

Olofsson defines the friction moment, M_f, as the critical moment of slippage; Livesey and Owen[6] define friction moment as the "coersive couple" or the couple required to restore zero curvature.

From the knowledge of the distribution of fiber slip and internal pressure of the fabric, Popper[8] derived expression for the energy loss during bending or the total frictional work loss due to relative fiber motions per length of yarn in bending as

$$U'_F = \frac{4}{3}\pi^2 (N_f \cdot EI_f)\sqrt{N_f \cdot r}\, D_f \mu \sqrt{\frac{C_1}{p_2^2}} \qquad (2.5)$$

where: N_f = the number of fibers in the yarn
$(EI)_f$ = the elastic rigidity of the fiber
μ = the coefficient of friction between fibers
D_f = the fiber diameter
p = the yarn spacing
r = the height to width ratio of the yarn cross-section.

The above equation predicts the total frictional work loss due to relative fiber motions in bending. It is a relationship between fiber properties, structural parameters of warp and filling yarns and that of fabric, imposed curvature of the fabric and total frictional work loss due to relative fiber motion. The structural variable in this equation involves crimp of the bent yarns, the spacing of the cross yarns and the imposed curvature (K_i) of the fabric.

In Section 1 it has been stated that for the bias bends, the warp and filling threads are under a curvature of ($K_i \cdot \sin^2\alpha$) and ($K_i \cdot \cos^2\alpha$) respectively for an imposed fabric curvature (K_i). Extending the analysis used in deriving equation (2.5) and knowing the fiber slippage distribution and the pressure distribution of the fabric along the fiber length, the expressions are derived for the frictional work loss per unit length of yarn in bias bent fabrics as

$$U'_{F(warp)} = \left[\frac{4}{3}\pi^2 (N_{f_1} \cdot EI_{f_1})\sqrt{N_{f_1} \cdot r}\, D_{f_1} \mu \sqrt{\frac{C_1}{p_2^2}}\right] \cdot K_i \sin^2\alpha \qquad (2.6)$$

$$U'_{F(filling)} = \left[\frac{4}{3}\pi^2 (N_{f_2} EI_{f_2})\sqrt{N_{f_2} \cdot r}\, D_{f_2} \mu \sqrt{\frac{C_2}{p_1^2}}\right] \cdot K_i \cos^2\alpha \qquad (2.7)$$

In general terms, equations (2.6) and (2.7) take the form,

$$U'_{F(warp)} = f(\text{fiber properties, warp yarn and fabric structural parameters}) \cdot K_i \sin^2\alpha \qquad (2.8)$$

and

$$U'_{F(filling)} = f(\text{fiber properties, filling yarn and fabric structural parameters}) \cdot K_i \cos^2\alpha \qquad (2.9)$$

or

$$U'_{F(warp)} = A_1 \cdot K_i \sin^2\alpha \qquad (2.10)$$

$$U'_{F(filling)} = A_2 \cdot K_i \cos^2\alpha \qquad (2.11)$$

where A_1 and A_2 are constants for warp and filling respectively.

Since the total length of warp and filling yarns per unit area of the fabric remains a constant for a given fabric taken at any orientation to warp or filling thread directions, equations (2.10) and (2.11) can be combined to give

$$U'_{F(total)} = U'_{F(warp)} + U'_{F(filling)} = \\ = A_1 \cdot K_i \sin^2\alpha + A_2 \cdot K_i \cos^2\alpha \qquad (2.12)$$

From the above equation, it is evident that the amount of total frictional energy loss due to relative fiber motions for bias bents of fabrics depends on the structural parameters of warp and filling yarns and that of the fabric, and the individual curvatures exerted on the warp and filling assemblies of yarns for an imposed curvature (K_i) of the fabric.

In some asymmetric fabrics as the fabric bends, the yarns move relative to each other. If these yarns are in contact, this involves a rubbing together of two adjacent yarns as the fabric bends and as energy is lost to friction. From the knowledge of the relative motion between the yarns and the body of the fabric, and the force acting between the adjacent yarns at each crossing point, Popper[8] derived expression for the energy loss or the frictional work loss due to relative yarn motion per length of yarn in bending as

$$U''_F = \frac{\mu F}{m} \frac{\ell n\left(\frac{\pi h_1}{p_2} + \sqrt{1 + \left(\frac{\pi h_1}{p_2}\right)^2}\right)}{\sqrt{1 + \left(\frac{\pi h_1}{p_2}\right)^2}} \frac{2}{\pi^2} p_2 \cdot K_i \qquad (2.13)$$

where: F is the normal force between yarns

h_1 is the wave height of the crimped warp yarn.

The amount of energy lost by this effect depends on the structural parameters of warp and filling yarns and that of fabric, the interyarn forces and the imposed curvature of the fabric. Fabrics in which adjacent yarns do not touch have a zero value of interyarn forces, and there is no frictional work loss due to this mechanism.

Using the previously used analysis in deriving equation (2.12), the total frictional work loss due to relative motions of adjacent yarns for bias bents of fabrics can be shown to be as

$$U''_{F(total)} = U''_{F(warp)} + U''_{F(filling)} = \\ = A_3 \cdot K_i \sin^2\alpha + A_4 \cdot K_i \cos^2\alpha \qquad (2.14)$$

where A_3 and A_4 are constants for warp and filling respectively. From the above equation, it is evident that the amount of total frictional energy loss due to relative motions of adjacent yarns for bias bends depends on the structural parameters of warp and filling yarns and that of the fabric, the interyarn forces and the individual curvatures exerted on the warp and filling assemblies of yarns for an imposed curvature (K_i) of the fabric.

Equations (2.13) and (2.14) could be combined to give the total frictional work loss, both due to relative fiber motions and relative yarn motions for bias bends

$$\bar{U}_F = U'_{F(total)} + U''_{F(total)} = A_1 \cdot K_i \sin^2\alpha + A_2 \cdot K_i \cos^2\alpha + \\ + A_3 \cdot K_i \cos^2\alpha + A_4 \cdot K_i \sin^2\alpha = (A_1 + A_3) \cdot K_i \sin^2\alpha + \\ + (A_2 + A_4) \cdot K_i \cos^2\alpha \qquad (2.15)$$

For the particular case of a geometrically balanced fabric in which warp and filling yarns are nominally identical and there are nominally equal numbers of warp and filling threads per unit width, $A_1 = A_2 = A$ and $A_3 = A_4 = A'$, equation (2.15) takes the form

$$\bar{U}_F = A \cdot K_i + A' \cdot K_i = (A + A') \cdot K_i \qquad (2.16)$$

This implies that for a dimensionally balanced fabric, the total frictional work loss will be a constant at any angle of bias bend. Both the applicability of the equations (2.15) and (2.16) and the agreement with the experimental results are presented in Chapter IV.

3. Analysis of the Mathematical Model of Frictional Effect.

The mathematical model of frictional effect reported by

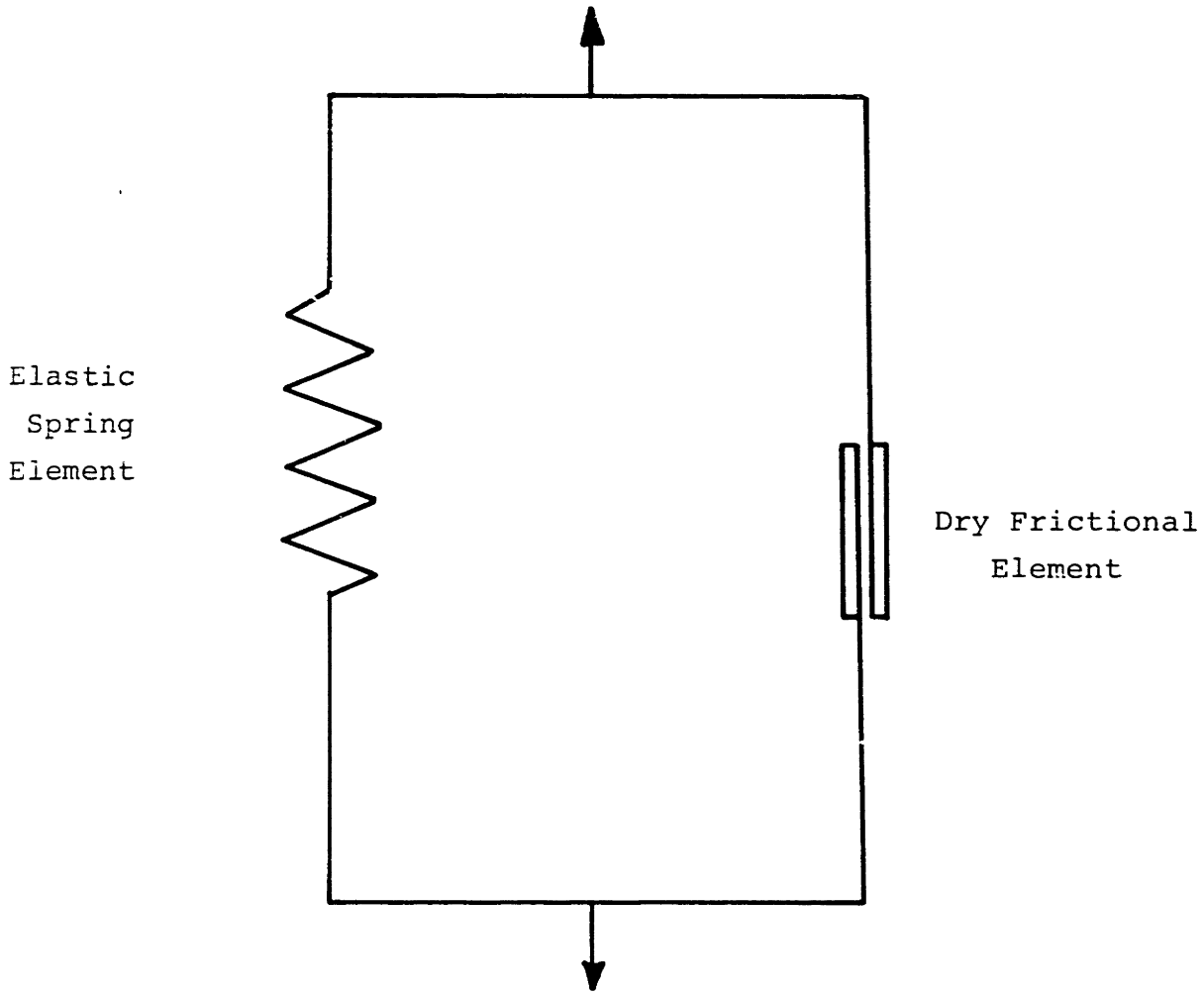

Figure 2-2
Mathematical Model of
Frictional Effect

Figure 2-3

Load-Deflection or Moment-Curvature Relation of Mathematical Model

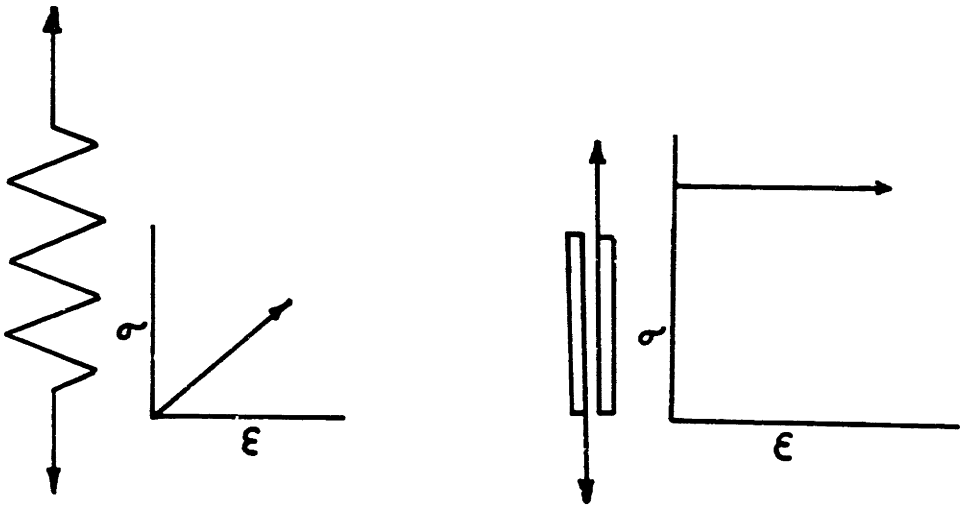

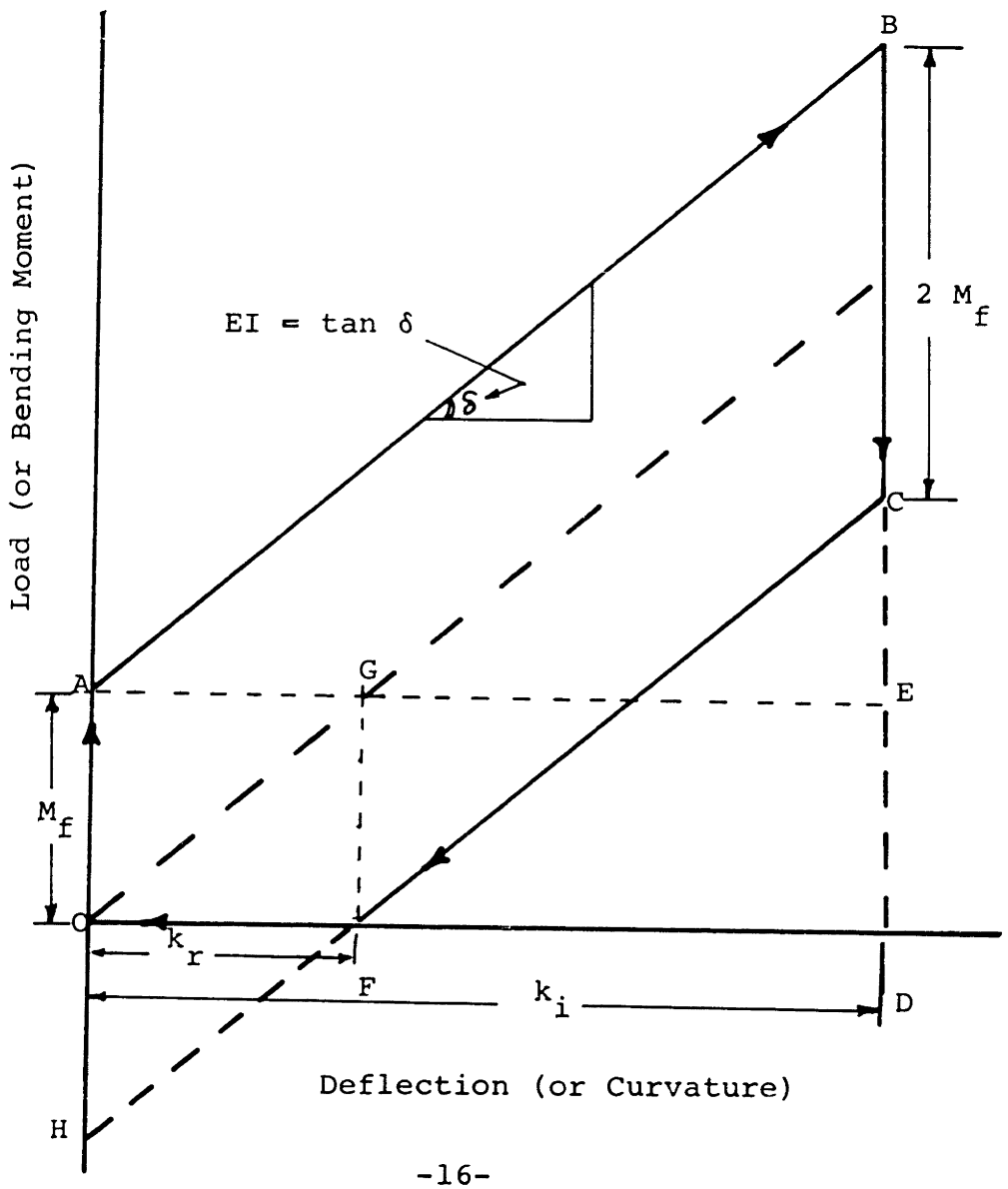

Popper[8] is shown on Figure 2.2. It consists of an elastic spring element and a dry-frictional element in parallel. The load-deflection (or moment-curvature) relation for this model is shown on Figure 2.3. The elastic term increases linearly with load, while the friction term is constant and always acts opposite to the direction of loading. This model could be described by two parameters: the elastic rigidity, and the friction moment. The magnitude of these quantities are functions of the geometry and properties of the elements of a structure. The slope of the moment-curvature relation will be referred to as the elastic-rigidity and the additive amount of moment which must be applied to overcome frictional effects will be referred to as the frictional moment.

The expressions for the energy balance for a loading-unloading (or bending-unbending) cycle of this mathematical model takes the form

$$U_T = U_{FL} + U_S \tag{2.17}$$

where: U_T is the total energy input
U_{FL} is the friction work loss during loading
U_S is the stored elastic energy

and for unloading (or unbending)

$$U_S = U_{FU} + U_R + V \tag{2.18}$$

where: U_{FU} is the friction work loss during unloading
V is the residual elastic energy.

It is important to note that at the end of the loading-unloading (or bending-unbending) cycle, when the system reaches equilibrium and shows an unrecovered displacement (or residual curvature), internal forces (or moments) in the spring element and the frictional element exist and oppose each other.

From the load-deflection (or moment-curvature) relation shown on Figure (2-3) the following relationships can be shown

$$U_T = \text{area OABD} = \frac{(2M_f + EI \cdot K_i)}{2} \cdot K_i \tag{2.19}$$

$$U_F = \text{area OAED} + \text{area FGED} = (2K_i - \frac{M_f}{EI}) \cdot M_f \tag{2.20}$$

$$U_R = \text{area FCD} = \left(\frac{EI \cdot K_i^2}{2} - M_f \cdot K_i + \frac{M_f^2}{2EI} \right) \tag{2.21}$$

$$V = \text{area HOF} = \frac{M_f^2}{2EI} \tag{2.22}$$

$$\text{Area of the Hysteresis Loop} = \text{area OABCF} = U_F + V \tag{2.23}$$

Extending the analysis of this model to textile structures, the expressions for the energy balance for the bending-unbending cycle of a fabric takes the form

$$U_T = 2\bar{U}_F + U_R + V \tag{2.24}$$

The elastic rigidity of a fabric will depend on the bending rigidity of the fibers and the friction moment on the amount of energy lost due to sliding friction.

From the above discussion it can be seen that the residual curvature of a fabric will be proportional to the magnitude of the residual elastic energy at the end of the bending-unbending cycle. This concept is further discussed in Chapter IV.

Chapter III
EXPERIMENTAL TECHNIQUES

1. Materials.

Two types of woven fabrics used in the experimental investigation were different both in fiber material and geometry,

(1) three plain-weave, unfinished cotton fabrics,

(2) six plain-weave, non-heat set multifilament nylon fabrics.

Further constructional details of these fabrics are given in Appendix A.

Samples of size 2" x .5" were prepared from each type of fabric at seven different angles of orientation between filling and warp thread directions. At least five samples were prepared so that the face, orientation, and position in the fabric were uniquely specified. Specimen preparation needs a careful control. Attention should be concentrated in cutting exactly .5" width of the specimens; particularly for warpwise or fillingwise specimens, care must be taken to ensure that an equal number of threads are included in all of the warpwise or fillingwise specimens. This is important because the slightest irregularity in the width of the specimen has a pronounced effect on the results. Then, ends of the prepared samples were stiffened by sticking at each end drafting tape 0.5" wide, so that the ends of the sample become of very high rigidity. This is essential from the point of view of the geometry of bending the specimen in the moment-curvature instrument which will be discussed in the succeeding section. All the specimens were tested under a controlled atmosphere of $65 \pm 2\%$ relative humidity and $68° \pm 4°F$.

2. Instrument for Measuring Moment-Curvature Relation.

MITEX Mk II[16] moment-curvature measuring instrument, Figure 3-1, obtained from IDR Enterprises, Inc., was used in the experimental investigation. This instrument was designed and constructed by Popper[8] to determine such quantities as elastic rigidity, friction-moment, residual curvature, and energy loss in bending.

The instrument[8] operates by imposing a constantly increasing

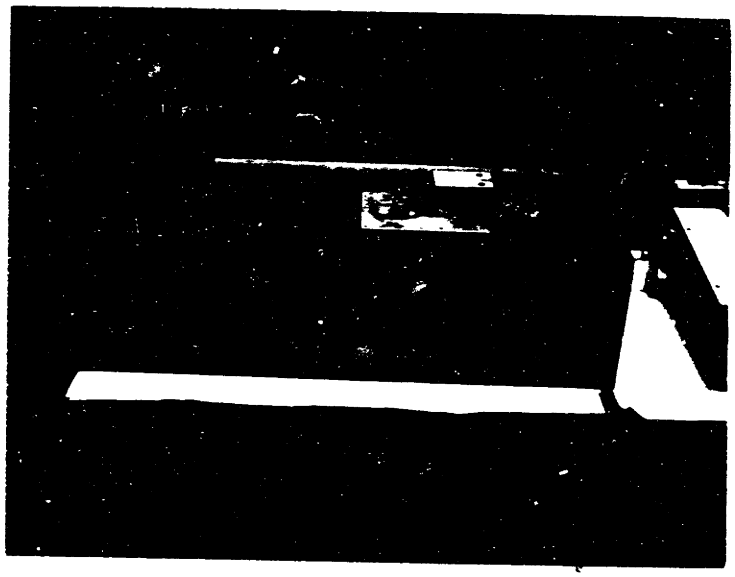

Figure 3-1a

MITEX Mk II Moment-Curvature Instrument

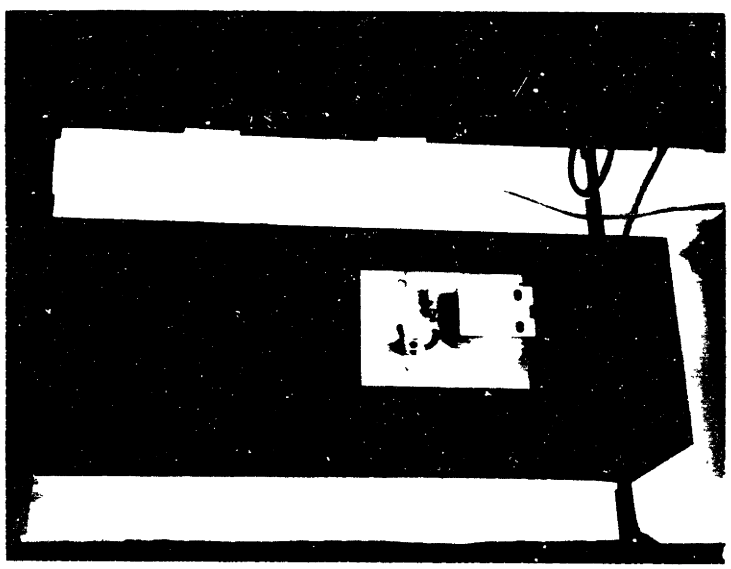

Figure 3-1b

Top View of Moment-Curvature Instrument

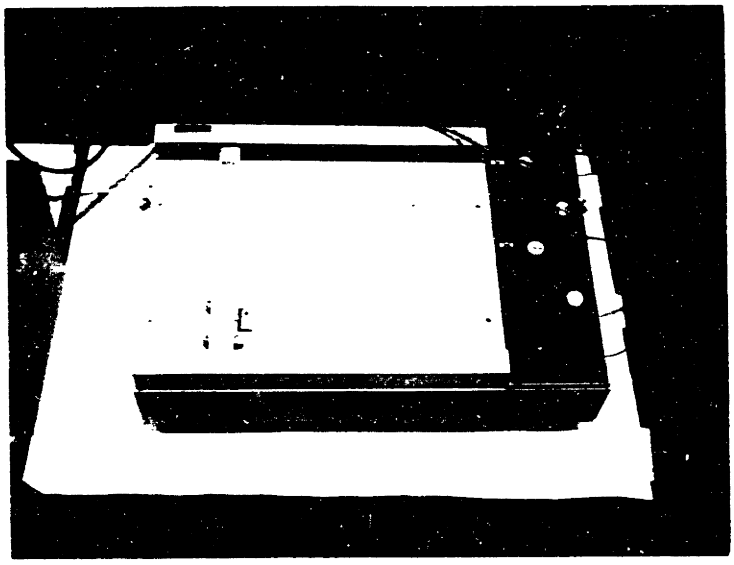

Figure 3-2

Hewlett Packard Model-135 X-Y Recorder

curvature to one end of the fabric sample which is mounted on a moving carriage. The other end of the sample is instrumented with a cantilever spring, a differential capacitor, and suitable circuitry to give a continuous output signal proportional to the displacement of the cantilever, and this displacement, in turn, is proportional to the bending moment. Thus, the output is a direct measure of the applied bending moment. This signal is fed to an X-Y Recorder Model 135, Figure 3.2, obtained from Hewlett-Packard Company, Moseley Division.

Since one end of the sample is held fixed, the moving end must execute a translation and rotation so that the sample is always in a circular arc of constant length. The curvature of this arc must increase linearly with time.

The equations of motion of the carriage bearing the moving jaw have been derived by Popper[8], using the method of Isshi[5]. Referring to Figure 3.3, let

ρ, θ = polar coordinates of point on carriage relative to fixed end of sample and original straight line of fabric

G = gage length of sample

θ_c = rotation angle of carriage

k = sample curvature.

To maintain a constant length of circular arc of the sample, the required translation of the carriage can be shown to be

$$\rho = \frac{G}{\theta} \sin\theta \tag{3.1}$$

To ensure that the tangent angle of the bent sample ends corresponds to that of a circular arc of appropriate radius, the required rotation of the carriage can be shown to be

$$\theta_c = 2\theta \tag{3.2}$$

The curvature of the sample at any position of the carriage is

$$k = \frac{2\theta}{G} \tag{3.3}$$

This means that if the angular position of the carriage is increased linearly with time, the curvature will increase linearly with time, and the boundary conditions of position and slope will correspond to

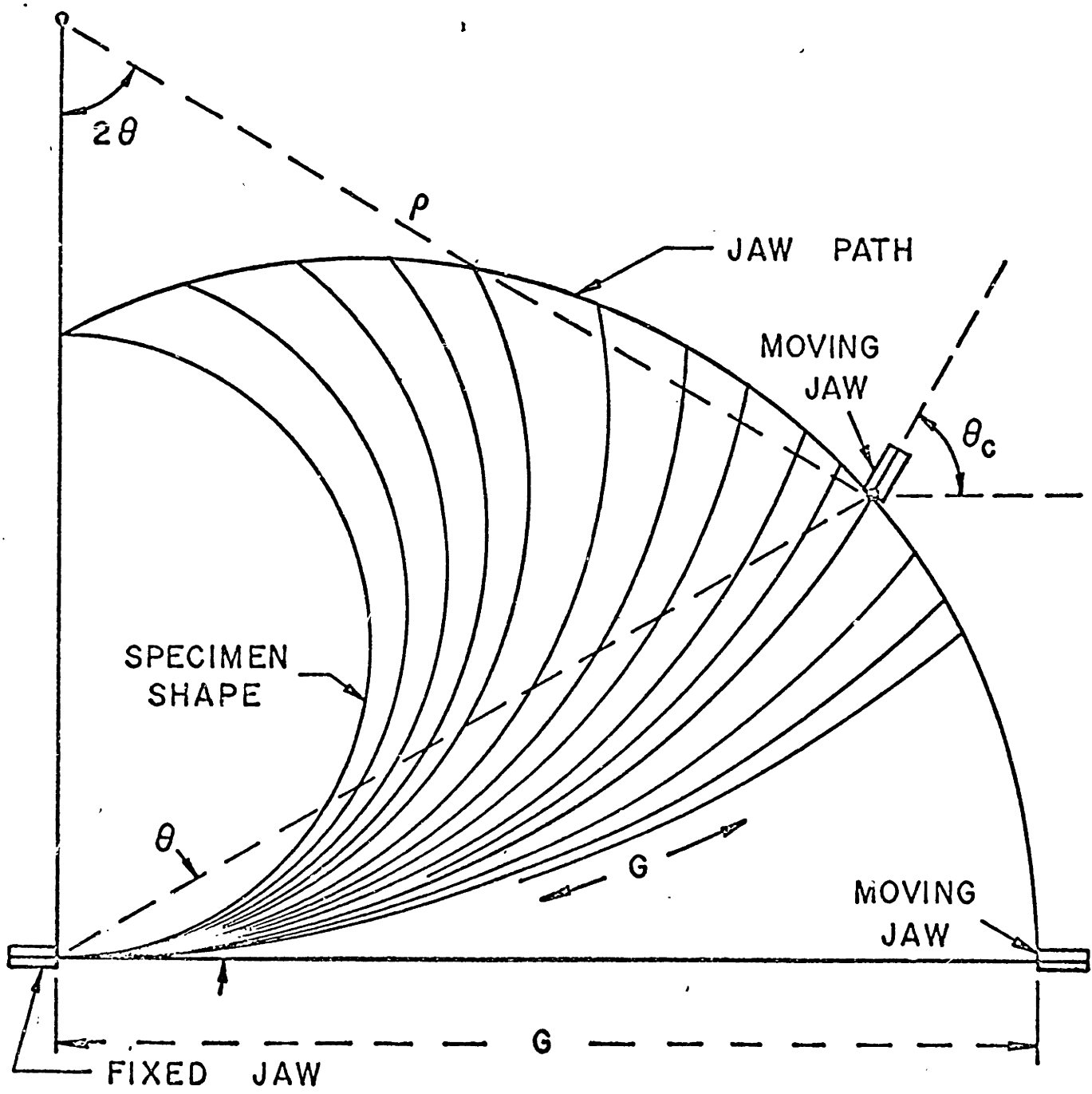

FIGURE 3-3

JAW PATH AND SPECIMEN SHAPE

that of a circular arc.

3. Method of Gripping Sample.

A four-point loading system described by Popper[8] was used on MITEX Mk II for gripping the sample. The sample is fixed between two sets of pins (fine drill bits .0135" diameter) on a double pin jaw, and bent by the couple set up by each set. The pins are separated by 1/4" and they can be individually adjusted to permit testing of samples of varying thickness.

One pair of pins is mounted on the moving carriage. The other pins are supported individually. One is fixed to the instrument frame and the other is mounted on a stiff cantilever spring.

Gage length (G), the distance between the inner pins on the double pin jaw, was kept at 1" and the samples were bent through an angle of 180° which, from the geometry of the instrument, is equivalent to a curvature of 3.141 (in^{-1}).

Care must be taken to ensure that the drafting tape used in stiffening the ends of the fabric sample is not protruding within the gage length region of 1" between the pins.

4. Calibration.

Both the curvature and bending moments must be calibrated to set the scales of the output moment-curvature curve. The rate of change of curvature is determined by determining the speed of the carriage (angular velocity of .3 RPM along the cam slot) relative to the chart, and applying equation (3.3). The moment calibration was done by preparing a steel strip .5" x .001" and performing the bending-unbending test on the instrument (Figure 3.4). The relation between force and output voltage was recorded. From this relation, the moment-voltage relation was computed. Refer to Figure 3.4.

5. Measurements of Friction Moment, Elastic Rigidity, Energy Loss in Bending and Bending Recovery.

Figure 3.5 illustrates the method of geometrical constructions used in the measurements of the quantities such as friction moment, elastic rigidity, total work loss, work recovered, and residual curvature.

The following equations could be further used to measure the other quantities

Sample: Steel (0.5" x 0.001"), Youngs Modulus (E) = 3×10^7 (psi)

Moment of Inertia (I) = $\frac{1}{12} \times \frac{1}{2} \times \frac{1}{10^7}$

= $\frac{1}{24} \times 10^{-9}$ (in^4)

x = 0.2 volts/inch

y = 50 millivolts/inch

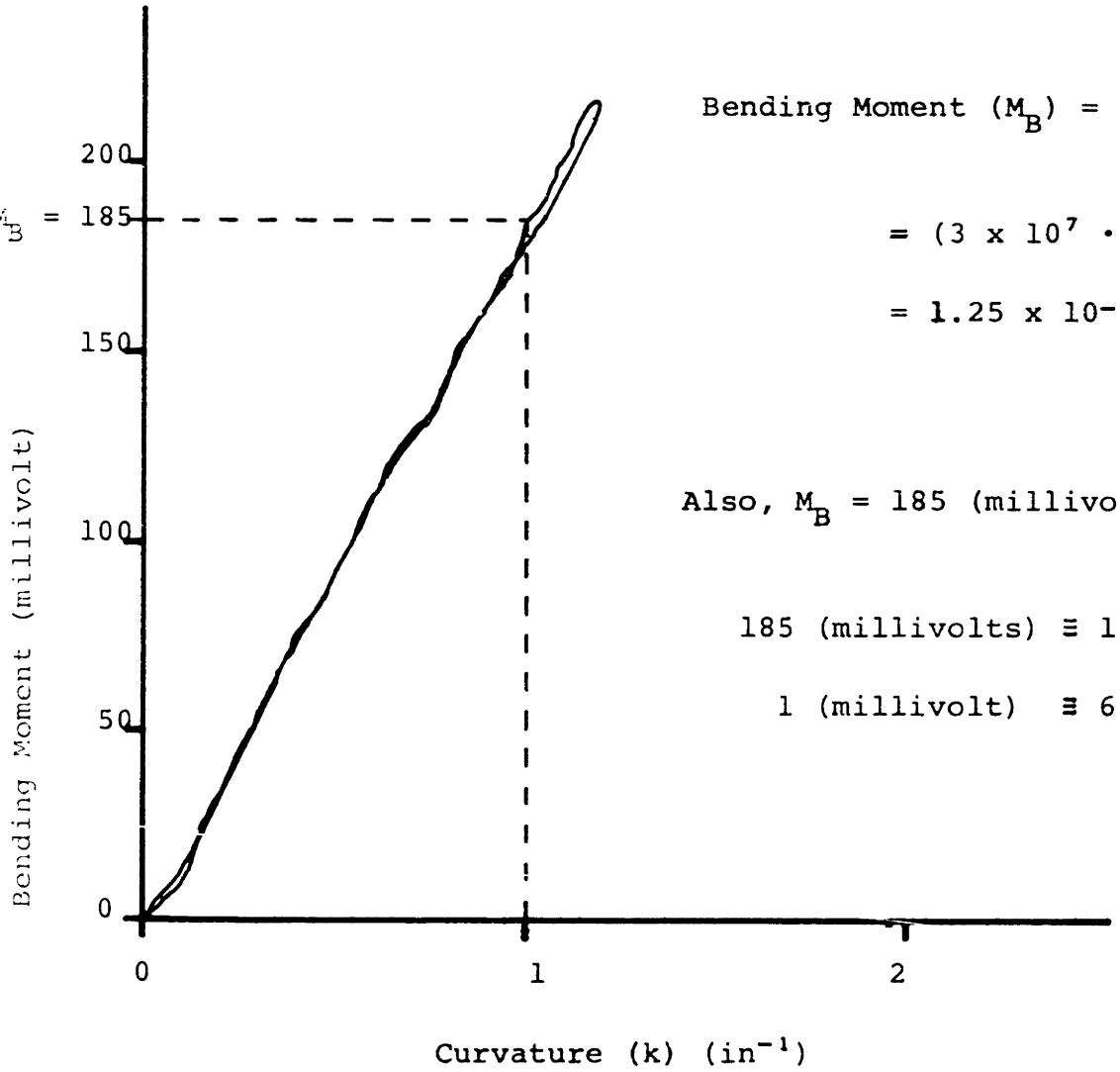

Bending Moment (M_B) = (E·I) · k

= $(3 \times 10^7 \cdot \frac{1}{24} \times 10^{-9}) \cdot 1$

= 1.25×10^{-3} (lb-in)

Also, M_B = 185 (millivolts)

185 (millivolts) ≡ 1.25×10^{-3} (lb-in)

1 (millivolt) ≡ 6.75×10^{-6} (lb-in)

Figure 3-4
Calibration Plot for Bending Moments

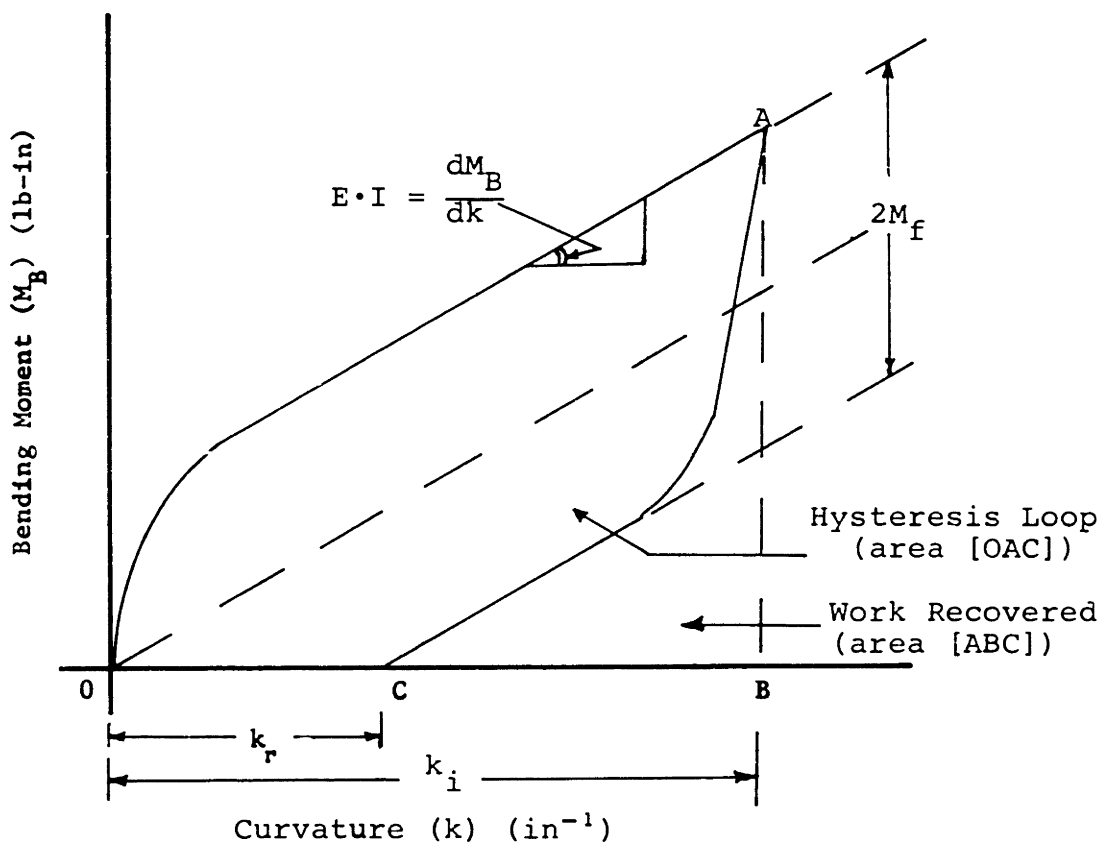

Figure 3-5

Typical Moment-Curvature Plot Measured for Fabrics

$$(R)\ \text{Bending Recovery} = \left(1 - \frac{k_r}{k_i}\right) \tag{3.4}$$

(U_F) Total Frictional Work Loss = [Total Work Loss - Unrecoverable Residual Elastic Energy] (3.5)

As an auxiliary study on the moment-curvature instrument, testing for cyclic loading, and the bending moment relaxation behavior holding the specimen at constant curvature bend has also been studied and the resulst are presented in Appendix D.

Chapter IV
RESULTS AND DISCUSSIONS

1. Measurements of Flexural Rigidity of Woven Fabrics Bent on the Bias.

Measurements of values for the elastic (flexural) rigidity have been deduced from the moment-curvature plots according to the method discussed in Chapter III, Section 5. The polar plots of the values of elastic rigidity for six plain-weave, multifilament nylon fabrics and three plain-weave cotton fabrics are shown on Figures (4-1) to (4-6) and (4-7) to (4-9) respectively.

The variation of the flexural rigidity of these fabrics with orientation obtained experimentally is seen to be in good agreement with the theoretically predicted values based on equation (2.3) which is the expression given by Cooper[2] corrected for a suitable geometric parameter. In obtaining the theoretically predicted values of elastic rigidity based on equation (2.3), $(EI)_{yF_1}$ and $(EI)_{yF_2}$ have been obtained by insertion of experimental values of M_B and K_i for test angles $\alpha = 90°$ and 0° respectively, and the sum of $(GI_p)_{yF_1}$ and $(GI_p)_{yF_2}$ has been deduced from measurements in three different directions, $\alpha = 0°$, 45°, and 90°. Chi-square tests have been performed to check the closeness of fit between the experimentally obtained values and the theoretically predicted values of flexural rigidity. Excellent fit has been obtained with all the nine fabrics of widely differing construction, both in cotton and in nylon. (See Appendix C)

2. Measurements of Total Energy Loss due to Friction for Woven Fabrics Bent on the Bias.

Measurements of values for the total energy losses that incur in bending both due to relative fiber motions and, in some asymmetric fabrics, also due to relative motions of adjacent yarns, have been deduced based on equation (2.15) as discussed in Chapter II, Section 3. The polar plots of the values of the total frictional work loss in a bending-unbending cycle for six plain-weave, multifilament nylon fabrics and three plain-weave cotton fabrics are shown on Figures (4-10) to (4-15) and (4-16) to (4-18) respectively.

To a first approximation, an expression has been deduced for predicting the total work loss due to frictional restraints in

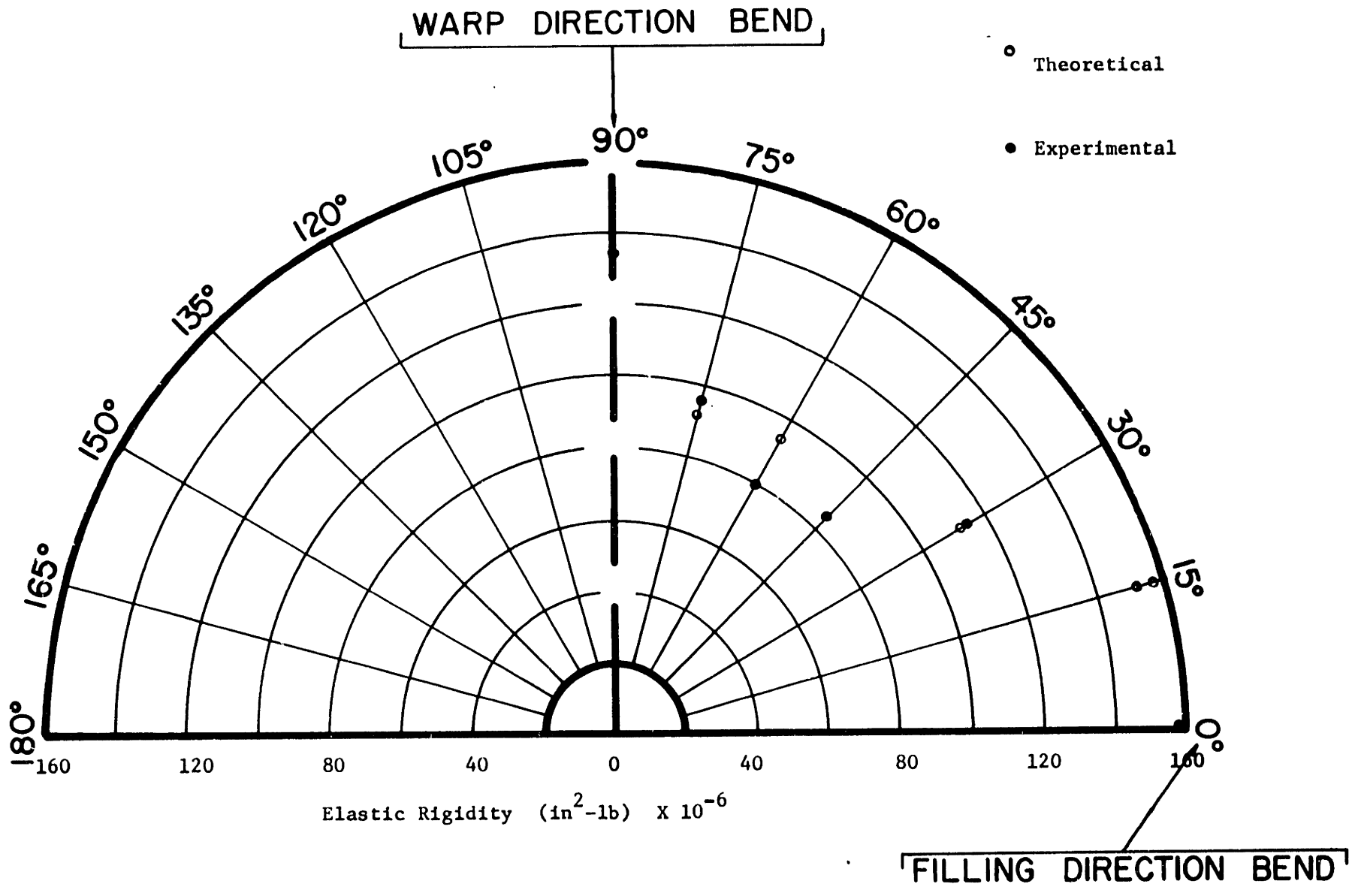

FIGURE 4-1

Directional Properties in Elastic Rigidity of Nylon-Fabric (N-1)

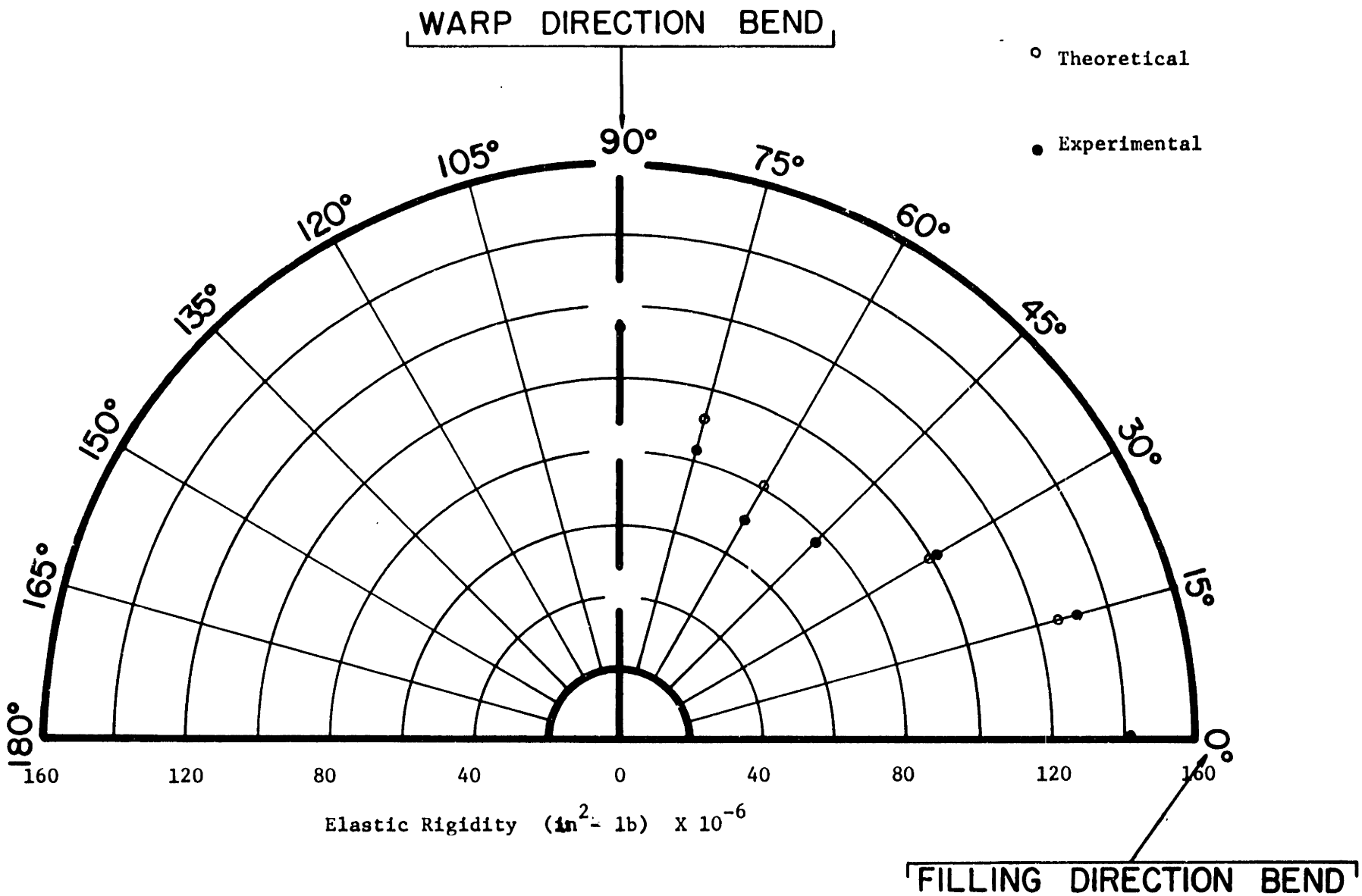

FIGURE 4-2

Directional Properties in Elastic Rigidity of Nylon Fabric (N-2)

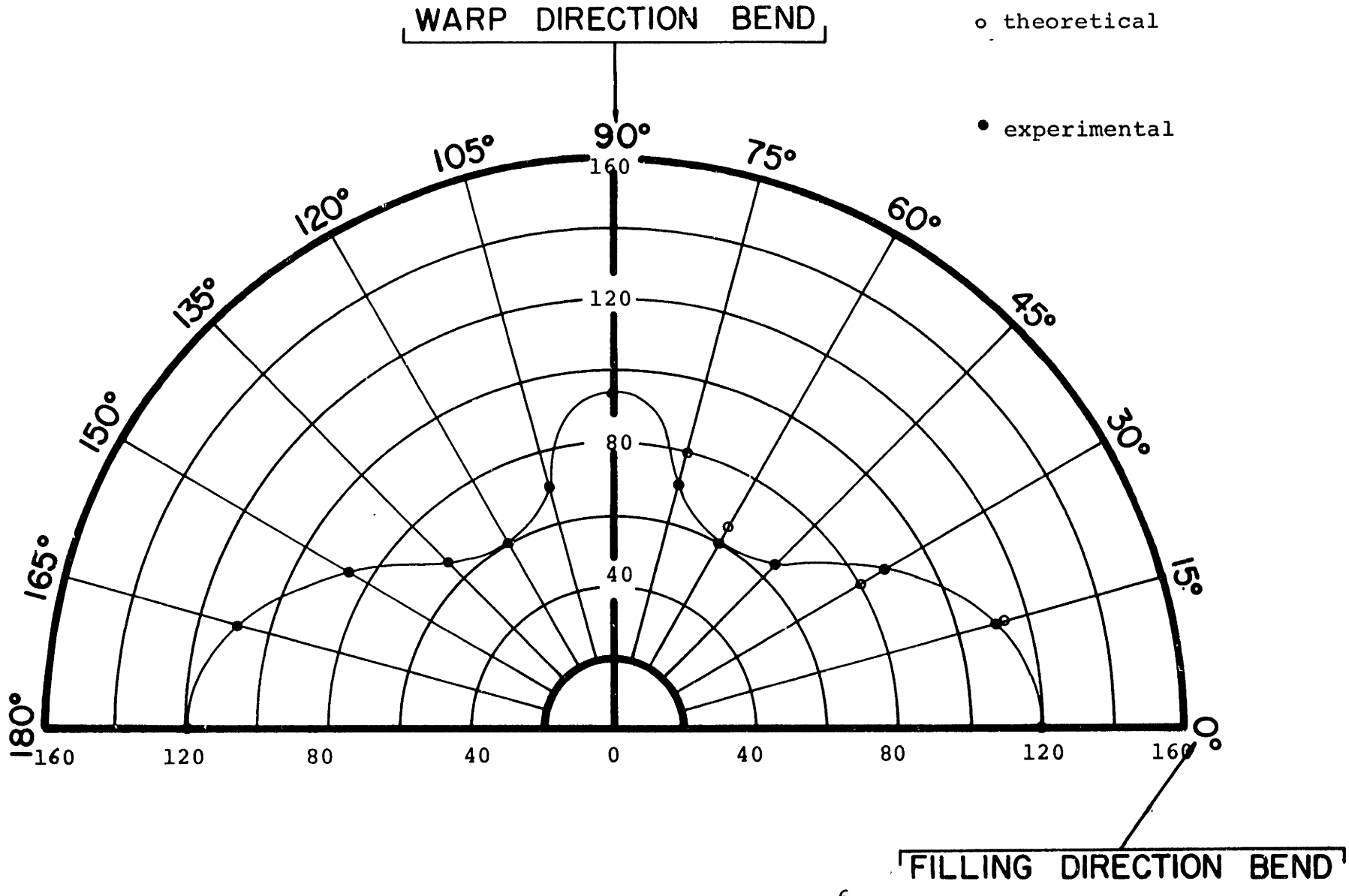

Elastic Rigidity (in^2 - lb) x 10^{-6}

Figure 4-3

Directional Properties in Elastic Rigidity of Nylon-Fabric (N-3)

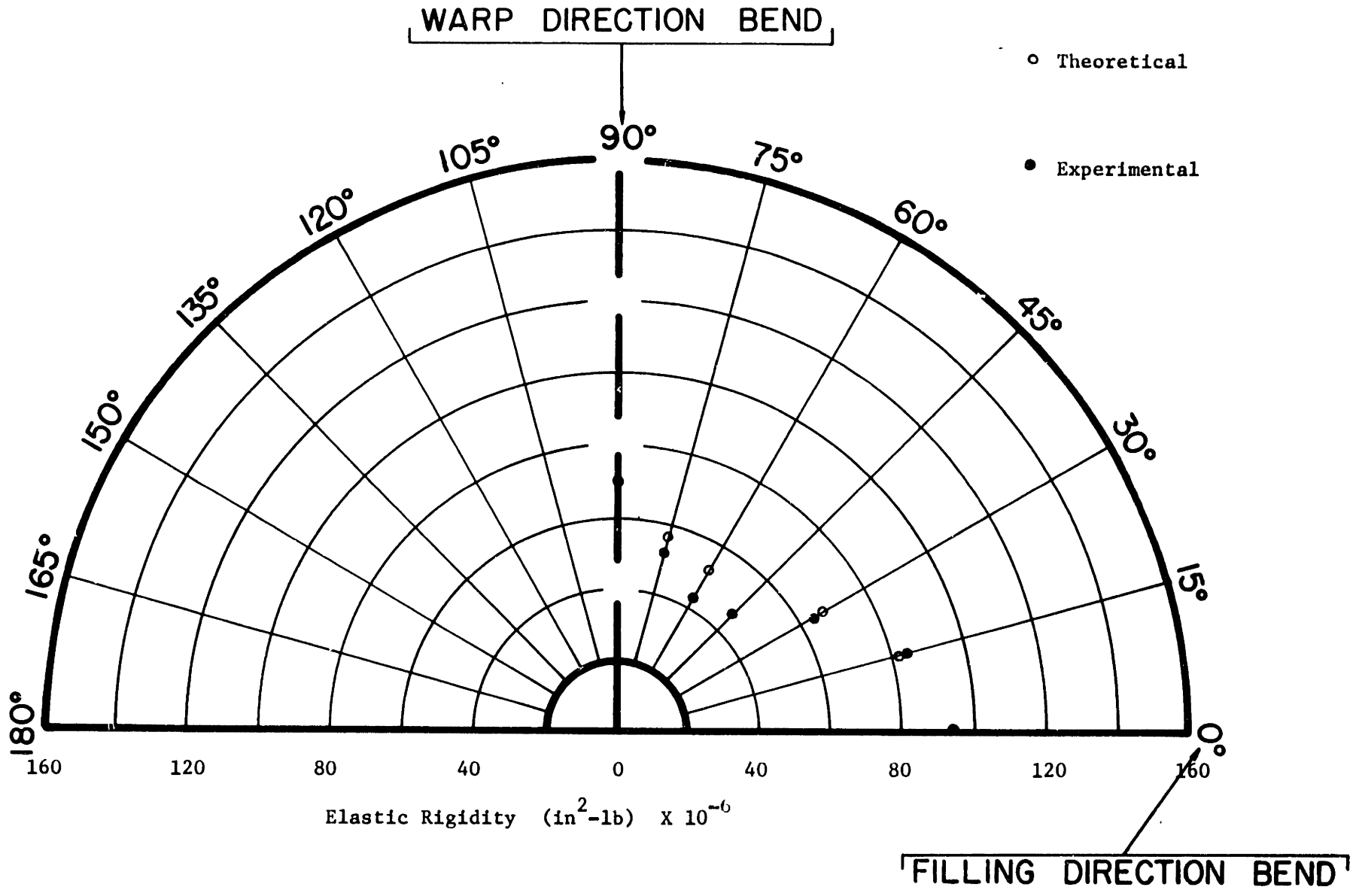

FIGURE 4-4

Directional Properties in Elastic Rigidity of Nylon -Fabric (N-4)

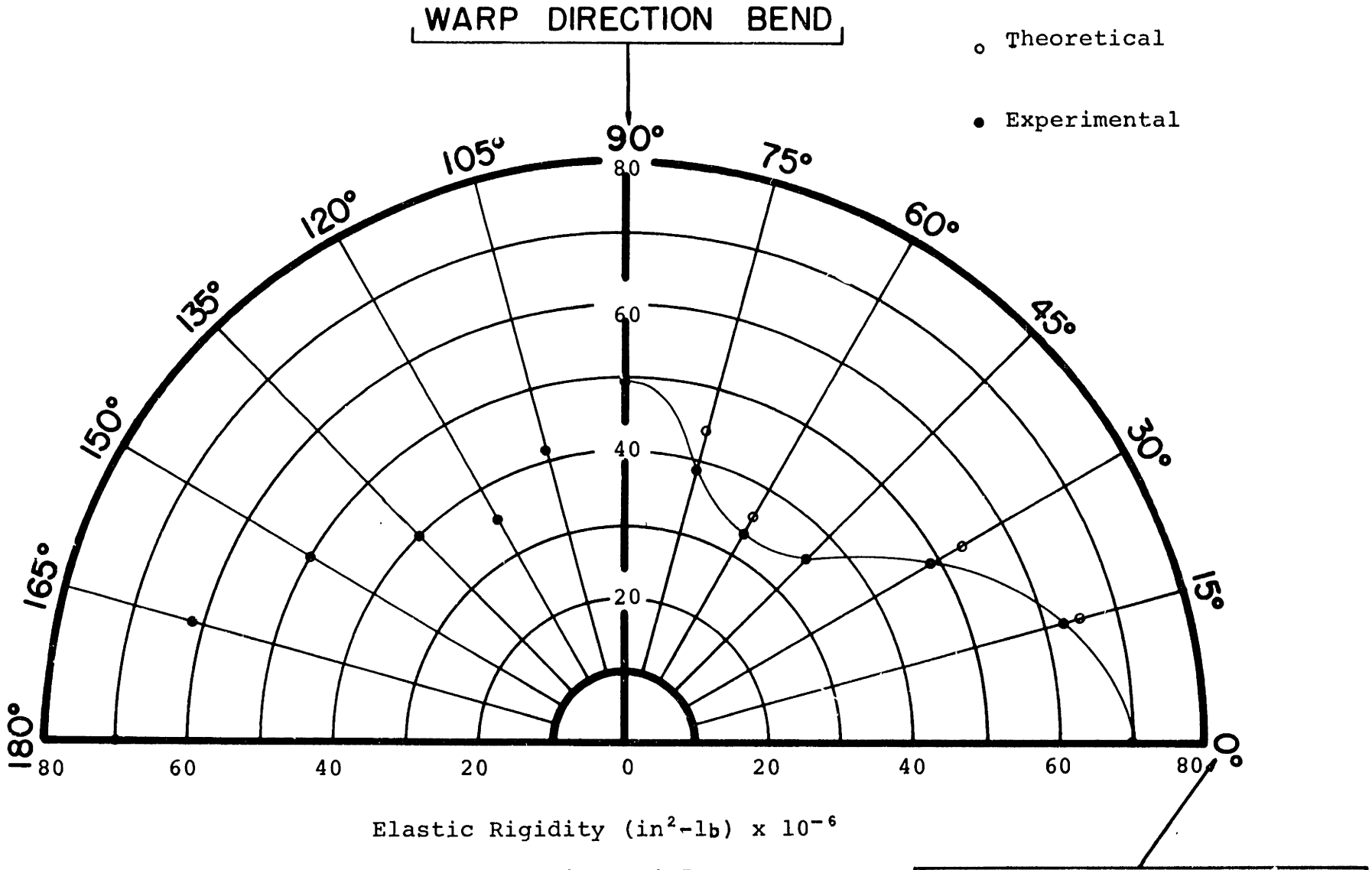

Figure 4-5

Directional Properties in Elastic Rigidity of Nylon-Fabric (N-5)

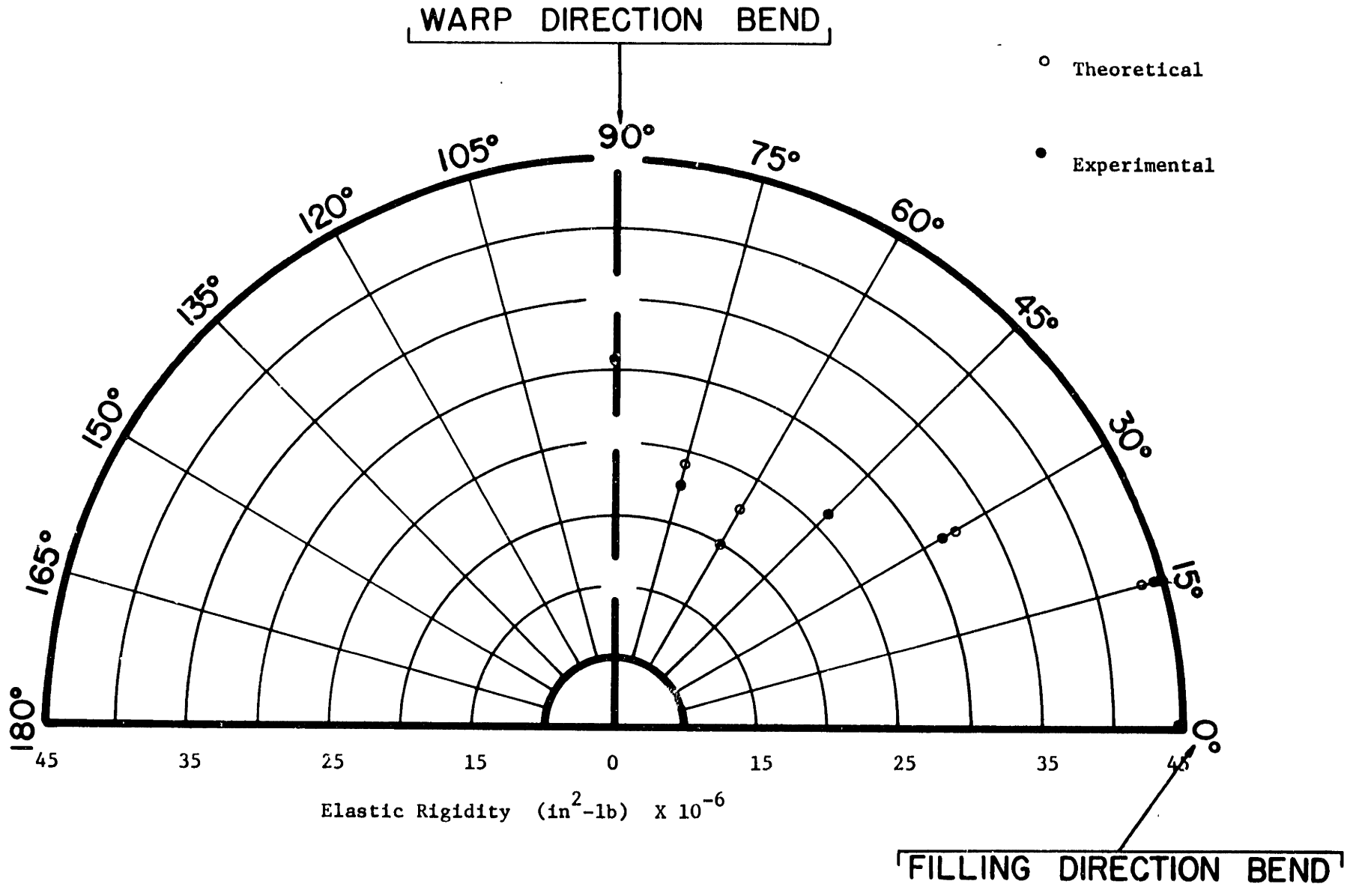

FIGURE 4-6

Directional Properties in Elastic Rigidity of Nylon-Fabric (N-6)

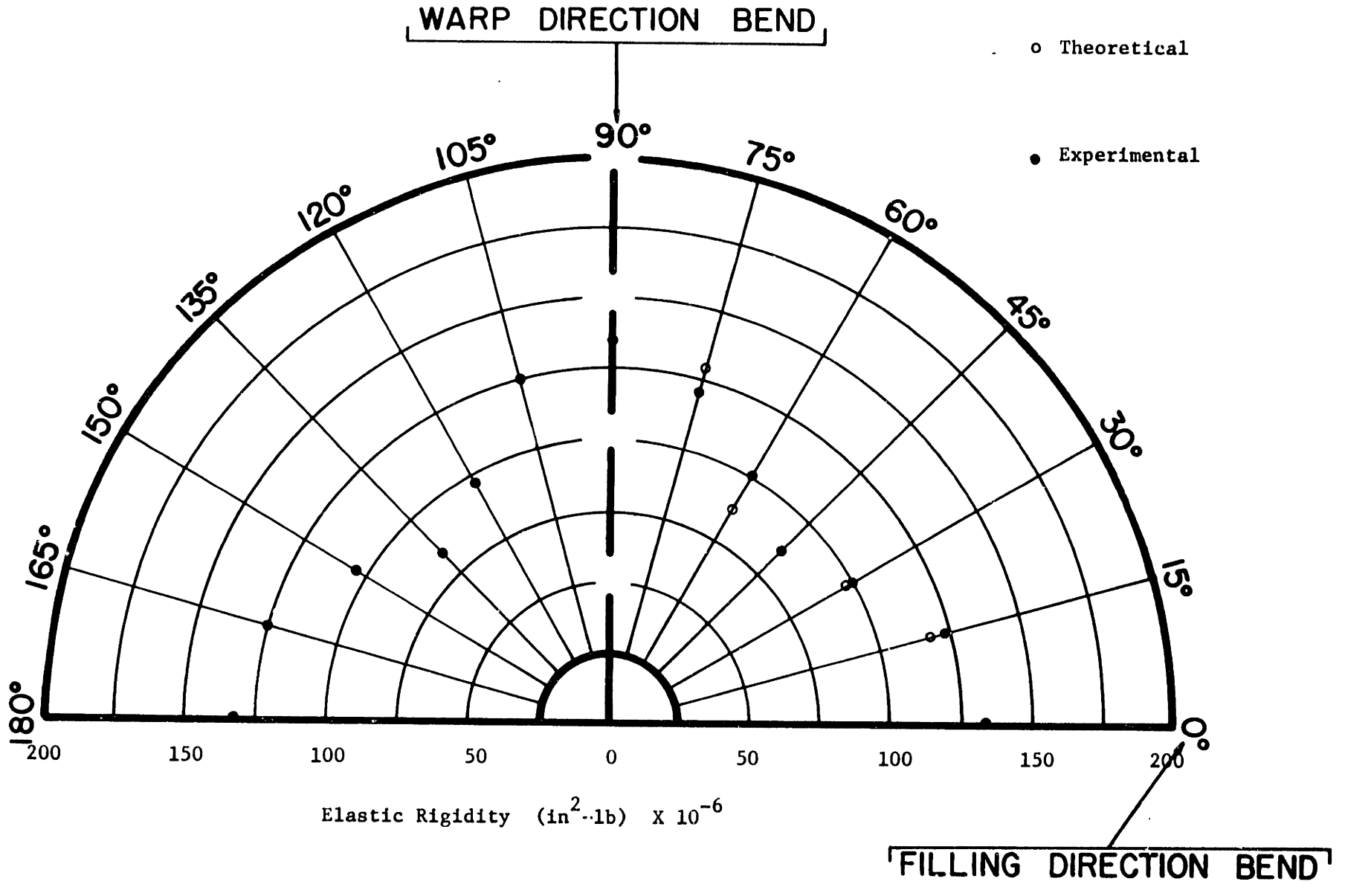

FIGURE 4-7

Directional Properties in Elastic Rigidity of Cotton-Fabric(dimensionally balanced) (C-1)

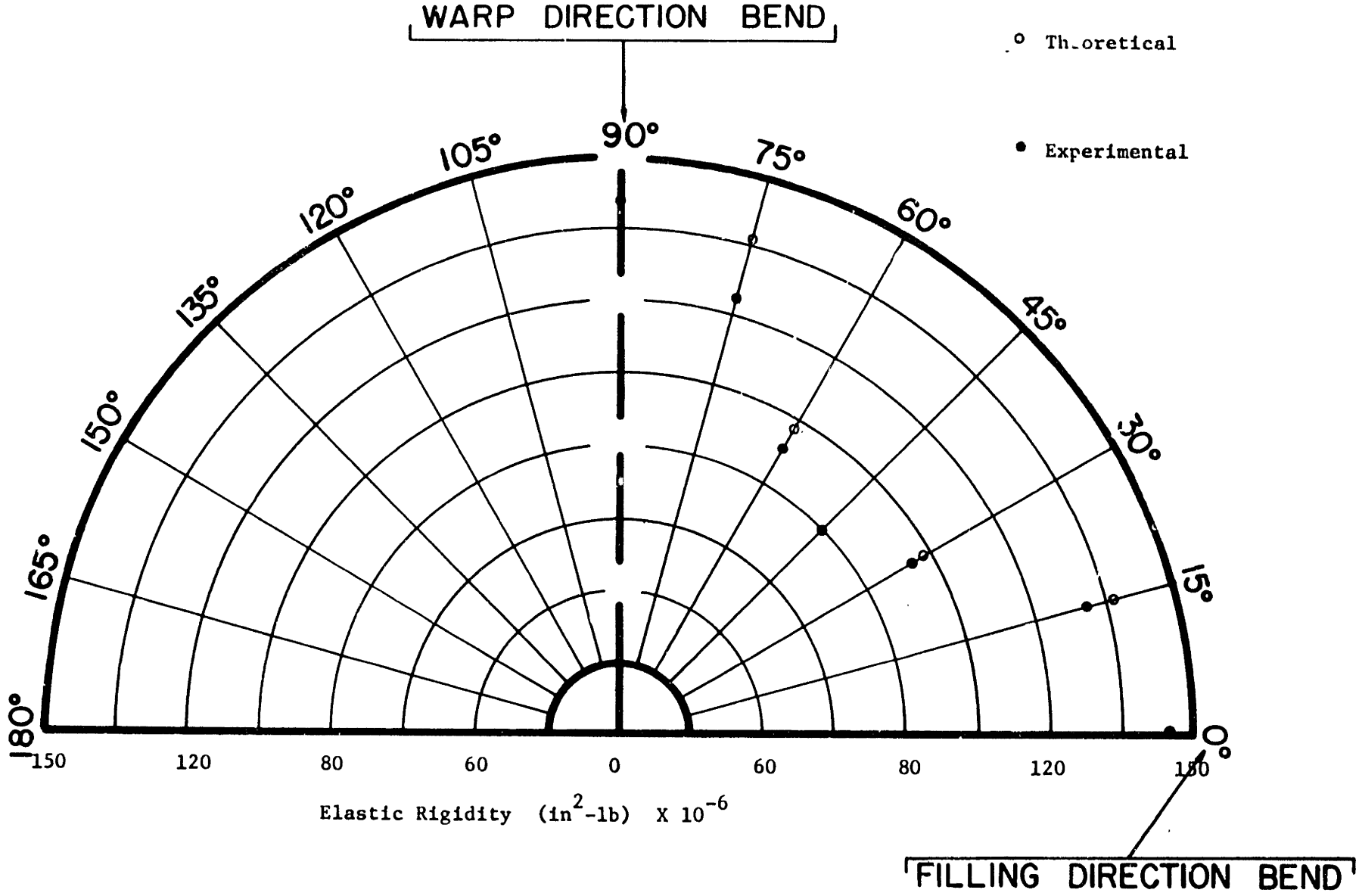

FIGURE 4-8

Directional Properties in Elastic Rigidity of Cotton-Fabric (C-2)

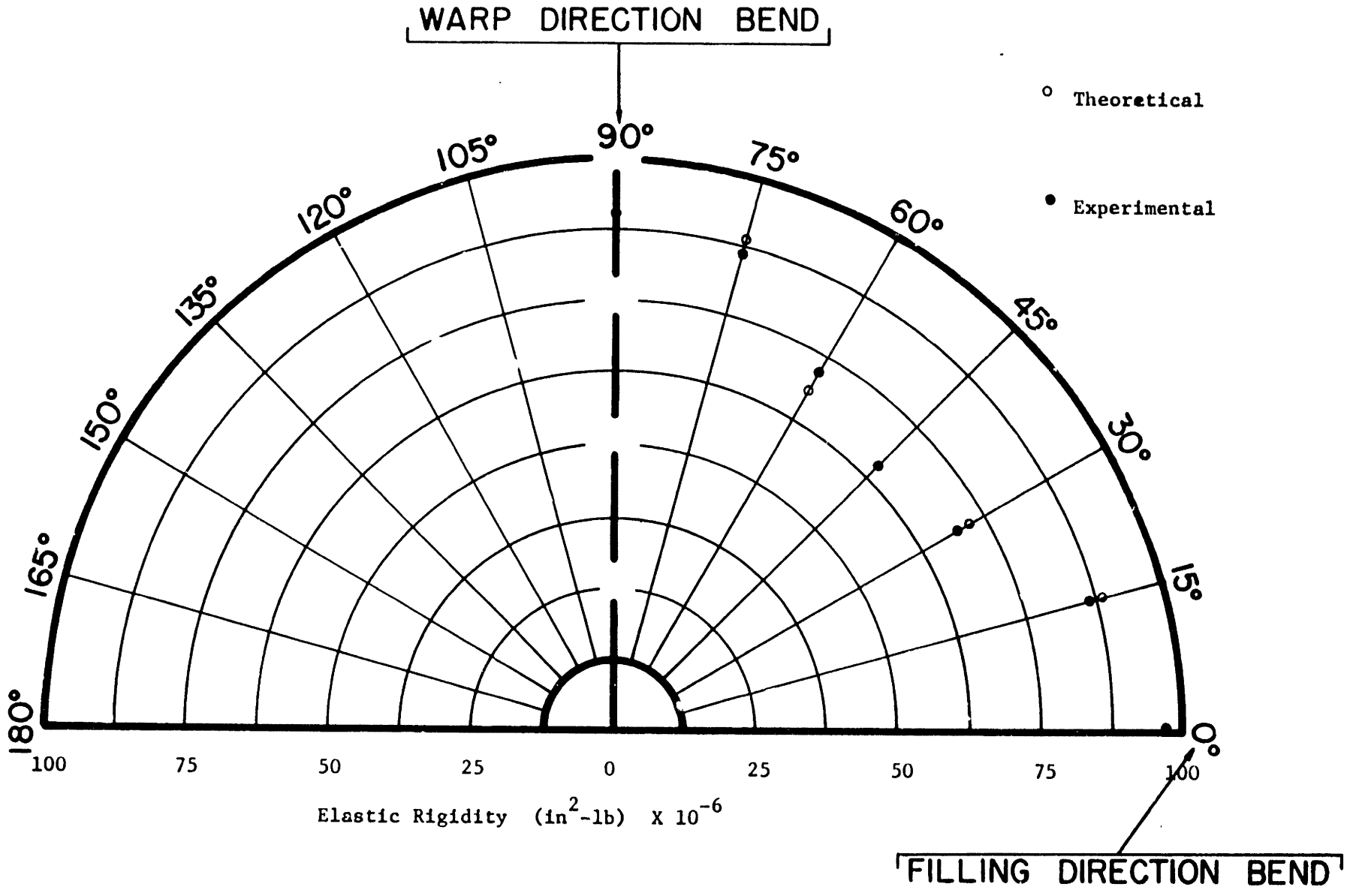

FIGURE 4-9

Directional Properties in Elastic Rigidity of Cotton-Fabric (C-3)

bending-unbending of a woven fabric at any orientation of bias bend in terms of the fiber properties, constructional parameters of warp and filling assemblies of yarn and that of the fabric, and the effective curvature of the component yarns. This equation (2.15) has been checked for the same nine fabrics. In obtaining the theoretically expected values of the total frictional work loss based on equation (2.15), the sum of A_1 and A_3 and the sum of A_2 and A_4 has been obtained directly by inserting experimental values in this equation for $\alpha = 90°$ and $0°$ respectively. By this means, the theoretical curves have been fitted to the experimental curves. Once again, chi-square tests have been performed to check the closeness of fit between the experimentally obtained values and the theoretically predicted values of the total frictional work loss and a good agreement has been observed with all the nine fabrics examined. (See Appendix C.)

For the particular case of a geometrically balanced fabric, since the fiber properties and constructional parameters of warp and filling yarns are nominally identical, it has been observed from equation (2.16) that the total frictional energy loss in bending is constant with angle of bend and is proportional to the imposed curvature of the fabric. This phenomenon is observed in Figure (4-16) where the total frictional work loss at any orientation of bend is constant.

It must be mentioned here that one additional frictional effect may occur for fabrics bent on the bias, namely that of yarn rotation at the crossing points due to the presence of a twisting moment. This effect has been neglected as a first approximation in the present analysis. Although this analysis is not complete, its results can be valuable in the interpretation of the frictional interactions observed. Since good agreement has been obtained between the experimentally observed values and the theoretically predicted values of the total frictional work loss based on the limited analysis, it could be deduced that frictional losses due to yarn rotation at crossing points are negligible in the multifilament nylon fabrics and cotton fabrics examined. The magnitude of this particular energy loss that may occur for fabrics bent on the bias would essentially be directly proportional to the magnitude of the inter-yarn pressure.

3. Unrecoverable Residual Elastic Energy as a Measure of Bending Recoverability.

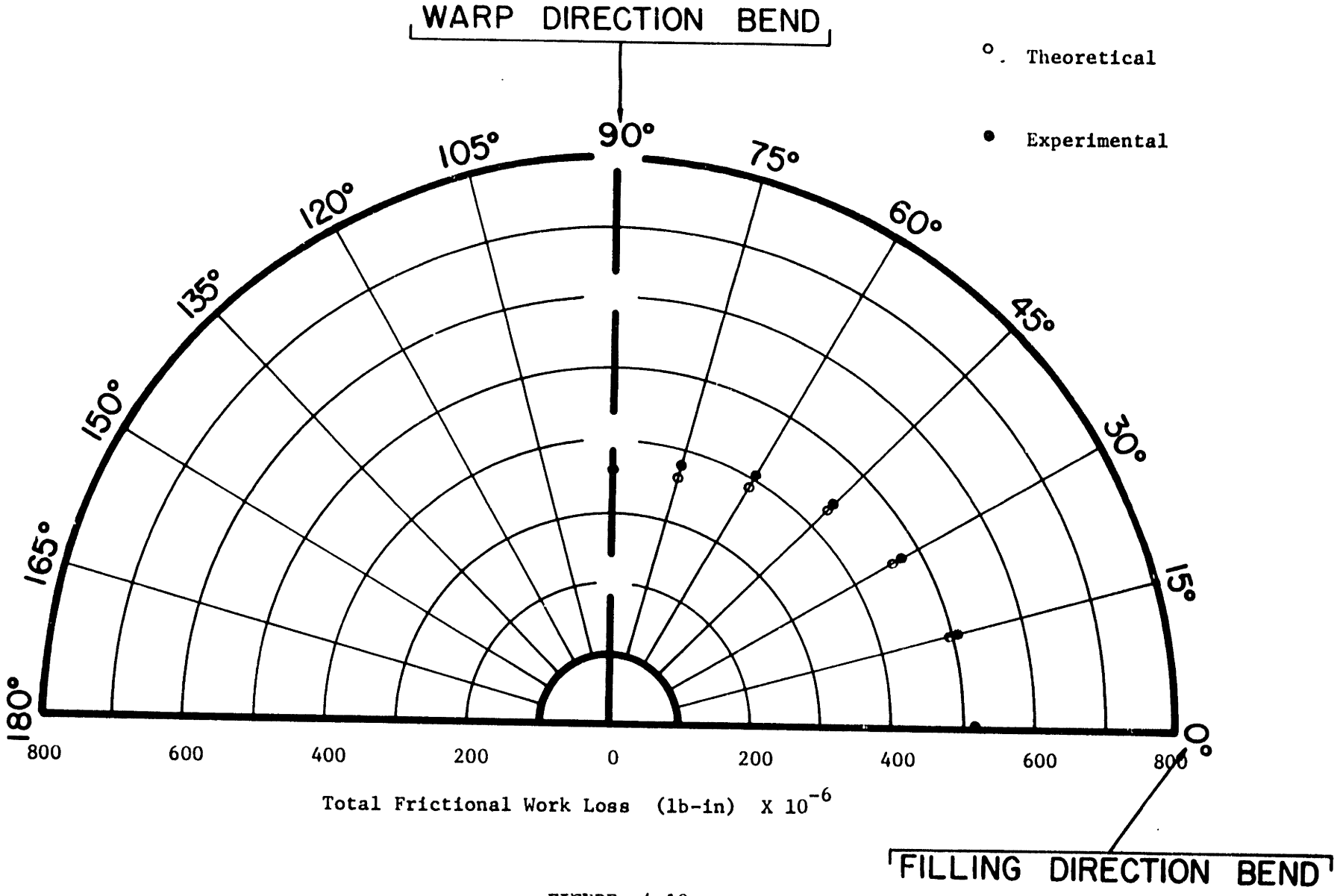

FIGURE 4-10

Directional Properties in Total Frictional Work Loss of Nylon-Fabric (N-1)

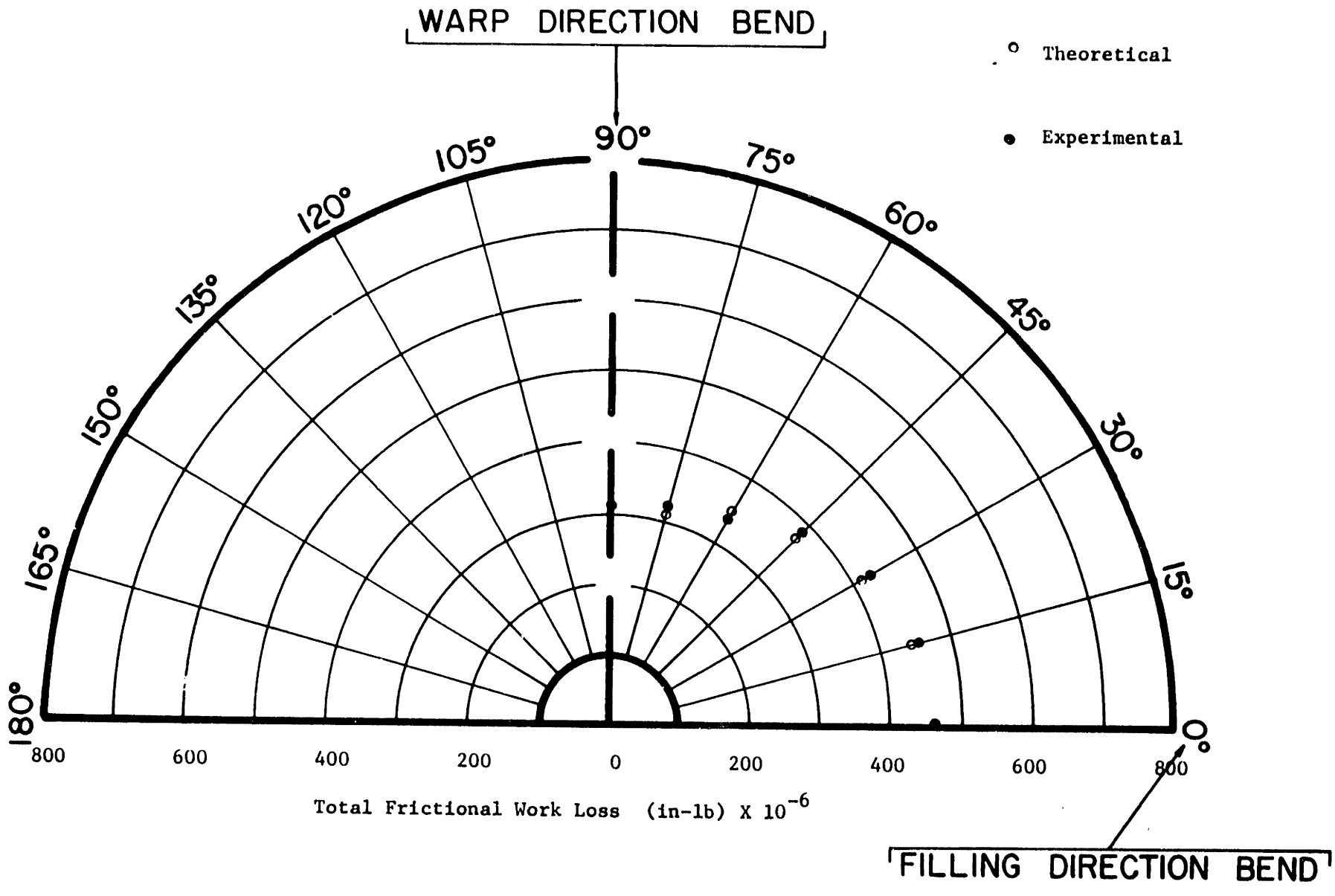

FIGURE 4-11

Directional Properties in Total Frictional Work Loss of Nylon-Fabric (N-2)

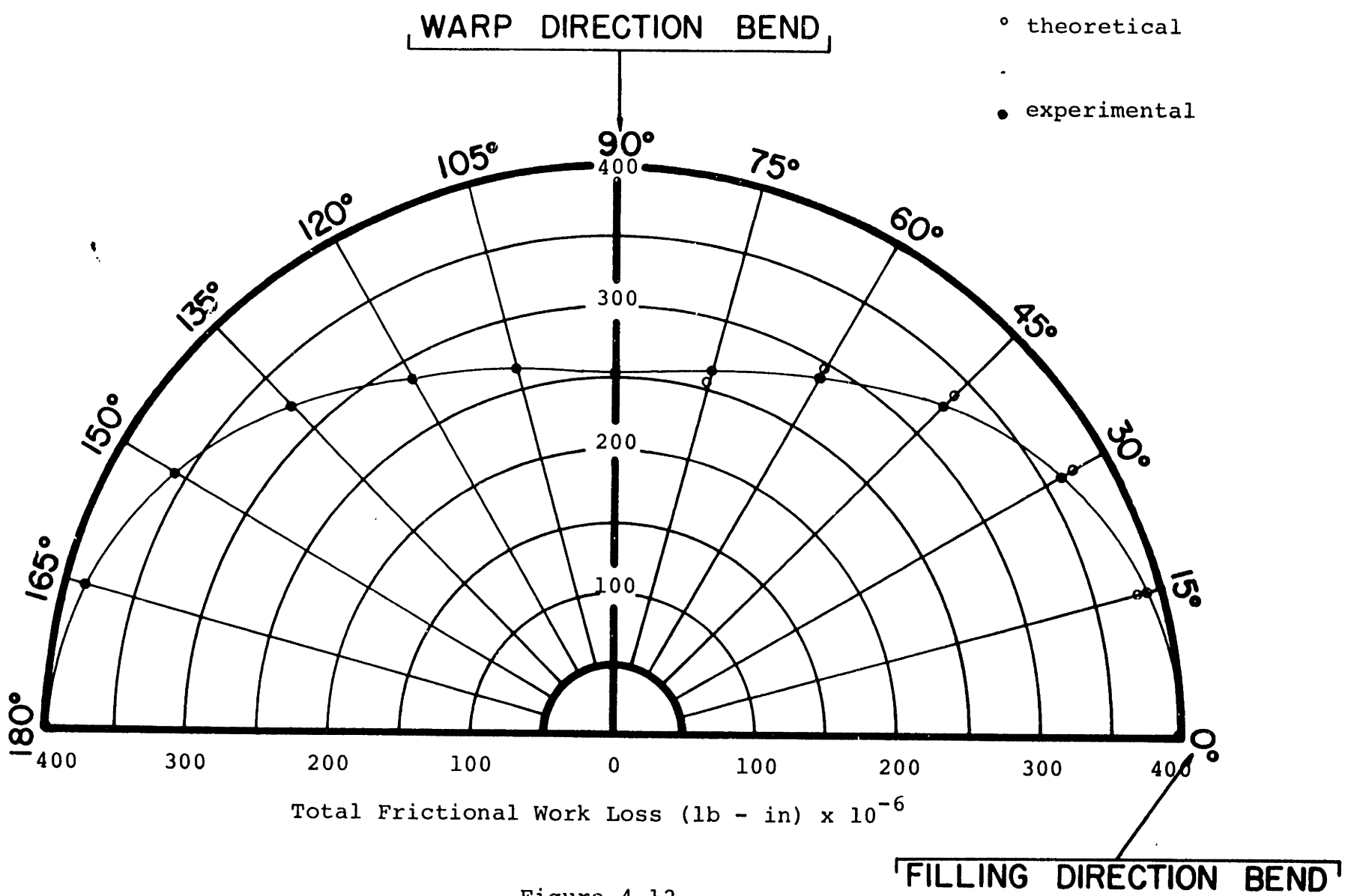

Figure 4-12

Directional Properties in Total Frictional Work Loss of Nylon-Fabric (N-3)

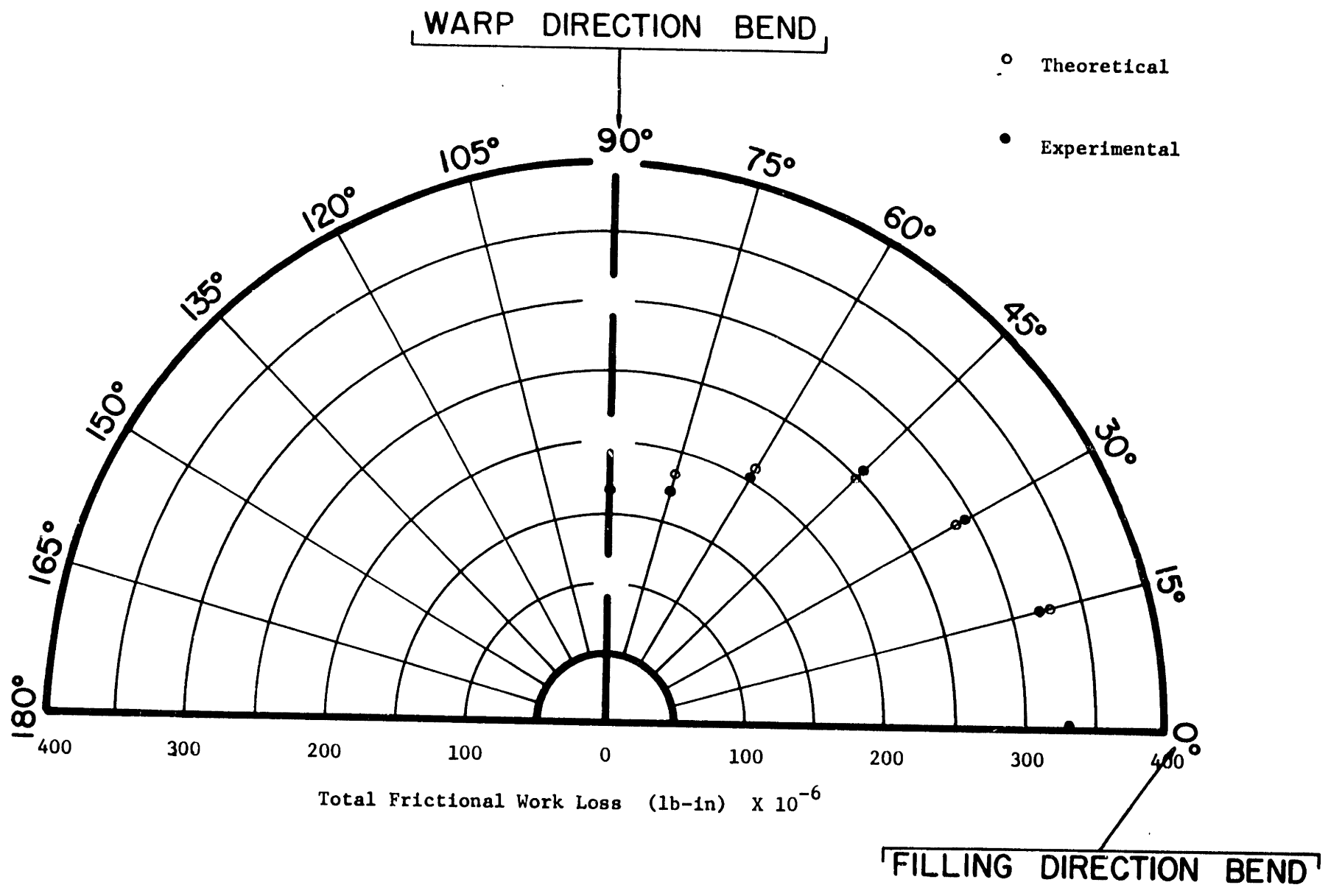

FIGURE 4-13

Directional Properties in Total Frictional Work Loss of Nylon-Fabric (N-4)

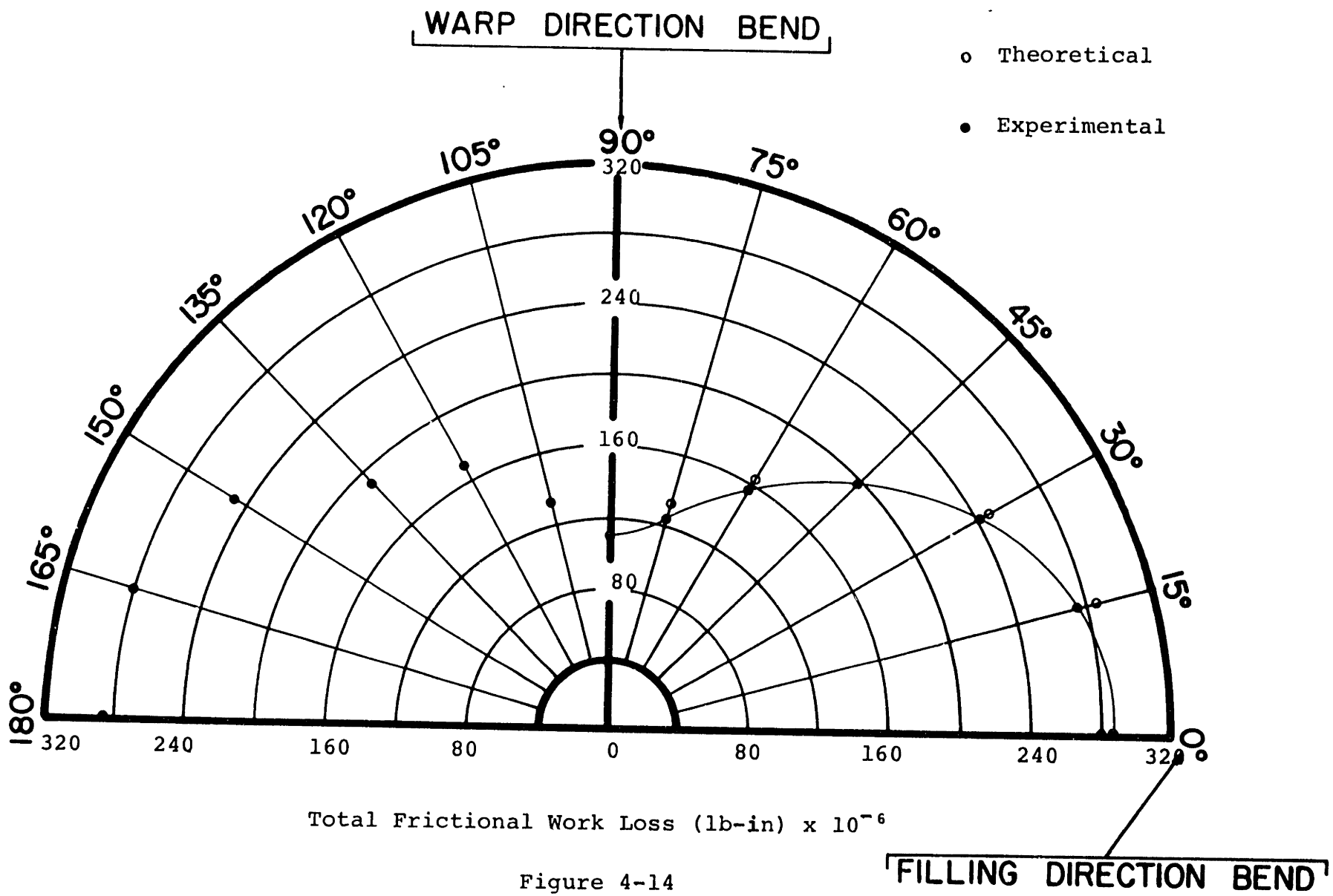

Figure 4-14

Directional Properties in Total Frictional Work Loss of Nylon-Fabric (N-5)

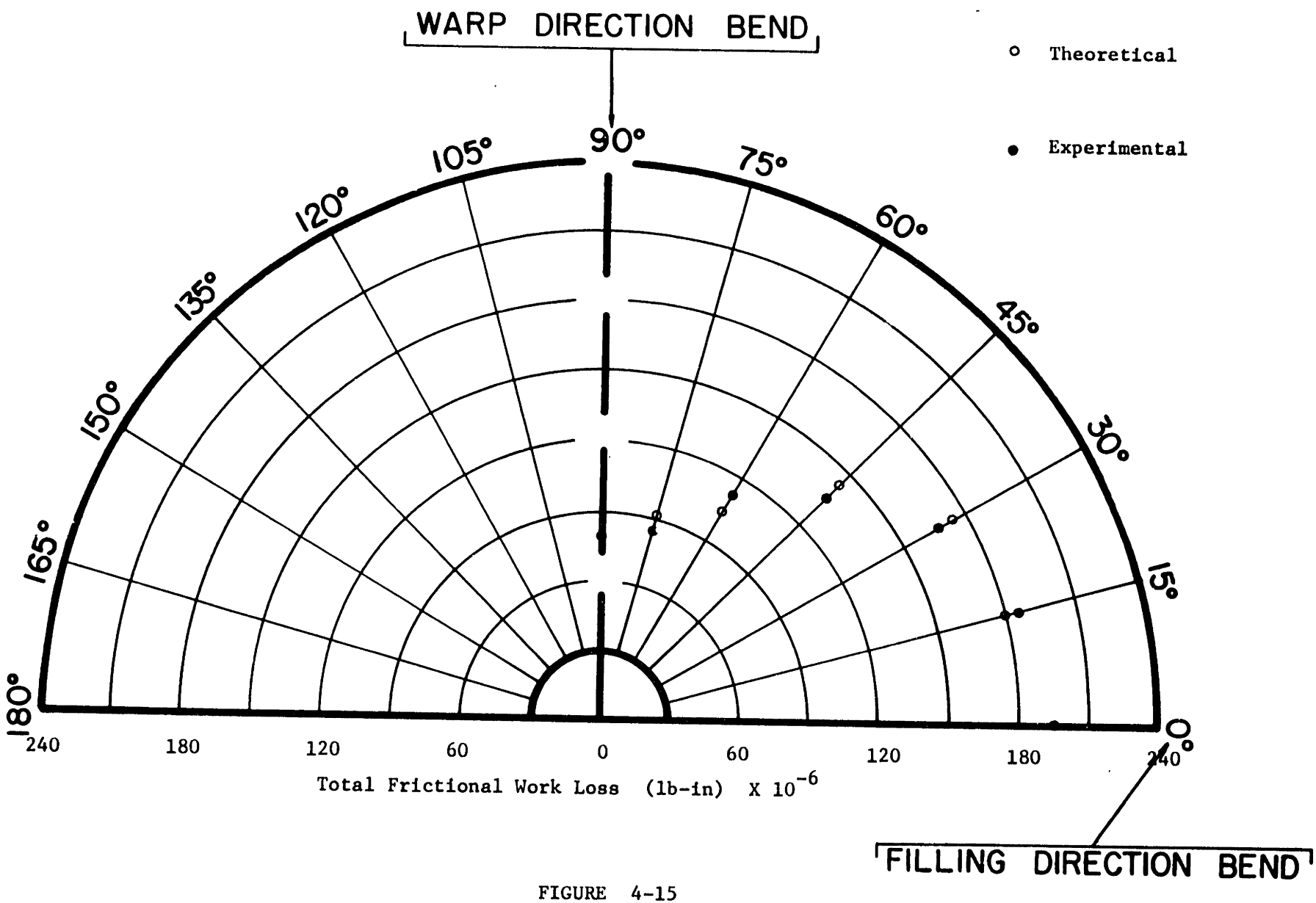

FIGURE 4-15

Directional Properties in Total Frictional Work Loss of Nylon-Fabric (N-6)

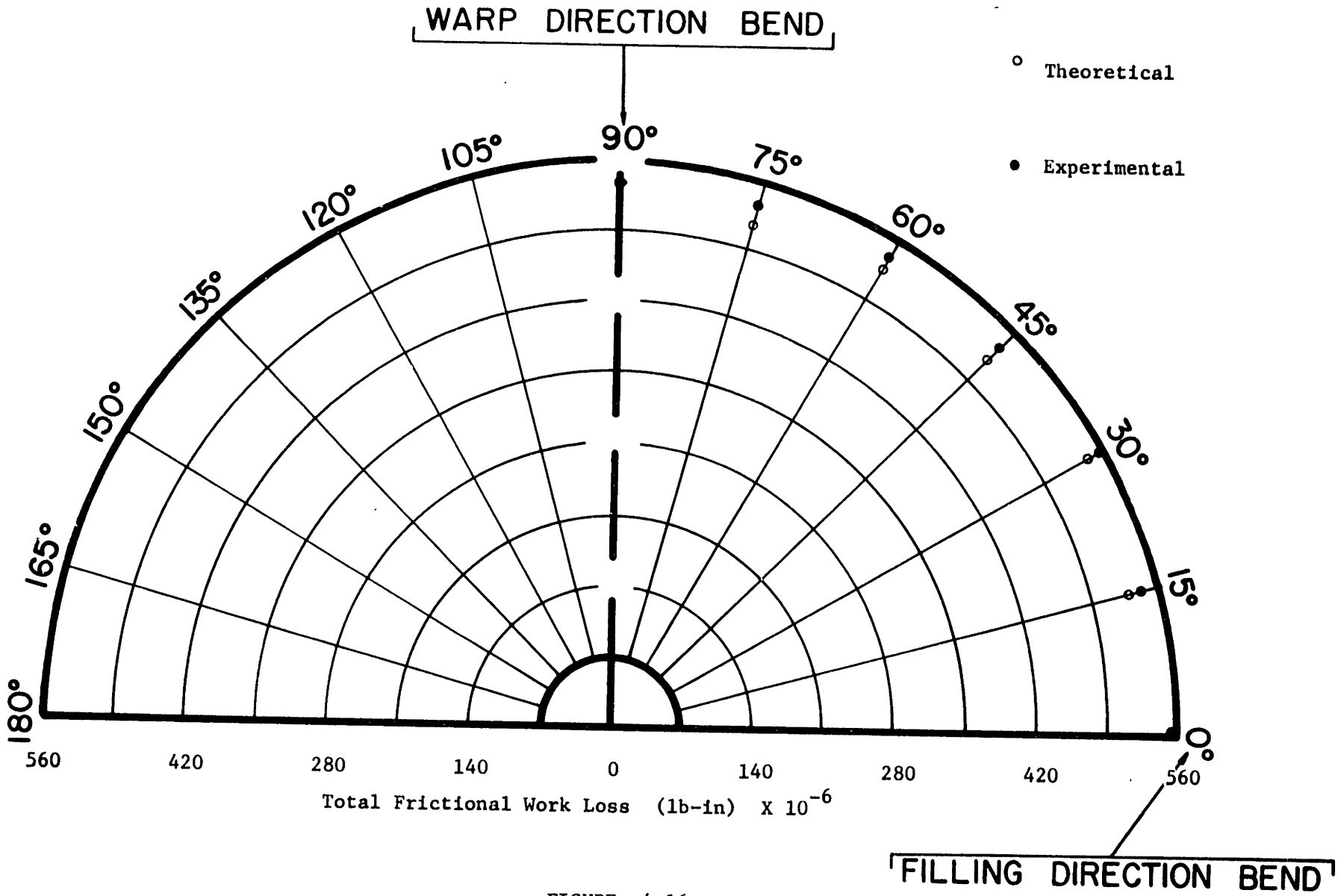

FIGURE 4-16

Directional Properties in Total Frictional Work Loss of Cotton-Fabric(dimensionally balanced)

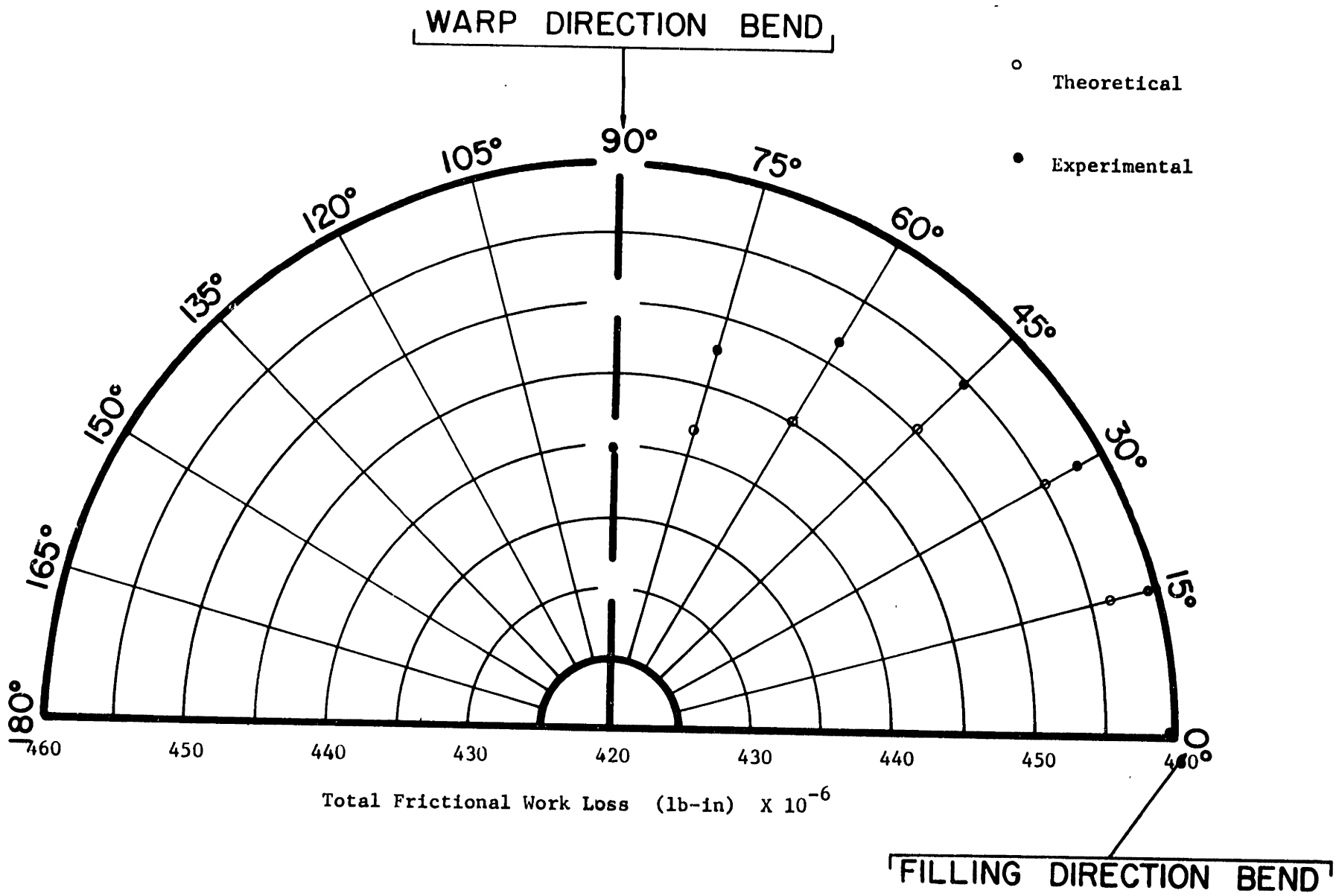

FIGURE 4-17

Directional Properties in Total Frictional Work Loss of Cotton-Fabric (C-2)

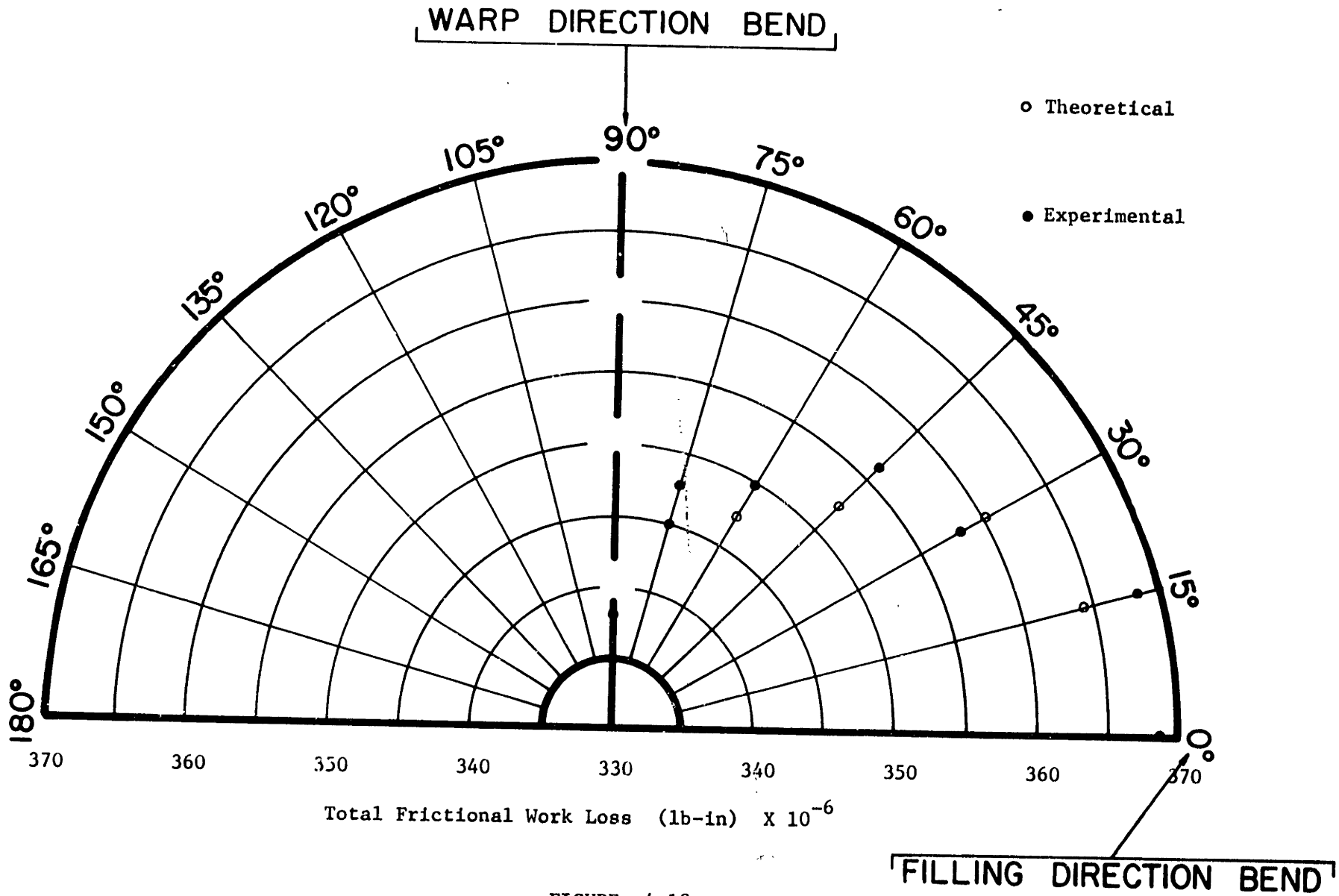

FIGURE 4-18

Directional Properties in Total Frictional Work Loss of Cotton-Fabric (C-3)

The model for investigating the friction in bending-unbending cycles of a woven fabric has been discussed in Chapter II, Section 3. In the present investigation an attempt has been made to analyze and quantitatively evaluate this conceptual model.

As discussed in the analysis presented in Chapter II, Section 3, the total energy that is put into the fabric in bending is partly dissipated in relative fiber motions and in some asymmetric fabrics also in relative motion of adjacent yarns against a frictional force and partly stored as elastic energy of the fibers. This is expressed by equation (2.17). On unloading a fabric, the stored elastic energy of the fibers becomes the driving force that unbends the fabric. This energy is partly dissipated, once again, in relative fiber motions and relative yarn motions (the motion is in the opposite direction to that which occurred during bending) against a frictional force, partly recovered as the fabric unbends, and a fraction of it remains unrecovered as residual elastic energy. This is expressed by equation (2.18). This residual elastic energy of the fibers that is left unrecovered at the end of the bending-unbending cycle is directly responsible for the residual curvature of the fabric. An expression has been deduced for the energy balance for a bending-unbending cycle of a fabric as:

> Total energy put into the fabric in bending = total energy loss in frictional restraints both in bending and unbending + energy recovered in unbending + unrecovered residual elastic energy.

This is expressed by equation (2.24).

The evaluation of the model presented in Chapter II, Section 3, relates one set of ensemble measurements, namely total energy input in bending a fabric, total energy loss in frictional restraints, energy recovered in unbending, and the unrecoverable residual elastic energy to another set of ensemble measurements, namely, elastic (flexural) rigidity of the fabric, the friction moment which is the additive amount of moment required to overcome frictional effects, and the imposed curvature of the fabric. The fundamental usefulness of the present analysis and the qualitative evaluation of the conceptual model have been exhibited in correcting the usually accepted concept of the hysteresis loop of bending-unbending cycle as representing the total energy loss due to frictional restraints. It has been shown in the present analysis

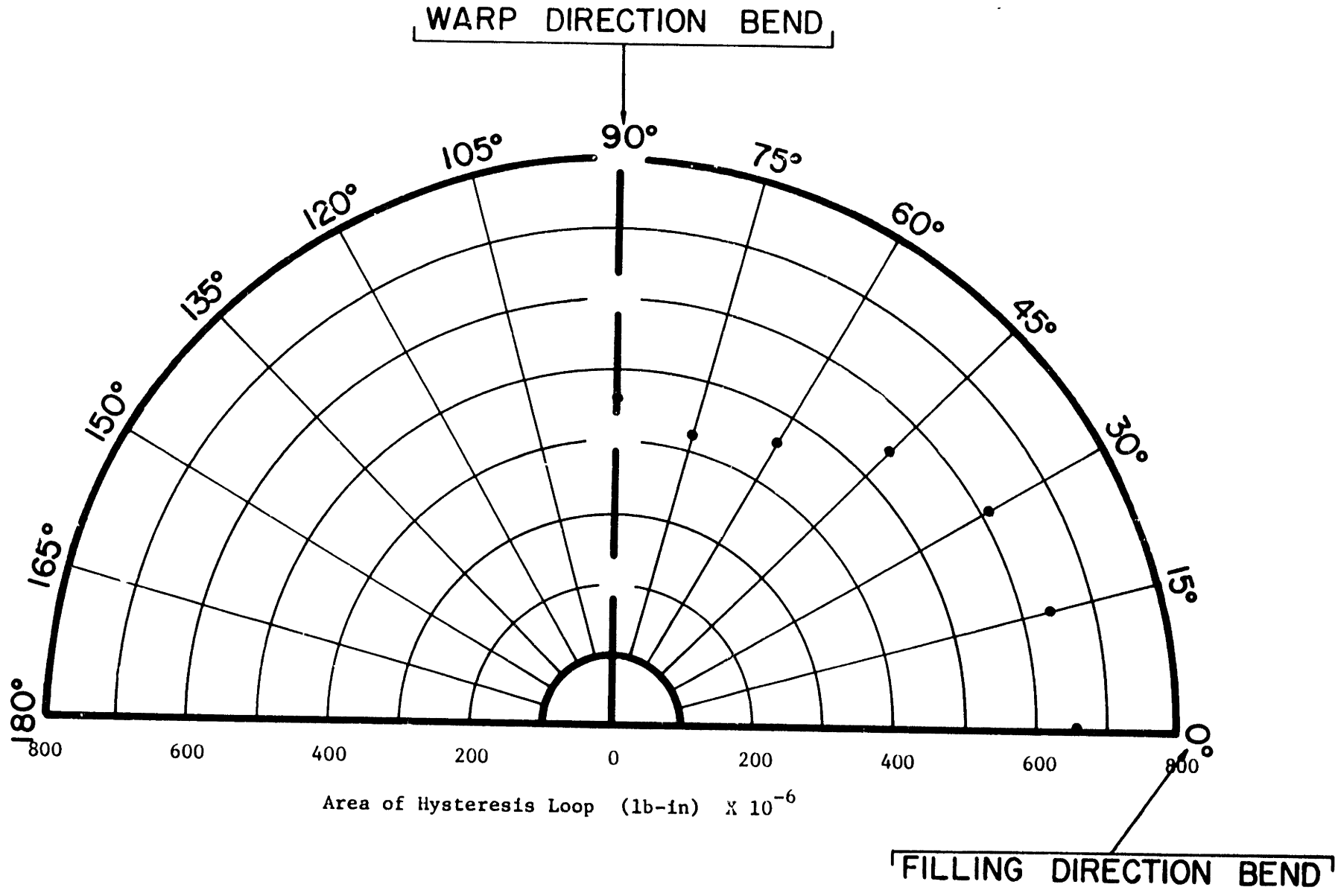

FIGURE 4-19

Directional Properties in Area of Hysteresis Loop of Nylon-Fabric (N-1)

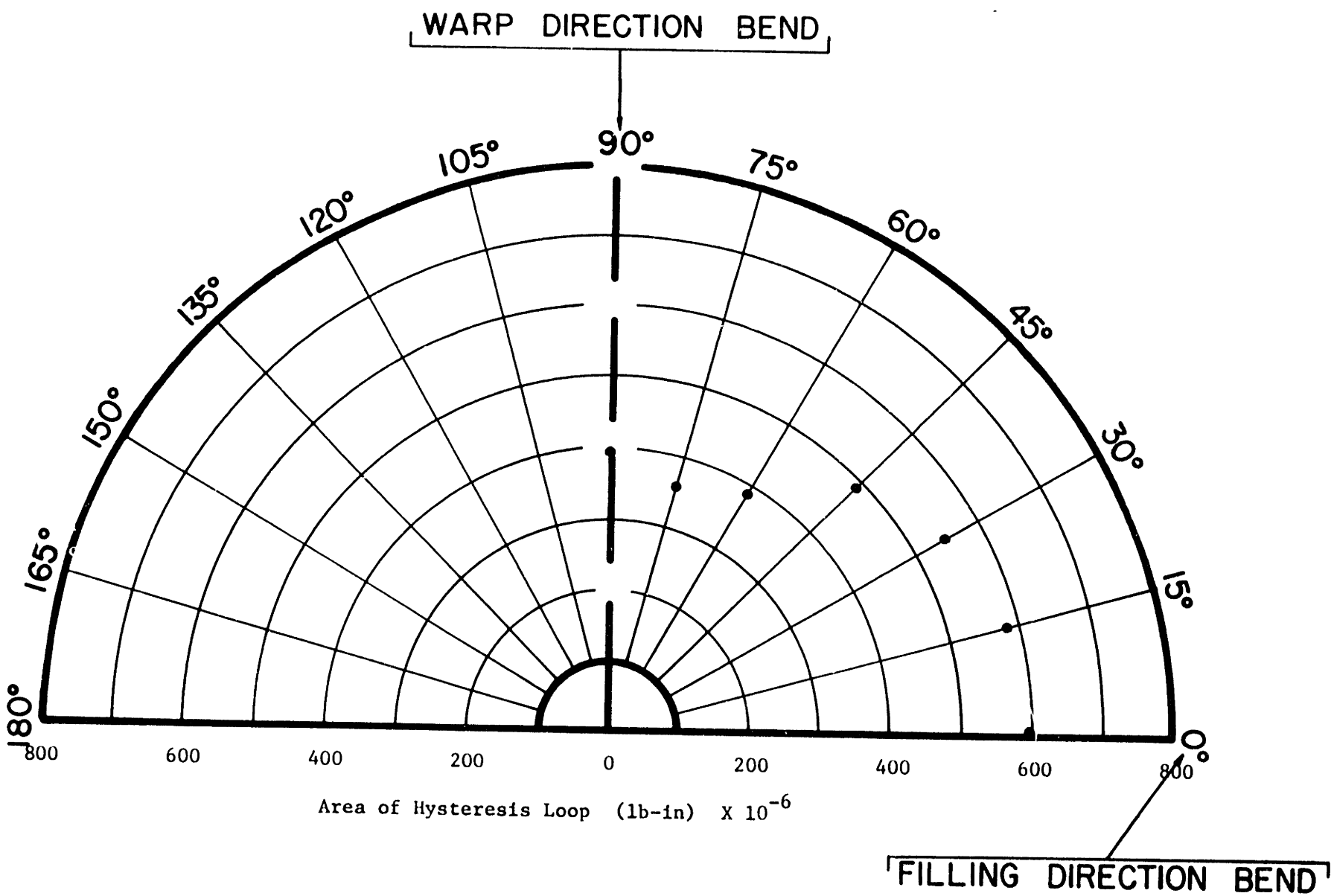

FIGURE 4-20

Directional Properties in Area of Hysteresis Loop of Nylon-Fabric (N-2)

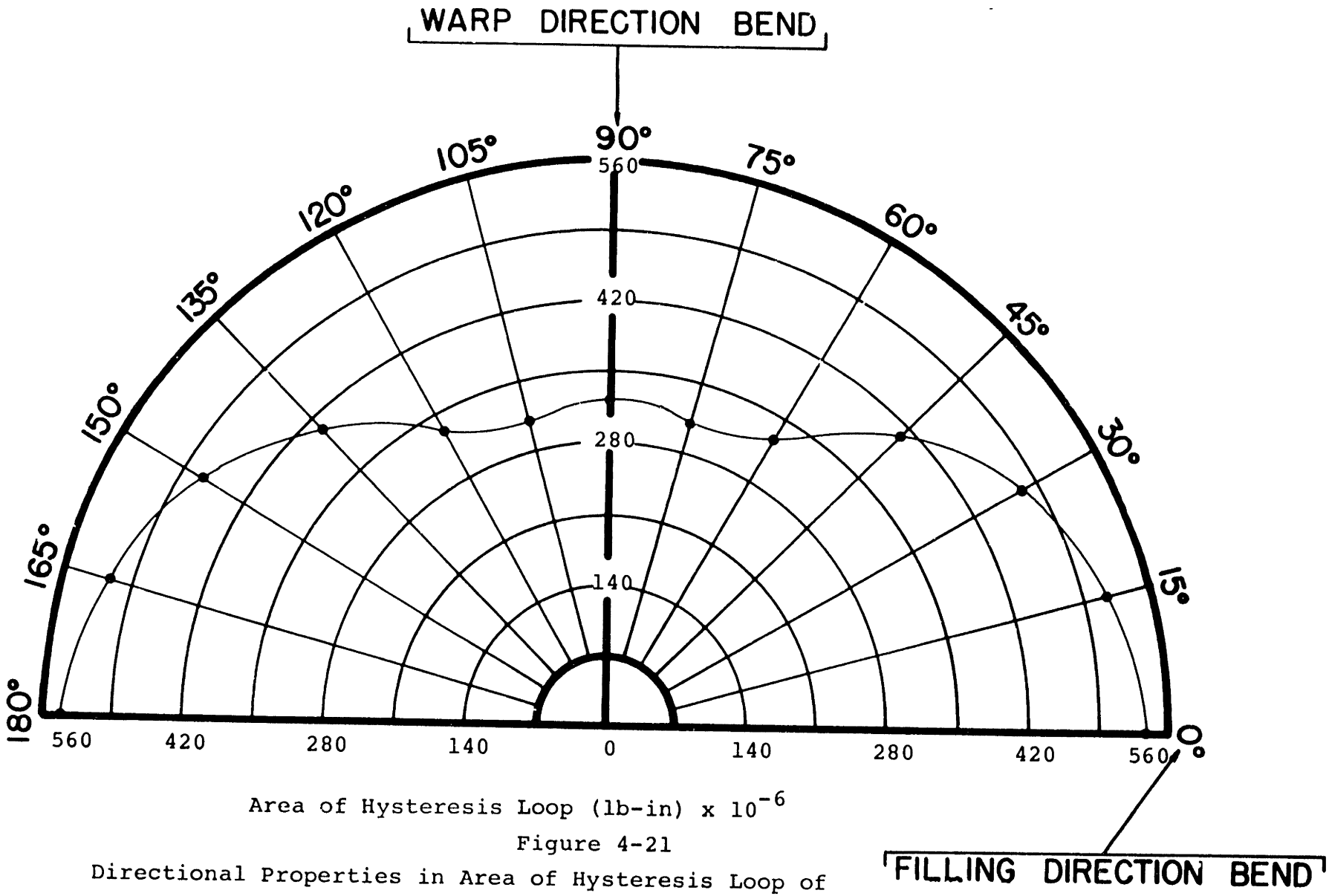

Figure 4-21

Directional Properties in Area of Hysteresis Loop of Nylon-Fabric (N-3)

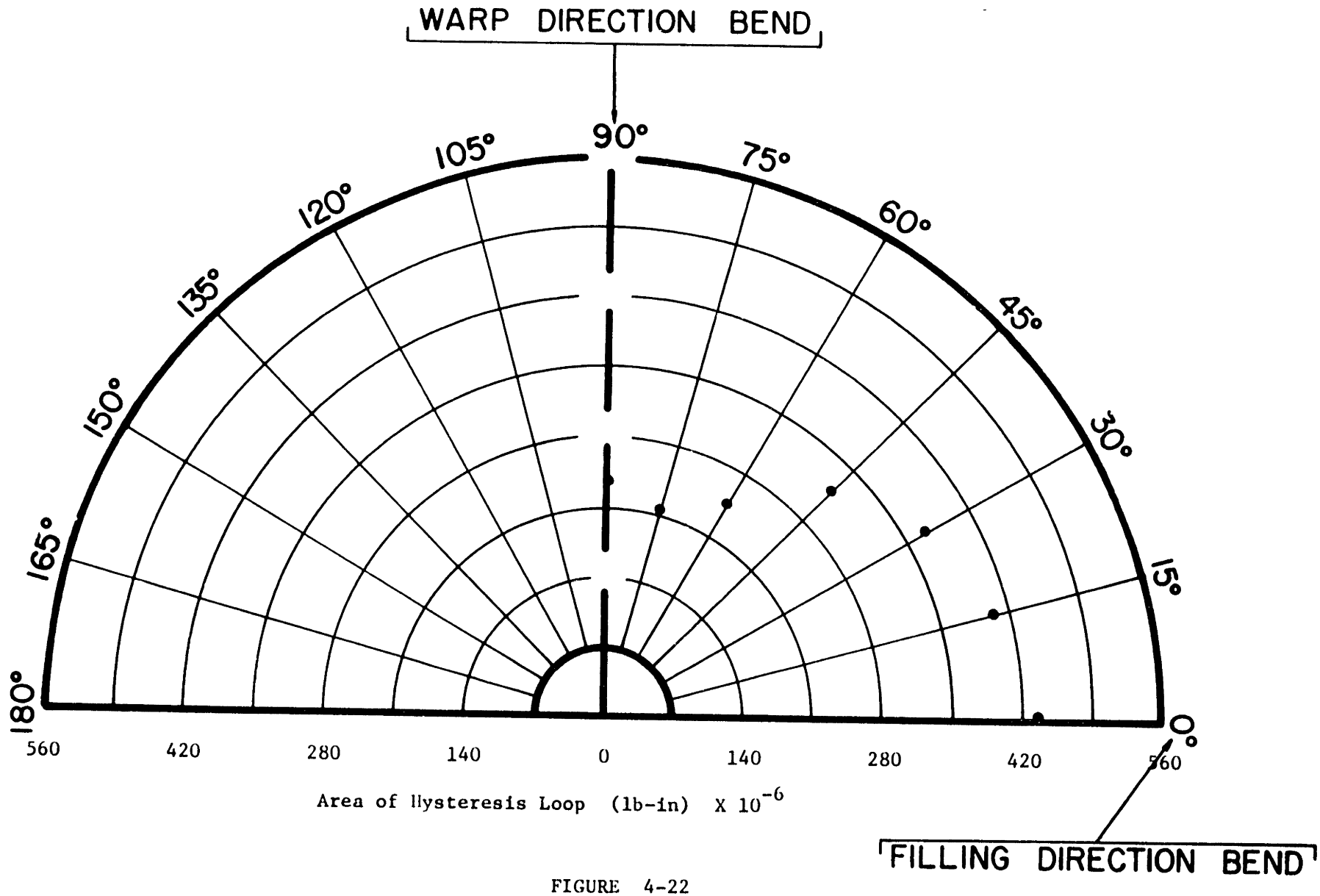

FIGURE 4-22

Directional Properties in Area of Hysteresis Loop of Nylon-Fabric (N-4)

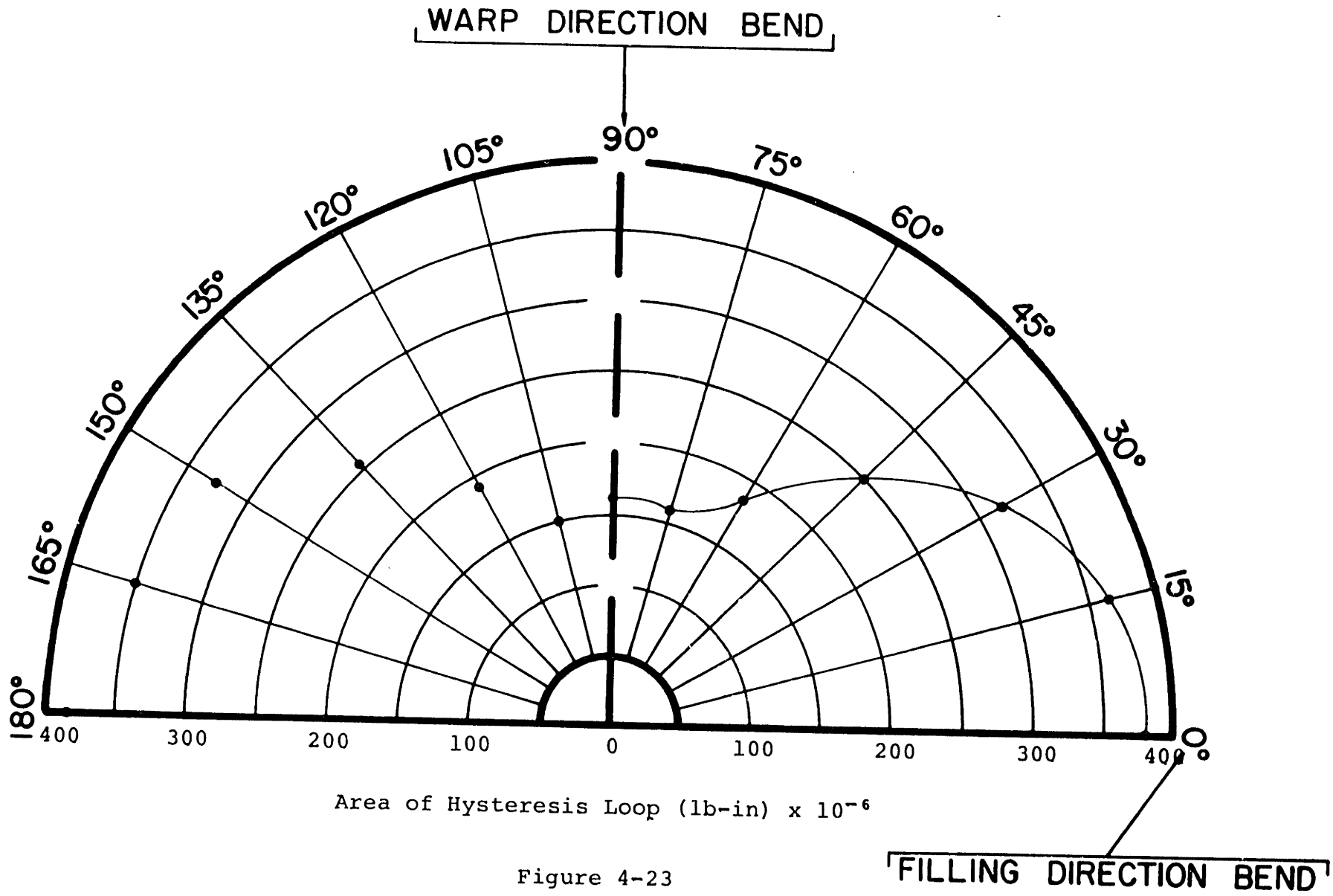

Figure 4-23

Directional Properties in Area of Hysteresis Loop of Nylon-fabric (N-5)

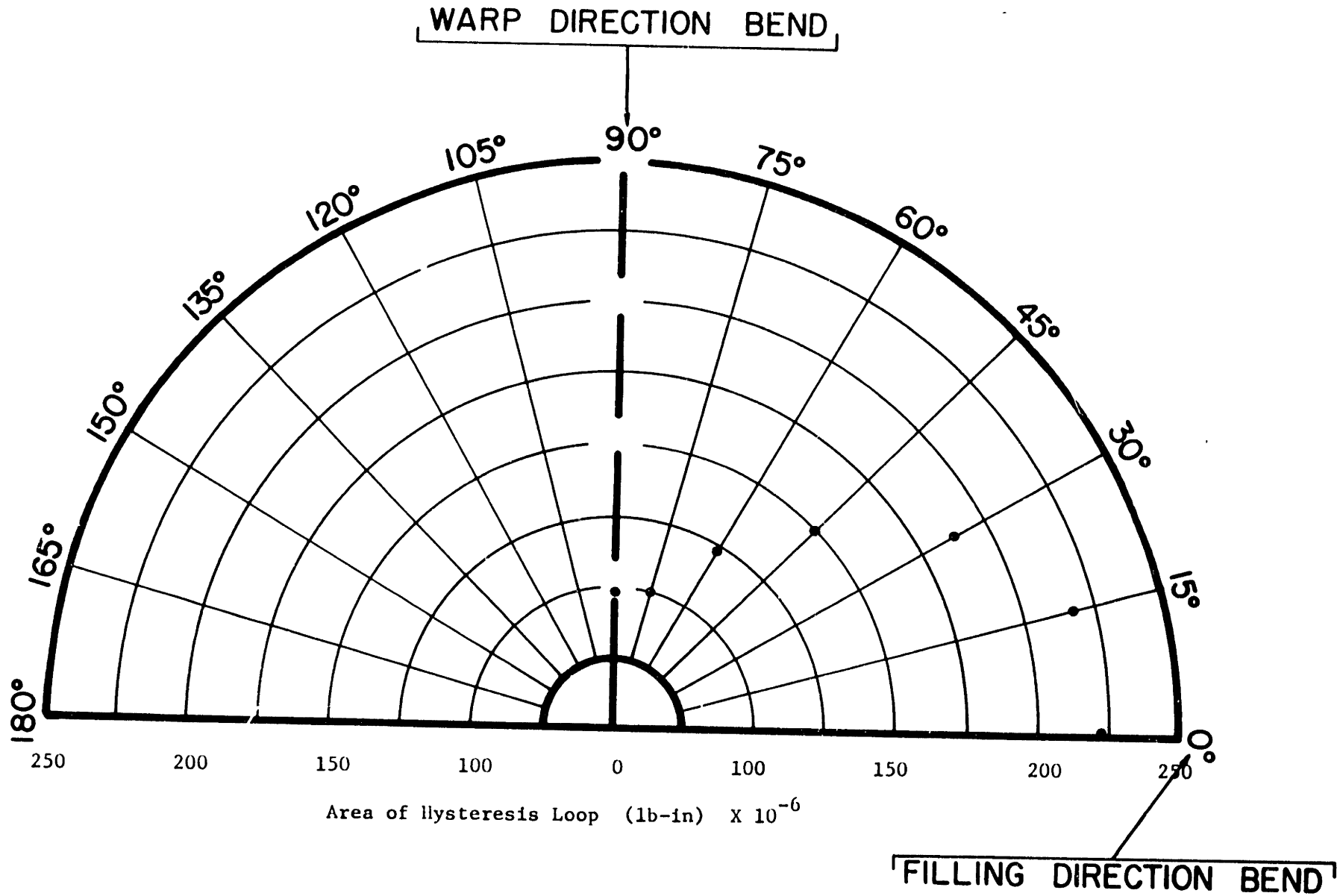

FIGURE 4-24

Directional Properties in Area of Hysteresis Loop of Nylon-Fabric (N-6)

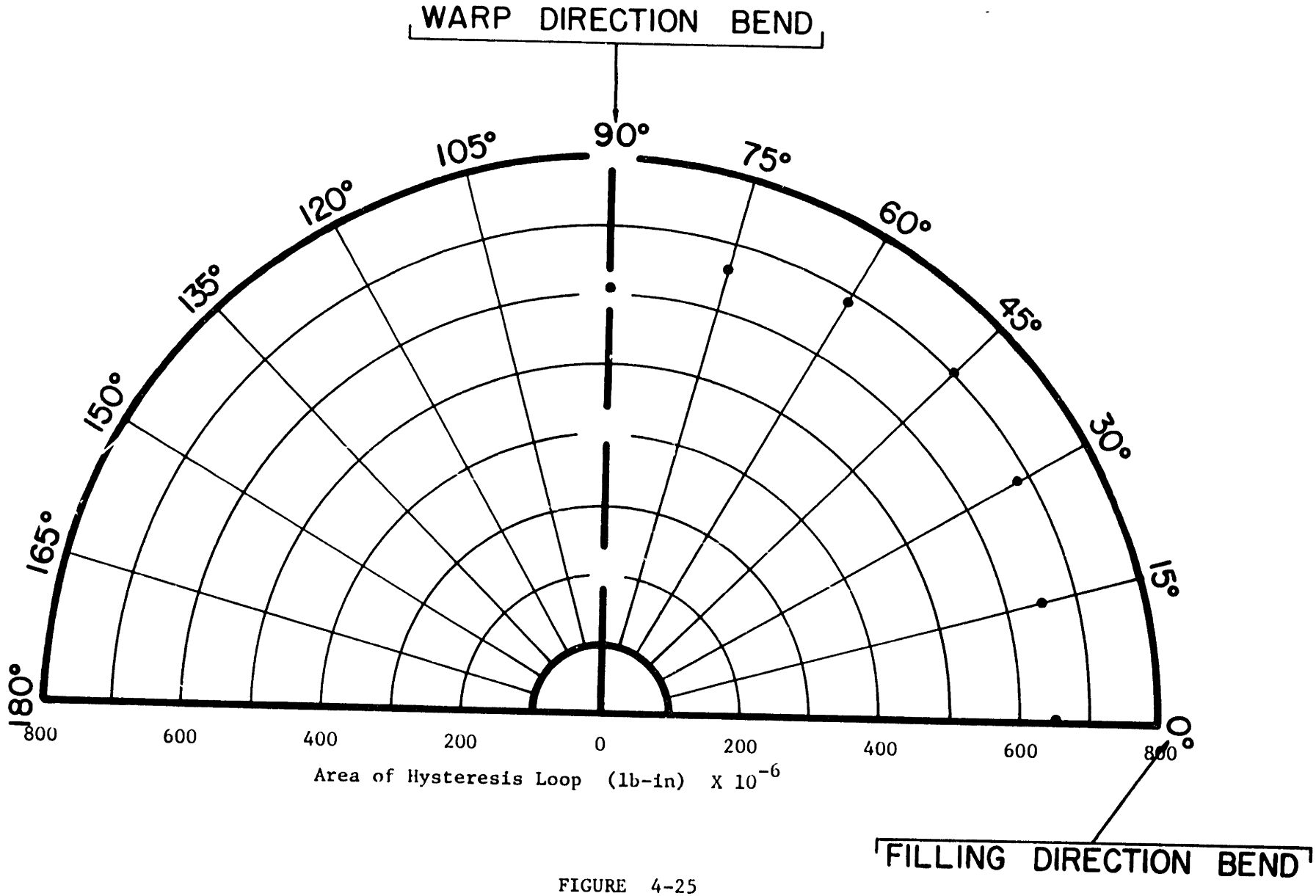

FIGURE 4-25

Directional Properties in Area of Hysteresis Loop of Cotton-Fabric(dimensionally balanced) (C-1)

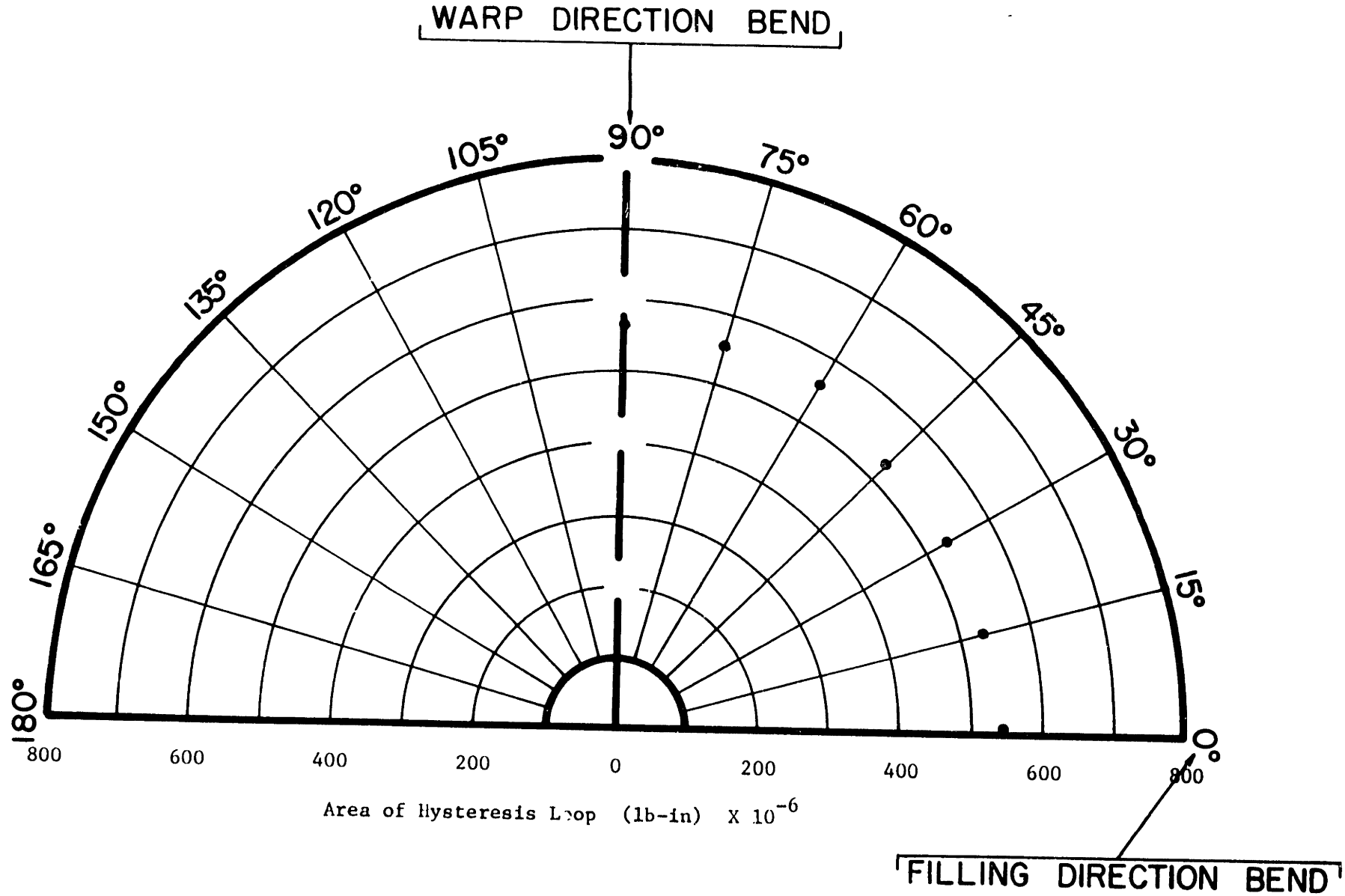

FIGURE 4-26

Directional Properties in Area of Hysteresis Loop of Cotton-Fabric (C-2)

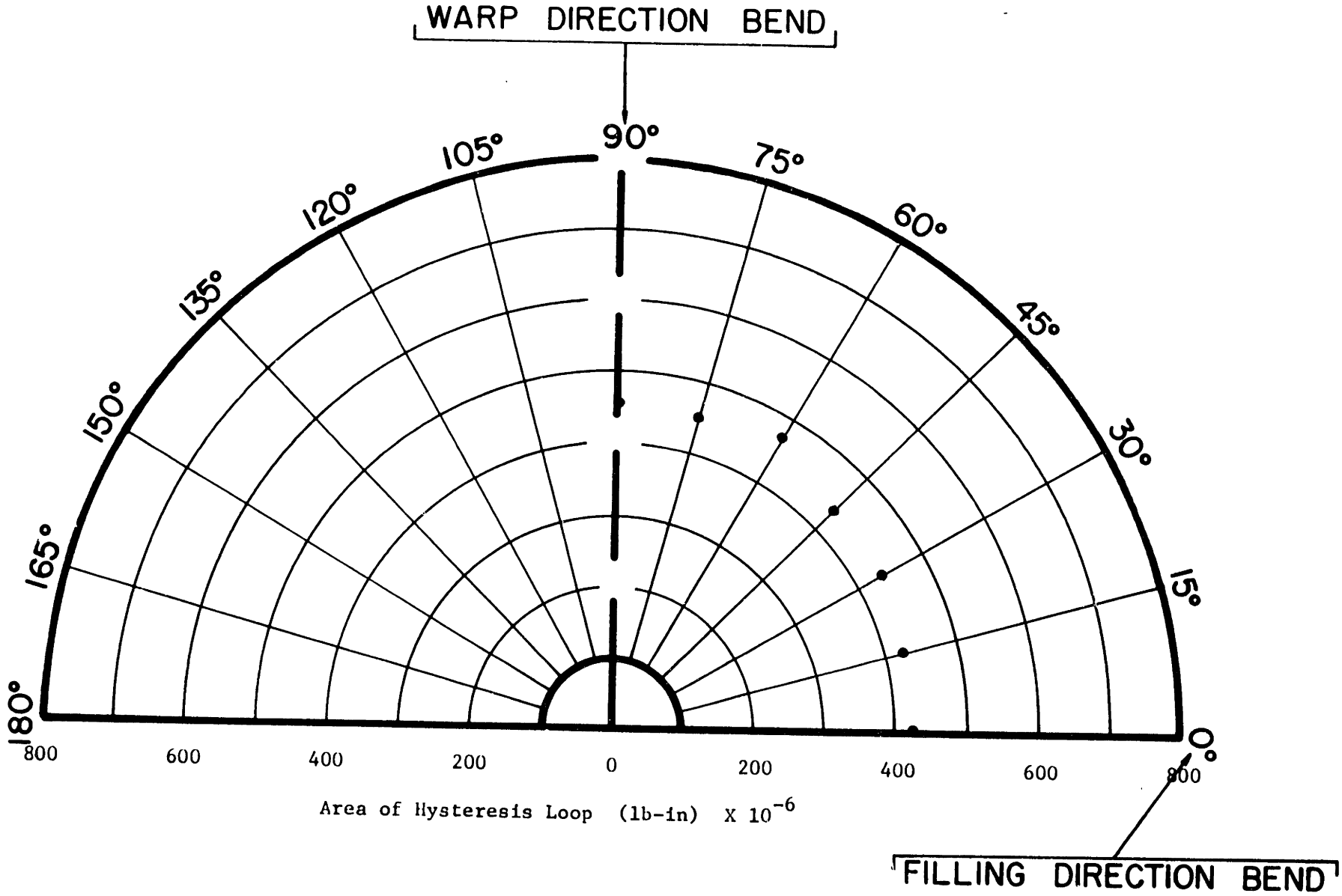

FIGURE 4-27

Directional Properties in Area of Hysteresis Loop of Cotton-Fabric (C-3)

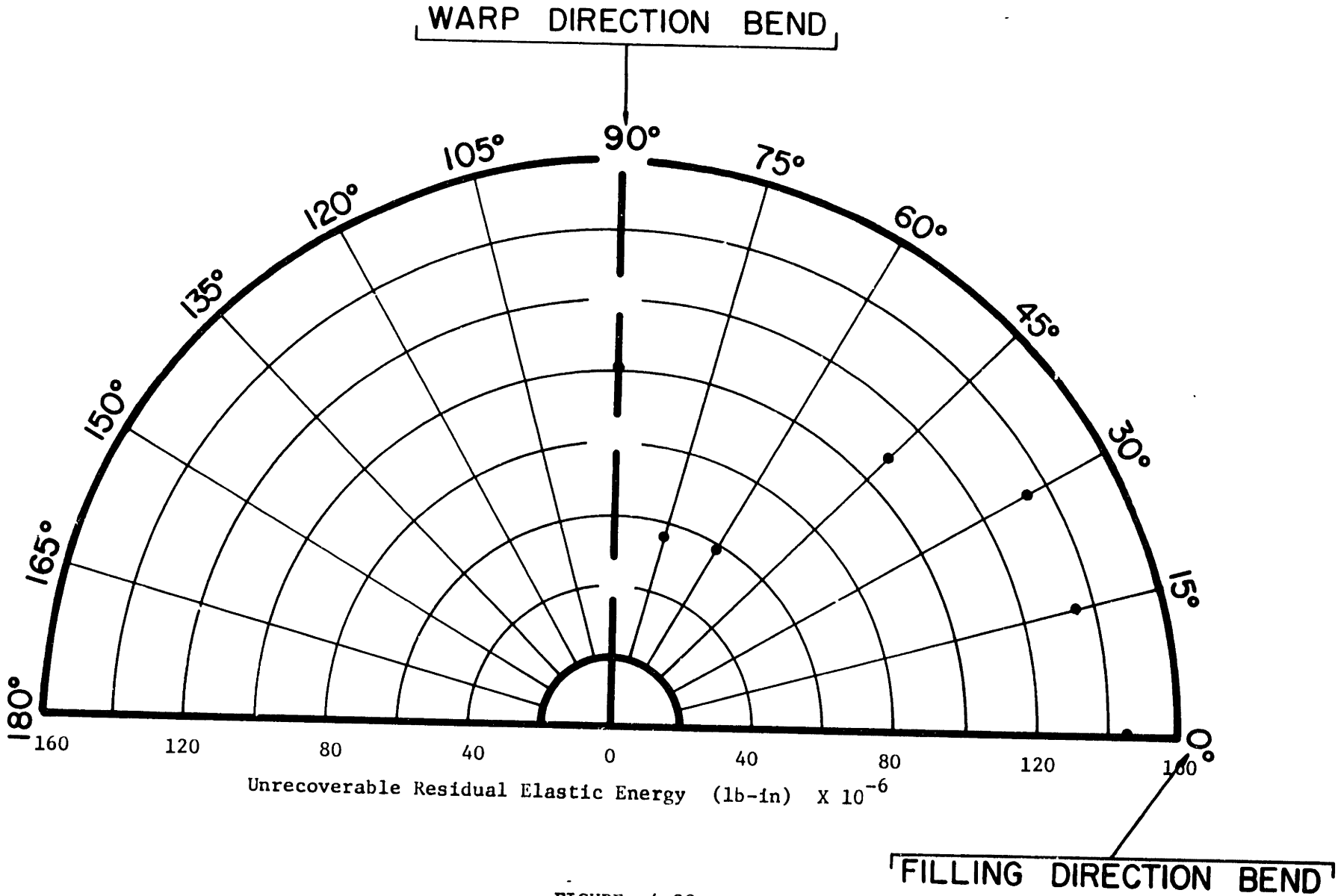

FIGURE 4-28

Directional Properties in Unrecoverable Residual Elastic Energy of Nylon-Fabric (N-1)

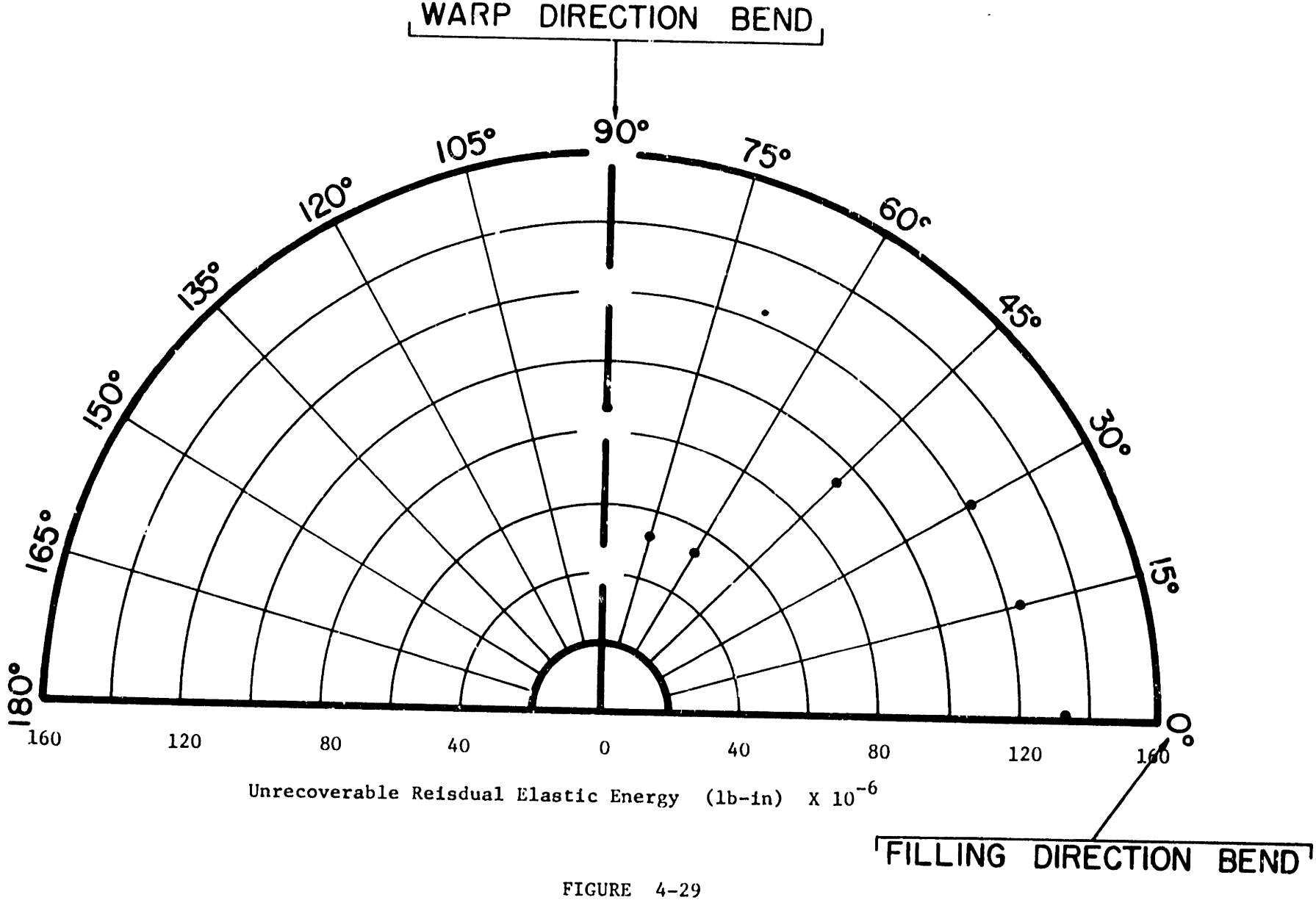

FIGURE 4-29

Directional Properties in Unrecoverable Residual Elastic Energy of Nylon-Fabric (N-2)

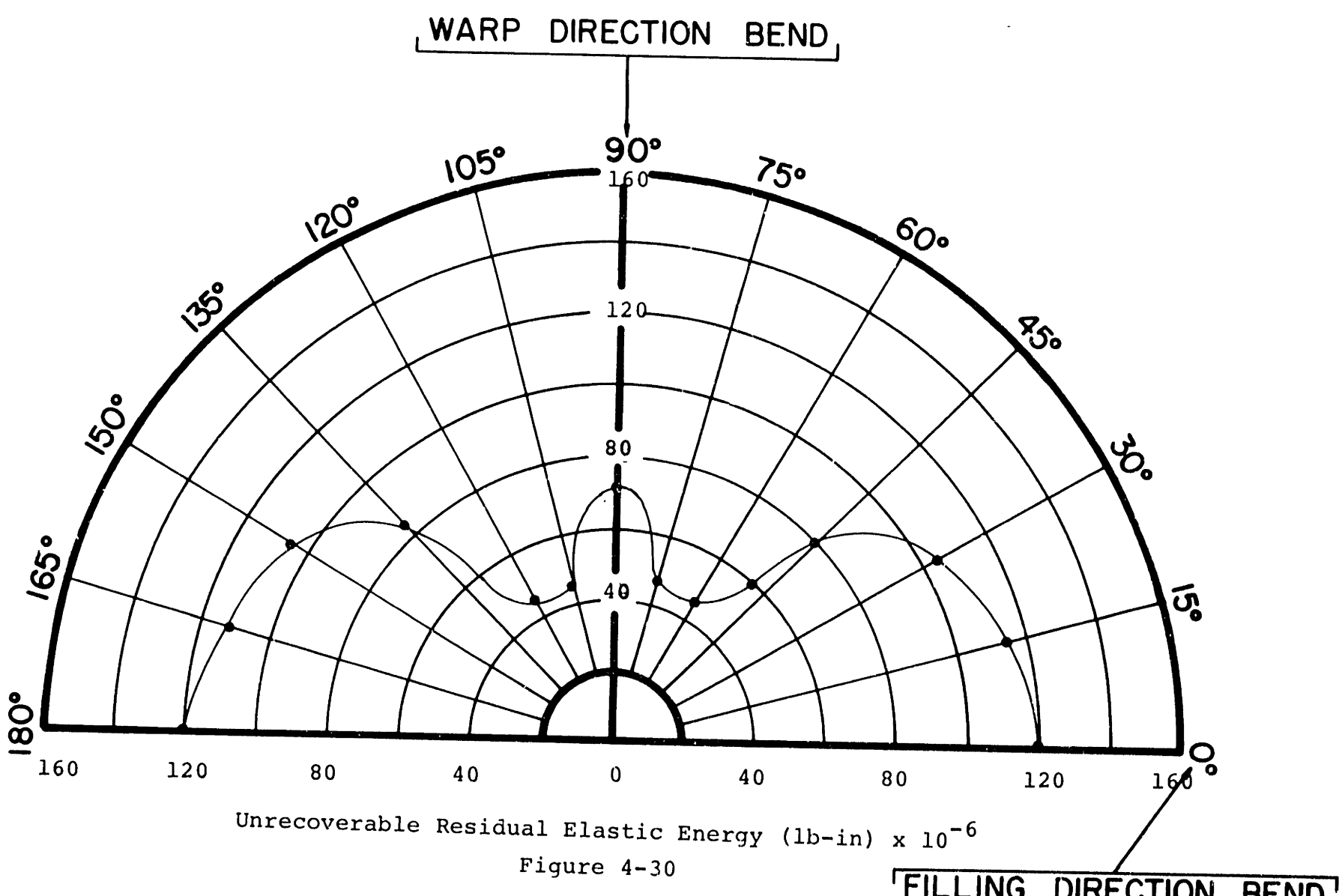

Unrecoverable Residual Elastic Energy (lb-in) x 10^{-6}

Figure 4-30

Directional Properties in Unrecoverable Residual Elastic Energy of Nylon-Fabric (N-3)

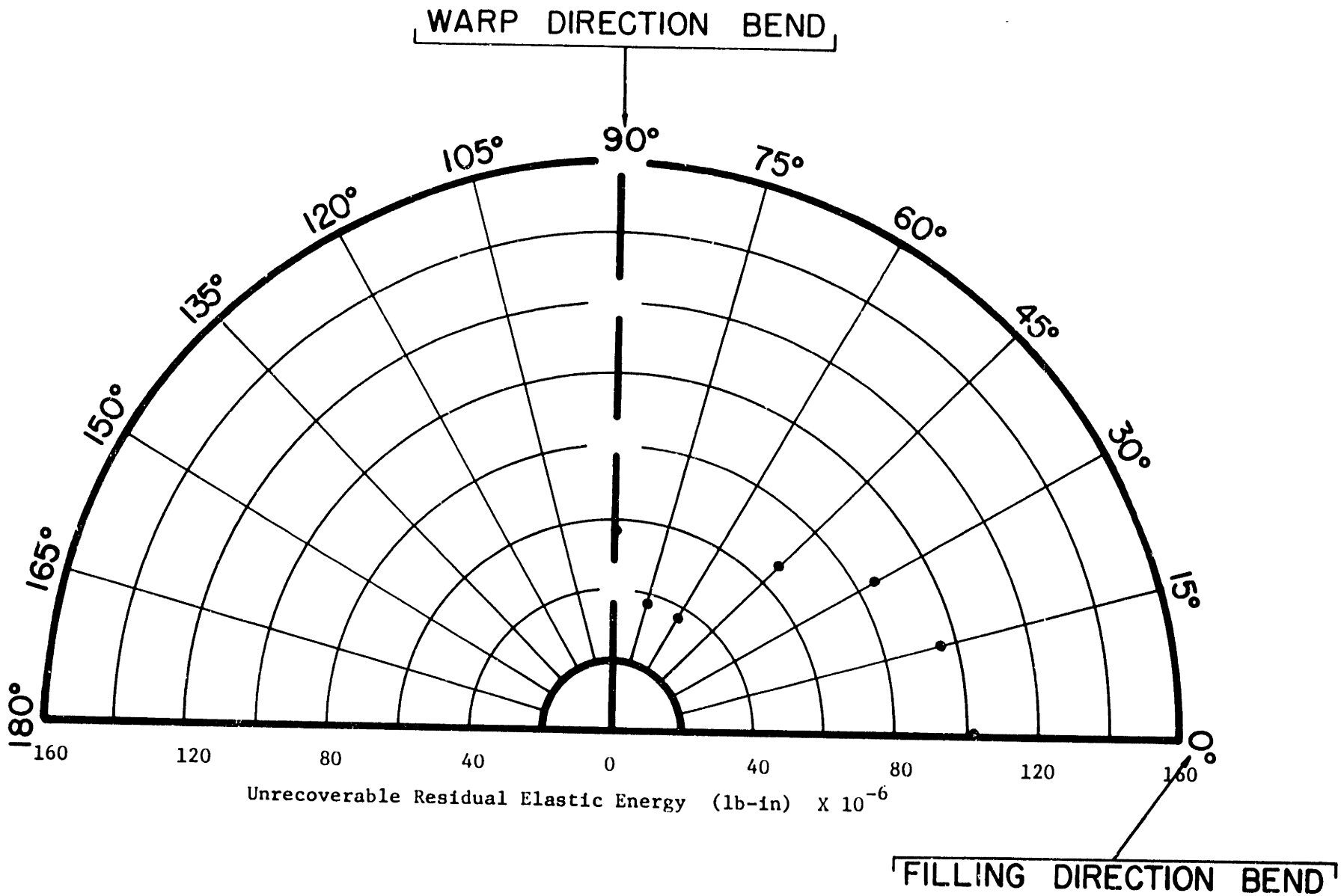

FIGURE 4-31

Directional Properties in Unrecoverable Residual Elastic Energy of Nylon-Fabric (N-4)

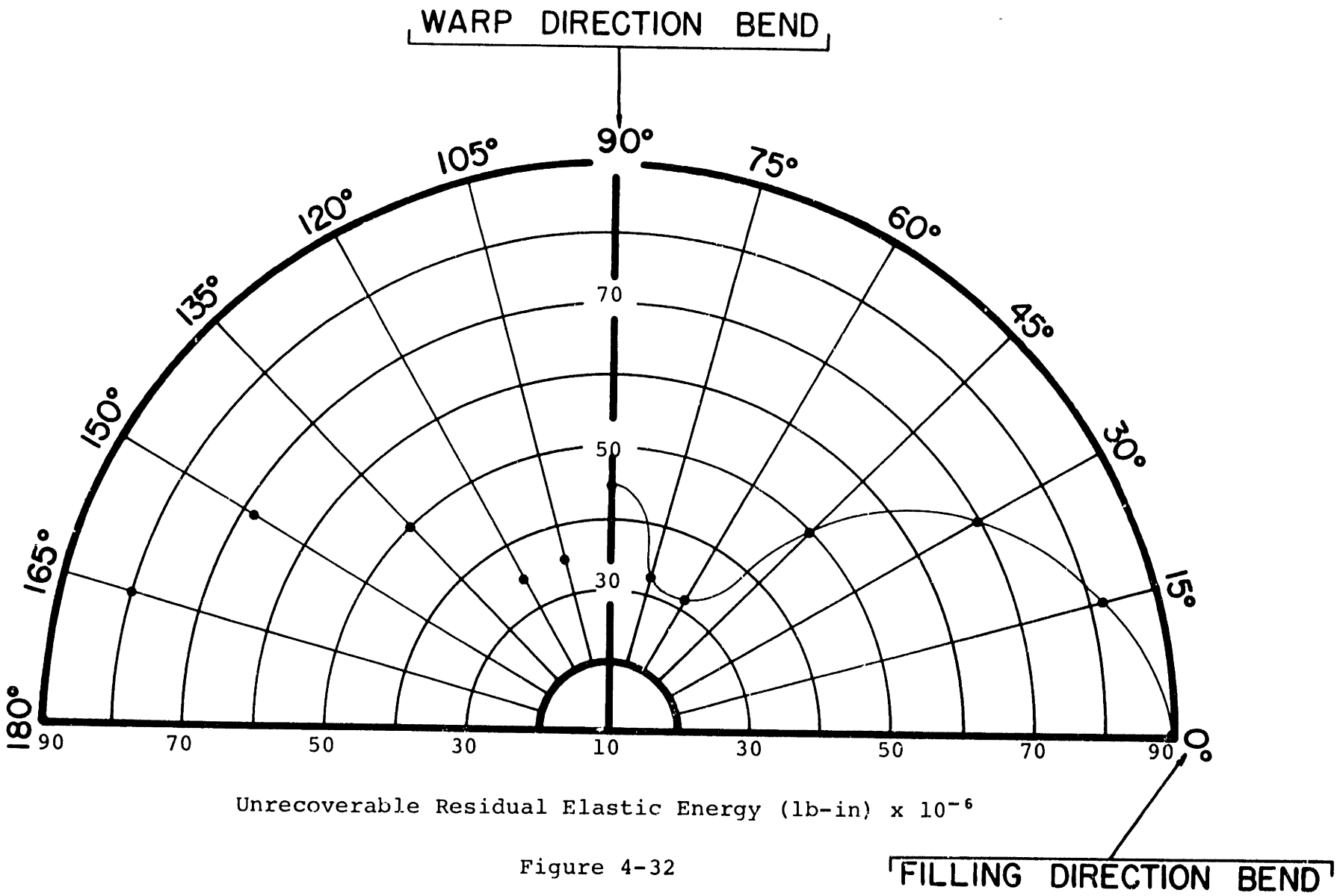

Figure 4-32

Directional Properties in Unrecoverable Residual Elastic Energy of Nylon-fabric (N-5)

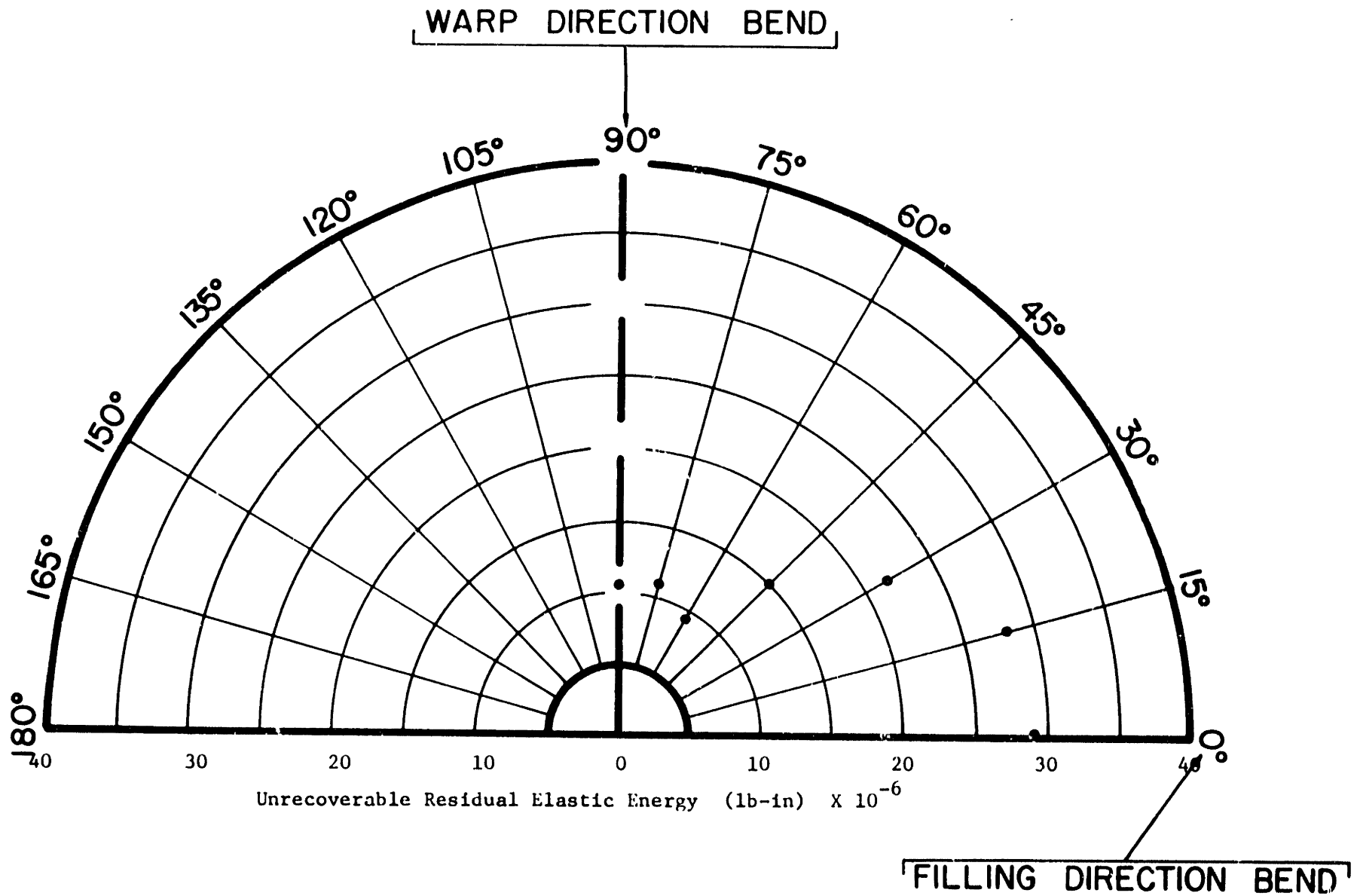

FIGURE 4-33

Directional Properties in Unrecoverable Residual Elastic Energy of Nylo-Fabric (N-6)

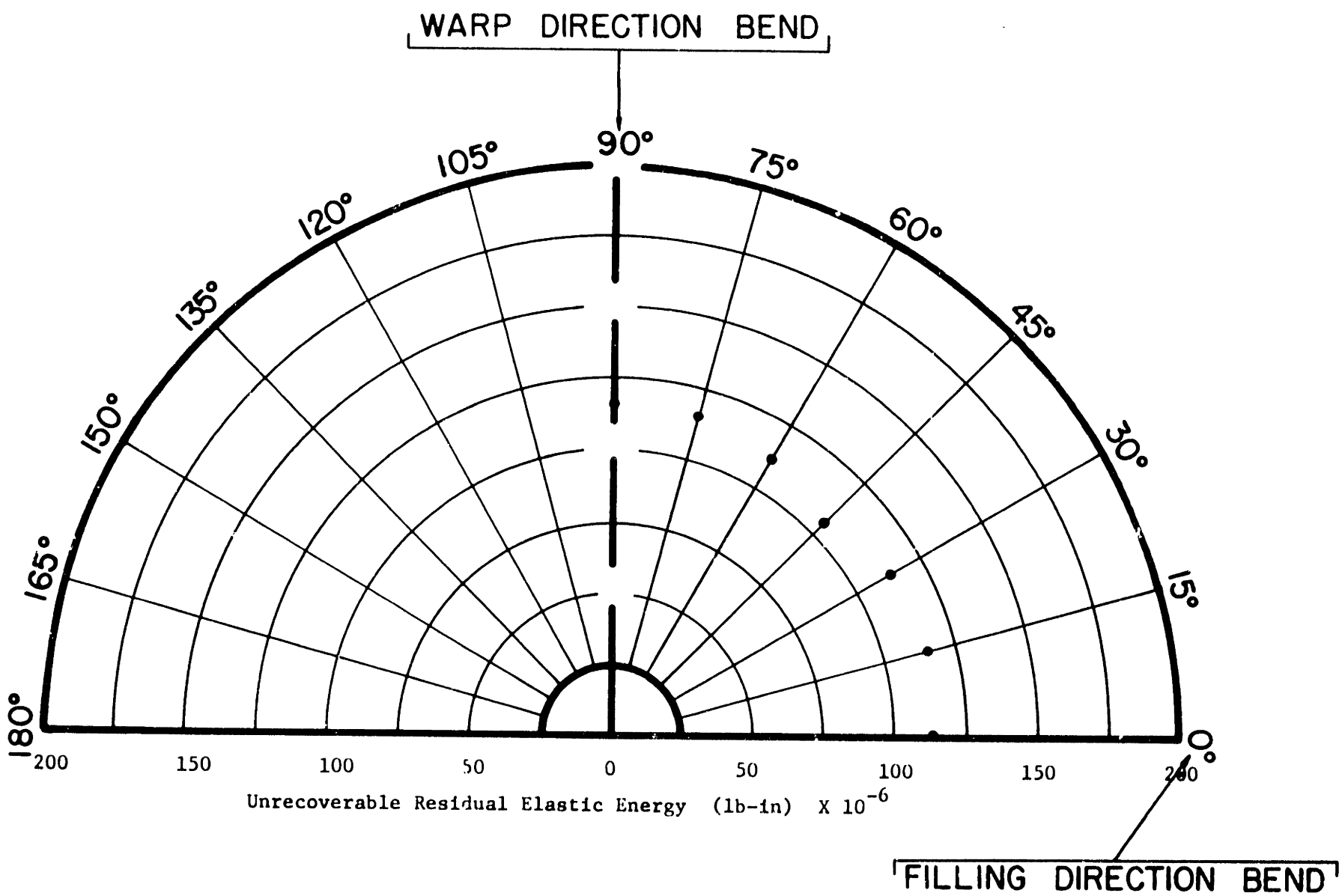

FIGURE 4-34

Directional Properties in Unrecoverable Residual Elastic Energy of Cotton-Fabric(dimensionally-balanced) (C-1)

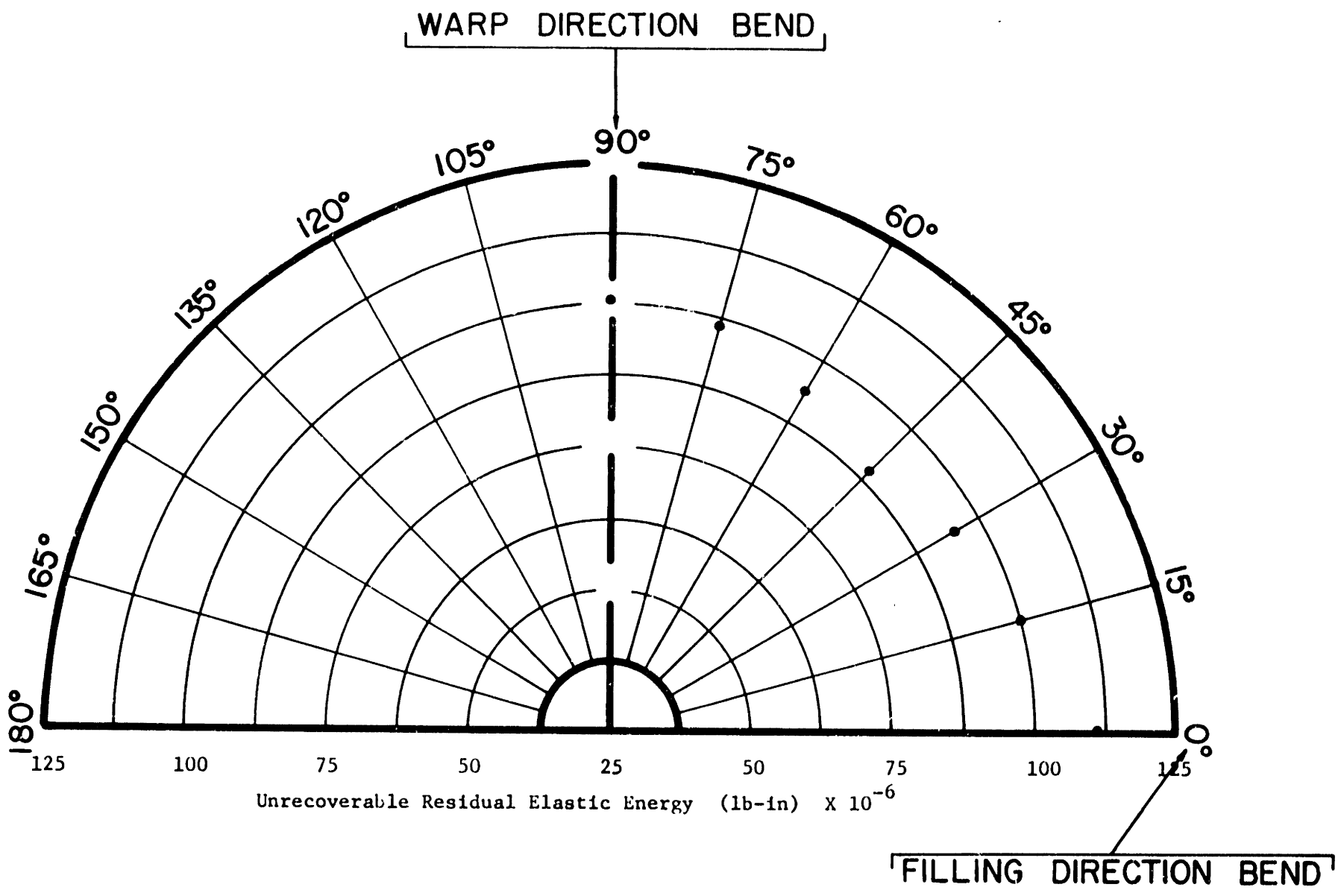

FIGURE 4-35

Directional Properties in Unrecoverable Residual Elastic Energy of Cotton-Fabric (C-2)

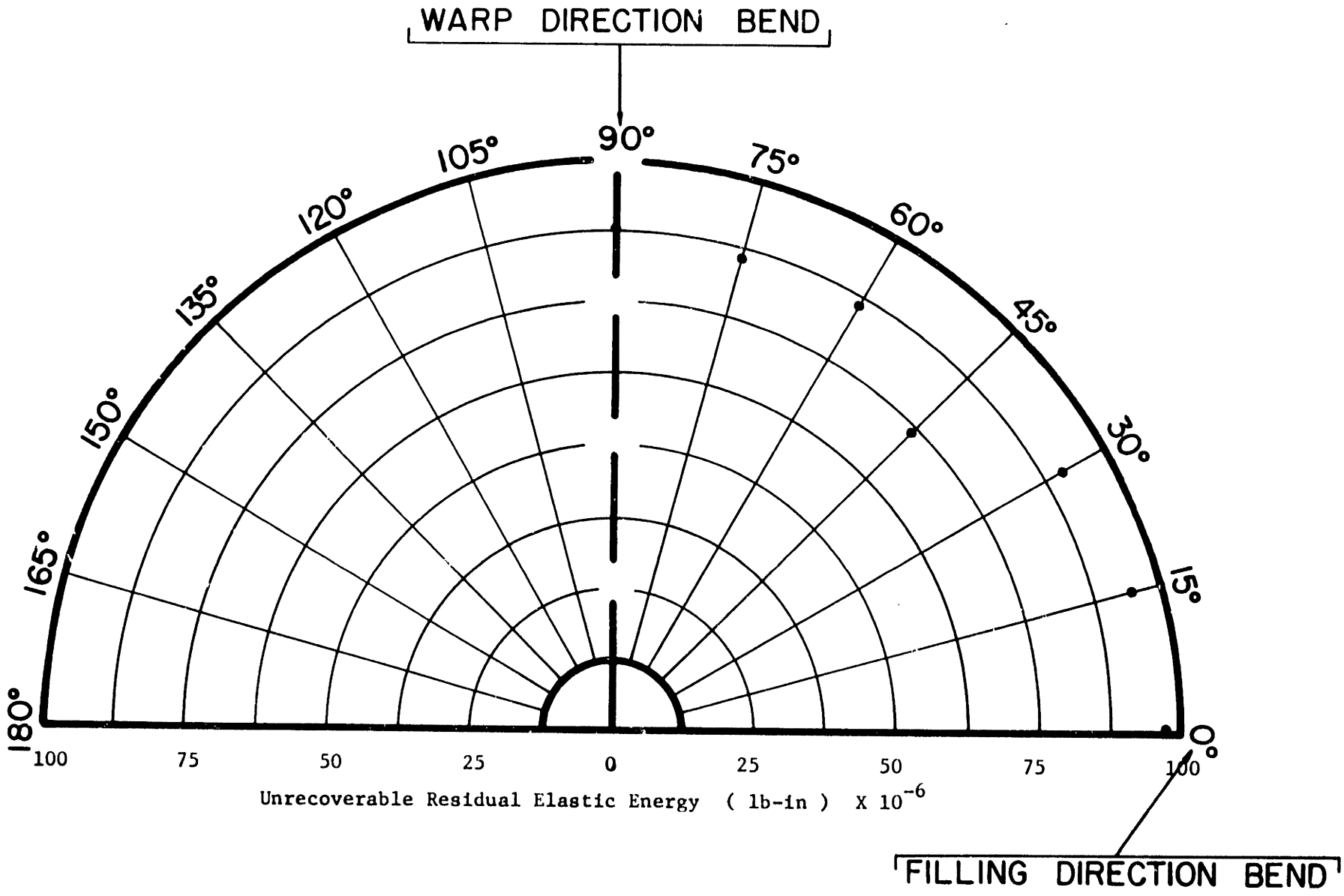

FIGURE 4-36

Directional Properties in Unrecoverable Residual Elastic Energy of Cotton-Fabric (C-3)

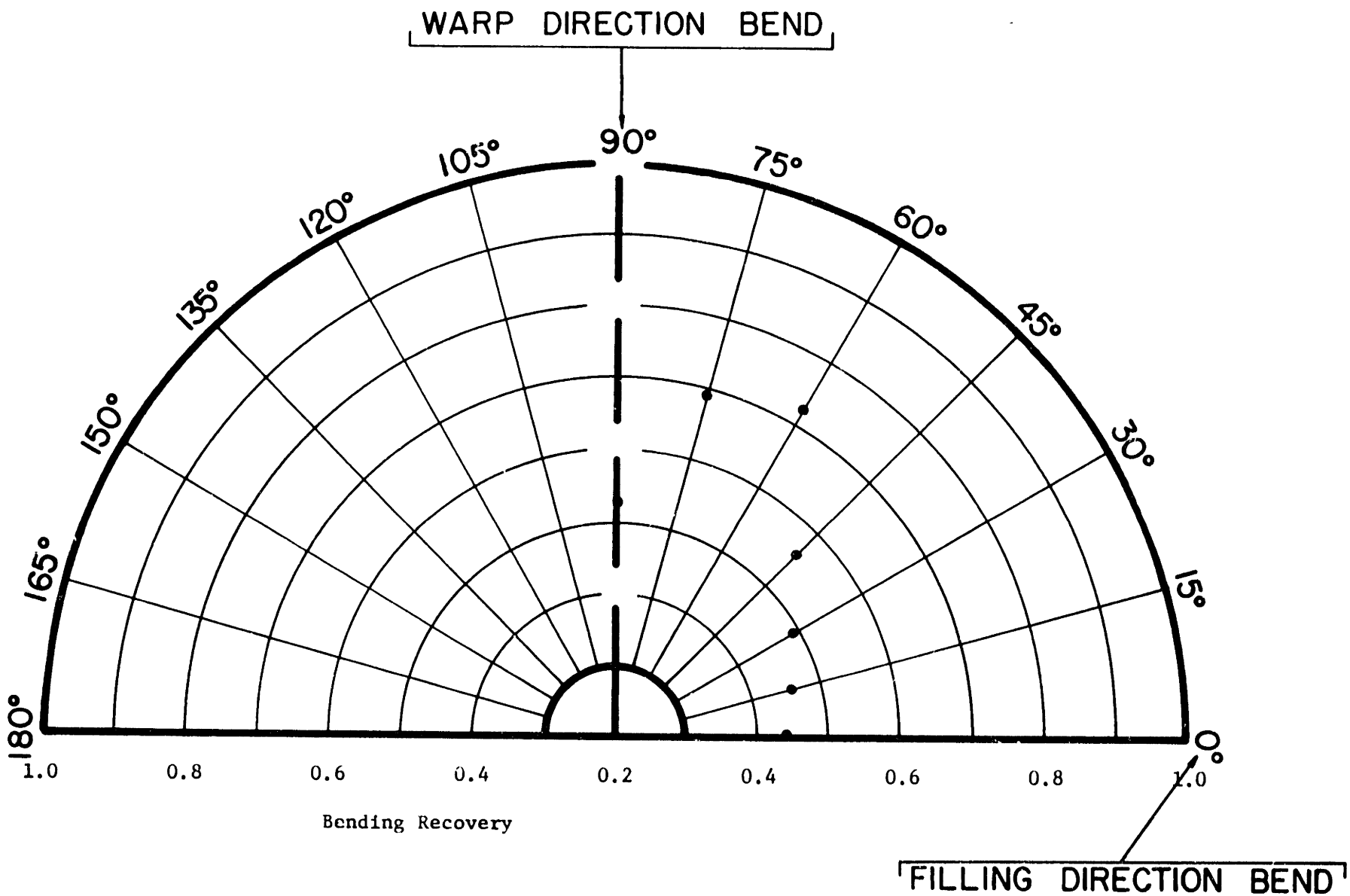

FIGURE 4-37

Directional Properties in Bending Recovery of Nylon-Fabric (N-1)

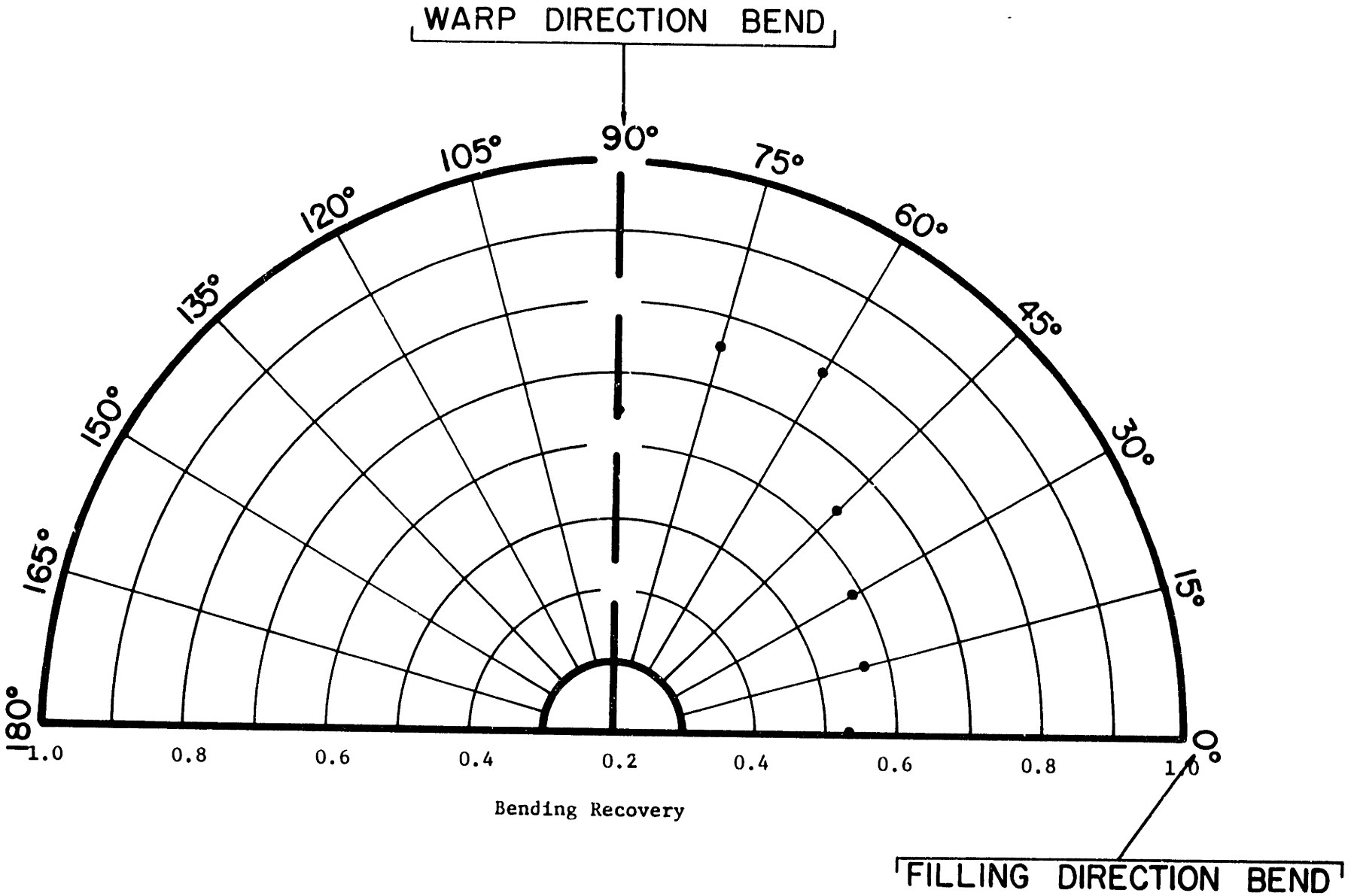

FIGURE 4-38

Directional Properties in Bending Recovery of Nylon-Fabric (N-2)

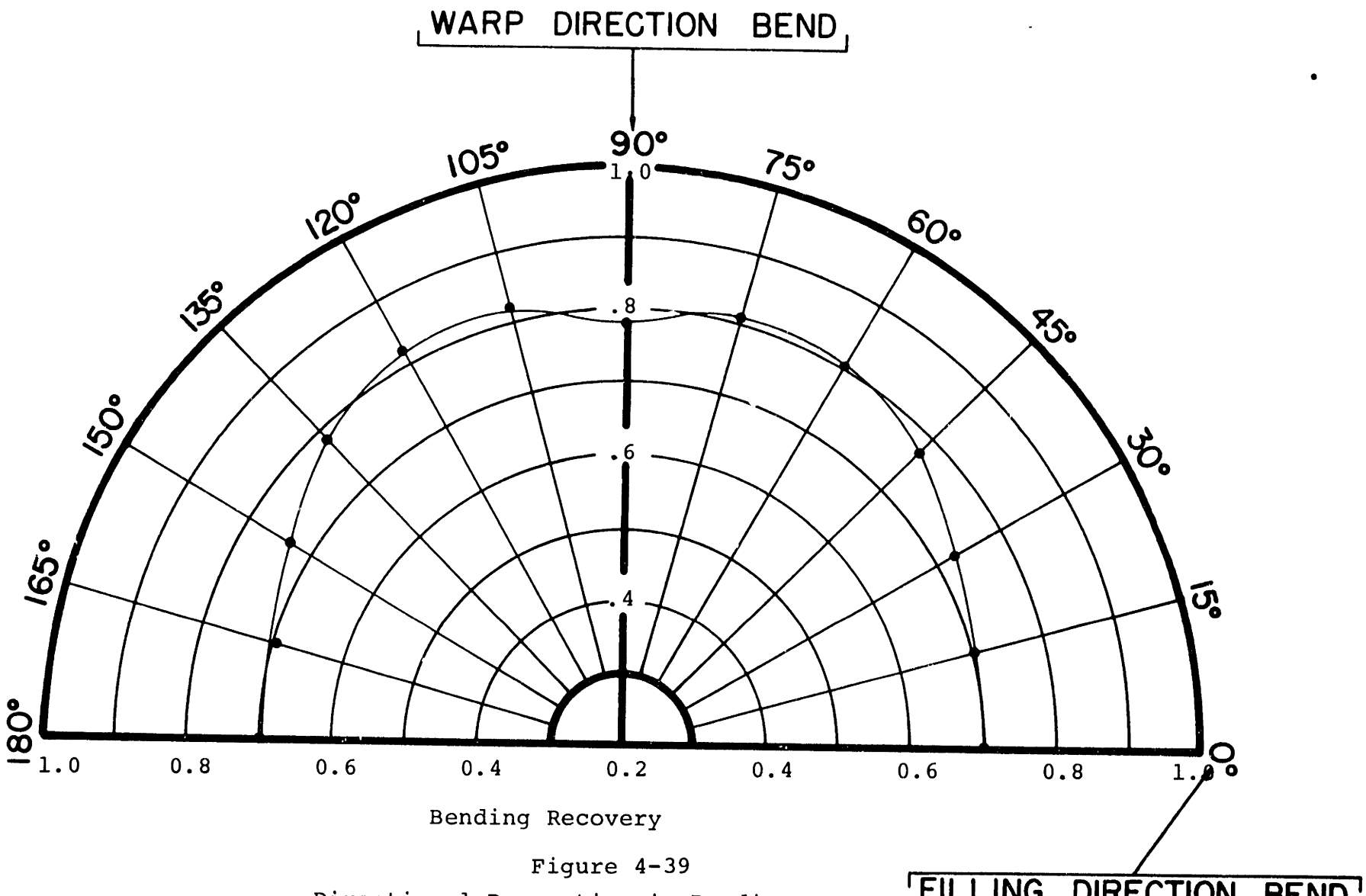

Figure 4-39
Directional Properties in Bending Recovery
of Nylon-Fabric (N-3)

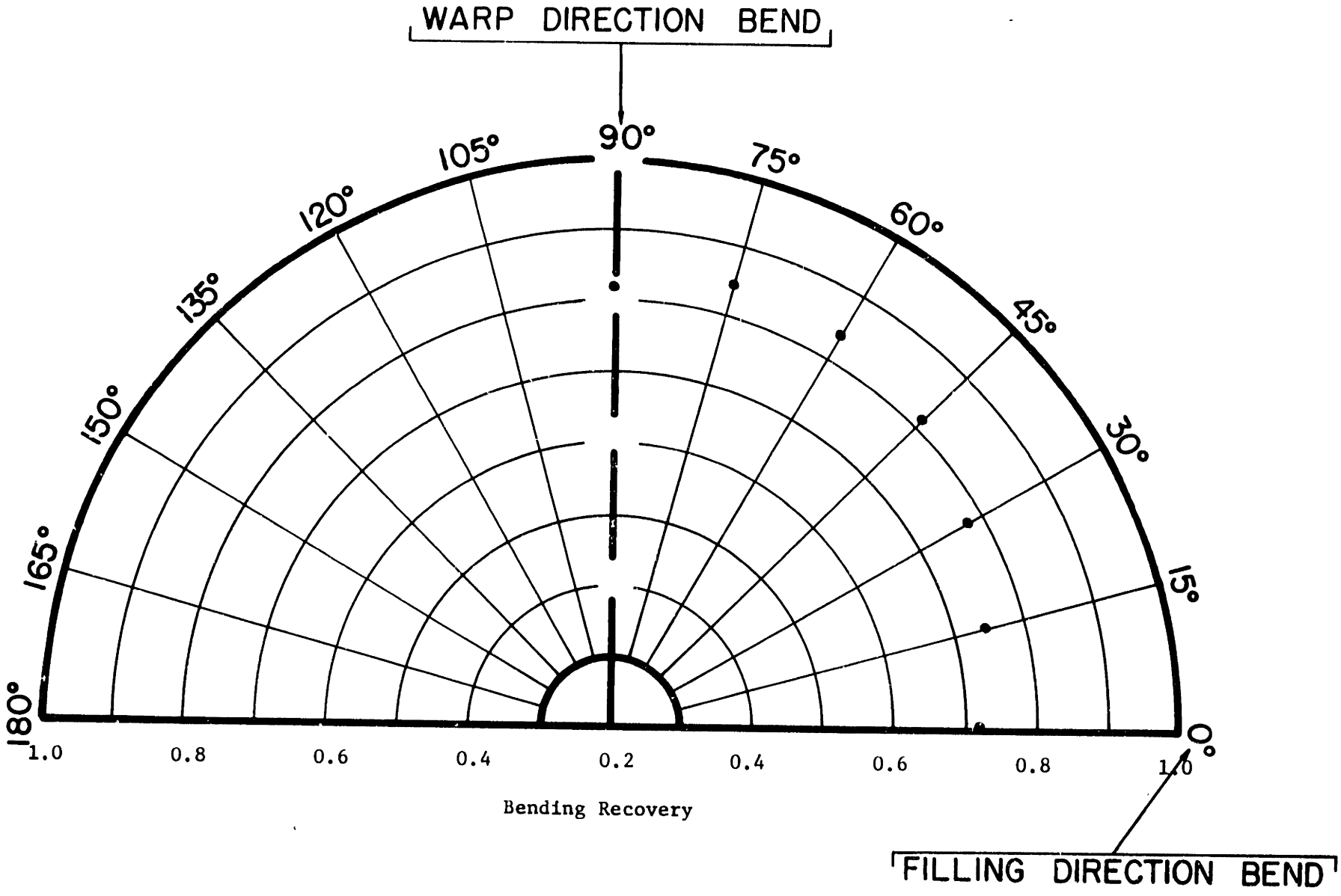

FIGURE 4-40

Directional Properties in Bending Recovery of Nylon-Fabric (N-4)

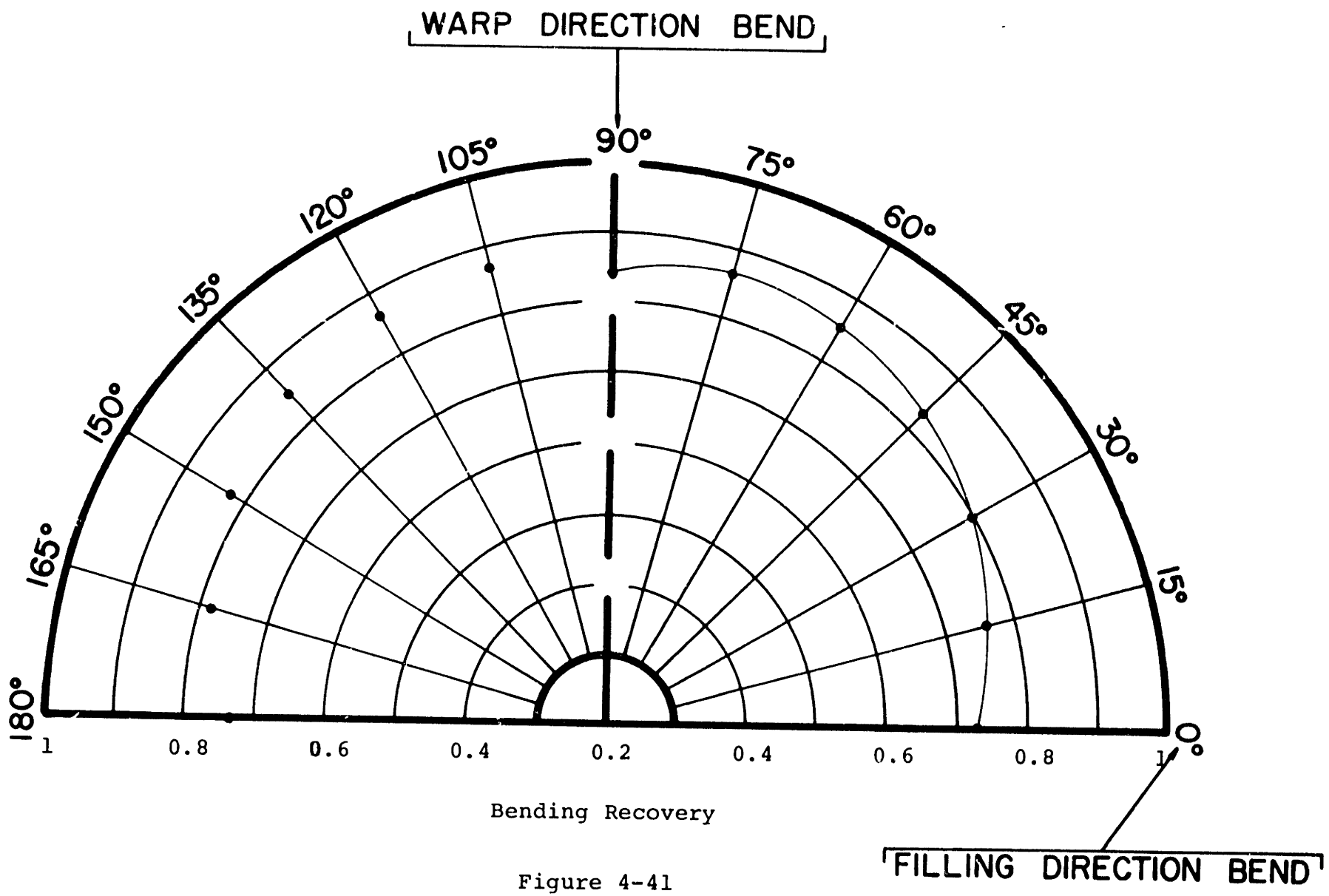

Figure 4-41
Directional Properties in Bending Recovery of Nylon-Fabric (N-5)

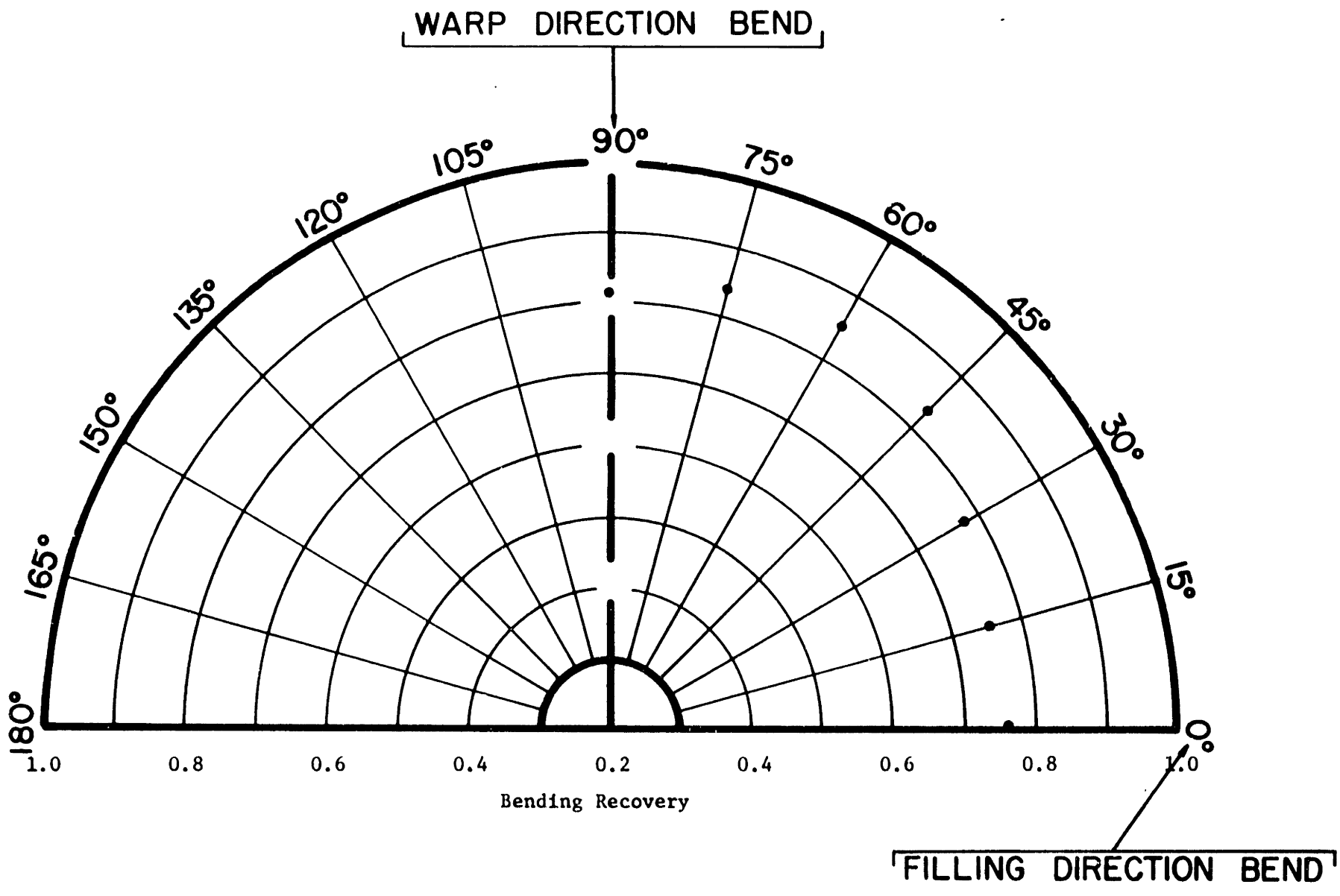

FIGURE 4-42

Directional Properties in Bending Recovery of Nylon-Fabric (N-6)

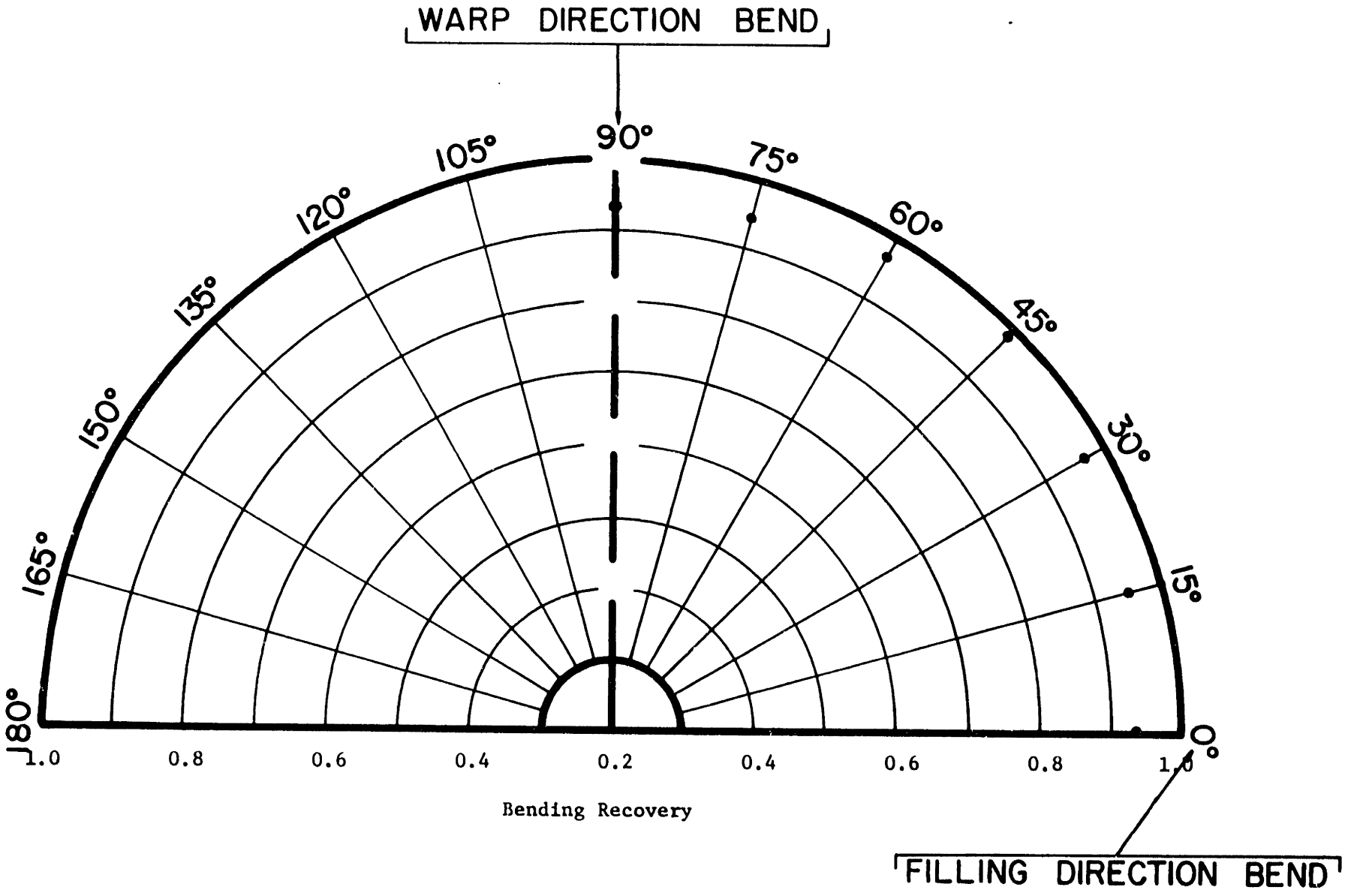

FIGURE 4-43

Directional Properties in Bending Recovery of Cotton-Fabric(dimensionally-

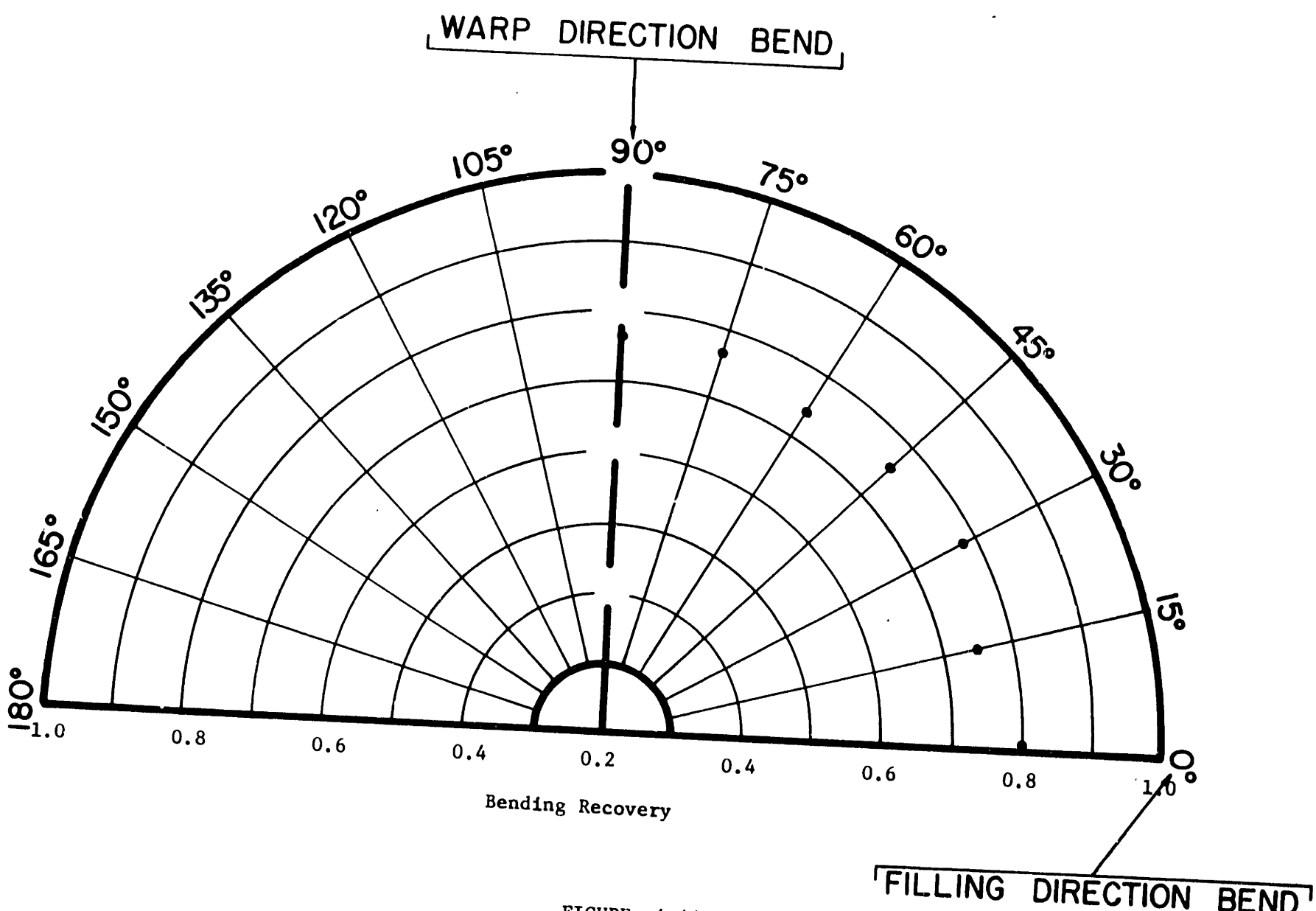

FIGURE 4-44

Directional Properties in Bending Recovery of Cotton-Fabric (C-2)

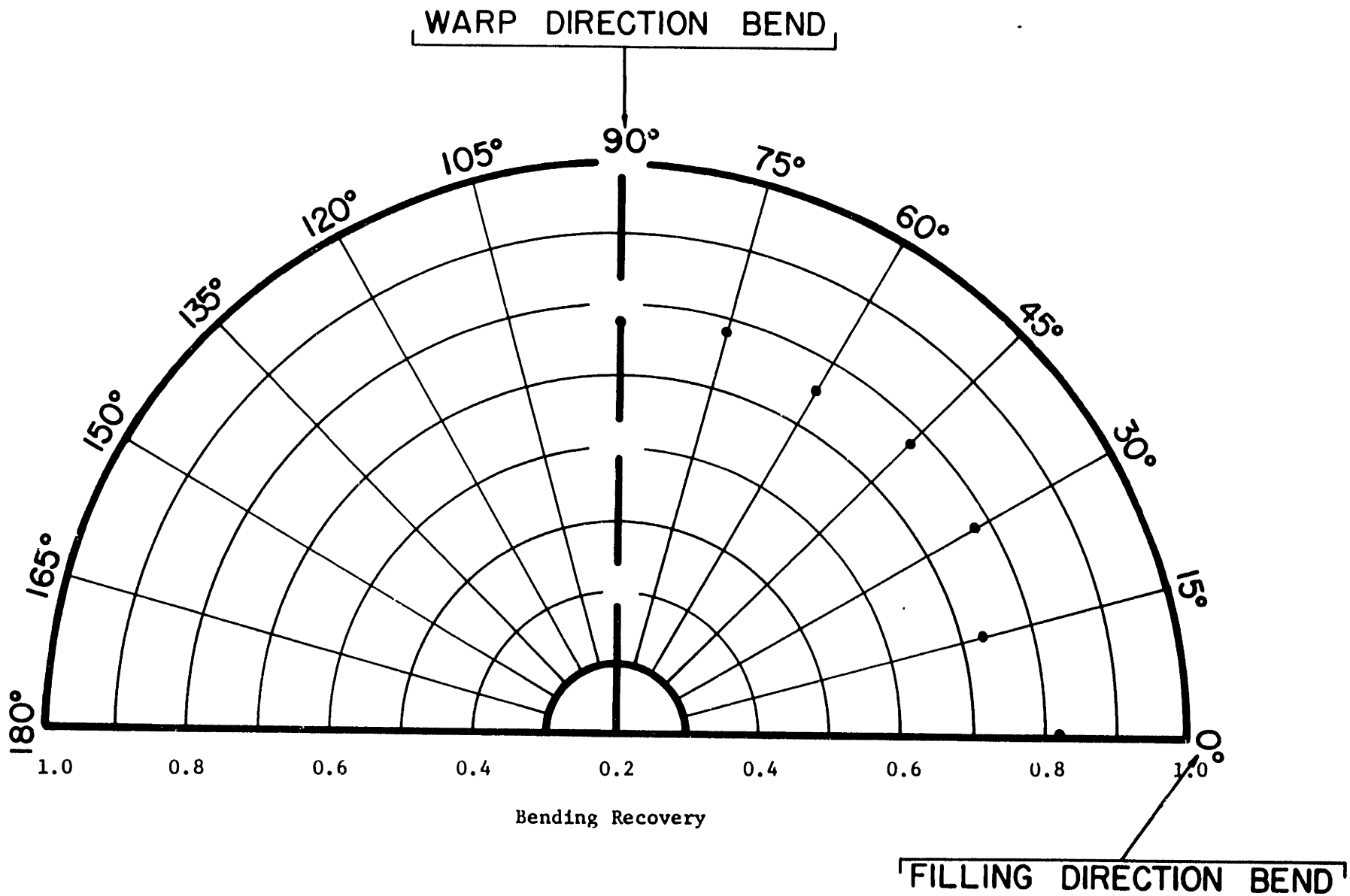

FIGURE 4-45

Directional Properties in Bending Recovery of Cotton-Fabric (C-3)

that, based on equation (2.23), we could say that the hysteresis loop represents the sum of the total energy loss in frictional effects and the unrecoverable residual elastic energy of the fibers. This residual elastic energy could certainly be activated and assisted by methods such as vibrations[1] in overcoming the frictional forces. The experimental data derived through use of equation (2.23) is shown on Figures 4-10 to 4-36 for all the nine fabrics examined.

From the experimental investigation a definite relationship has been observed between the unrecoverable residual elastic energy and the bending recoverability of the fabric.

For the plain-weave, multifilament nylon fabrics, the nimimum residual elastic energy occurs around 60° orientation of bias bend when the bending recovery is maximum; and for plain-weave cotton fabrics, the residual elastic energy minima occur at an angle of 45° orientation when the bending recovery is the best.

4. Bending Behavior as a Function of Structural Variables.

Considering only the case of frictional losses due to fiber-to-fiber motion during fabric bending, we may apply equations (2.12), (2.6), and (2.7) directly for the experimental series of nylon fabrics. Equation (2.6) must be multiplied by N_1 (warp per inch) and (2.7) by N_2 (filling per inch) to give a measure of frictional loss per sample 1/2" x 1" or 1/2 square inch. Noting that both warp and filling yarns are 400 denier, but that the warp has 68 filaments vs. the filling 136 filaments, we can substitute $N_{f_2} = 2\,N_{f_1}$ to give

$$U'_{F(total)} = (\text{constant})\left[\sqrt{\frac{C_1}{p_2^2}}\cdot N_1 \sin^2\alpha + \sqrt{\frac{C_2}{p_1^2}}\cdot\frac{N_2}{2}\cos^2\alpha\right] \qquad (4.1)$$

The latter term, a structural variable, is in effect a measure of fabric tightness.

To determine the validity of the above equation, measured values of total friction work losses for nylon series are plotted on Figures (4-46) to (4-49) as functions of the structural variable. Equation (4.1) predicts a linear relation. It is clearly seen that the measured values of friction increase with structural tightness. The agreement is good at all angles of bending.

To express equation (2.1) in more convenient terms

$$(E\cdot I)_{yF_1} = (E\cdot I)_{y_1}\,\frac{p_2}{(S_t - S_r)} \qquad (4.2)$$

Figure 4-46

Total Frictional Work Loss vs. Structural Parameter

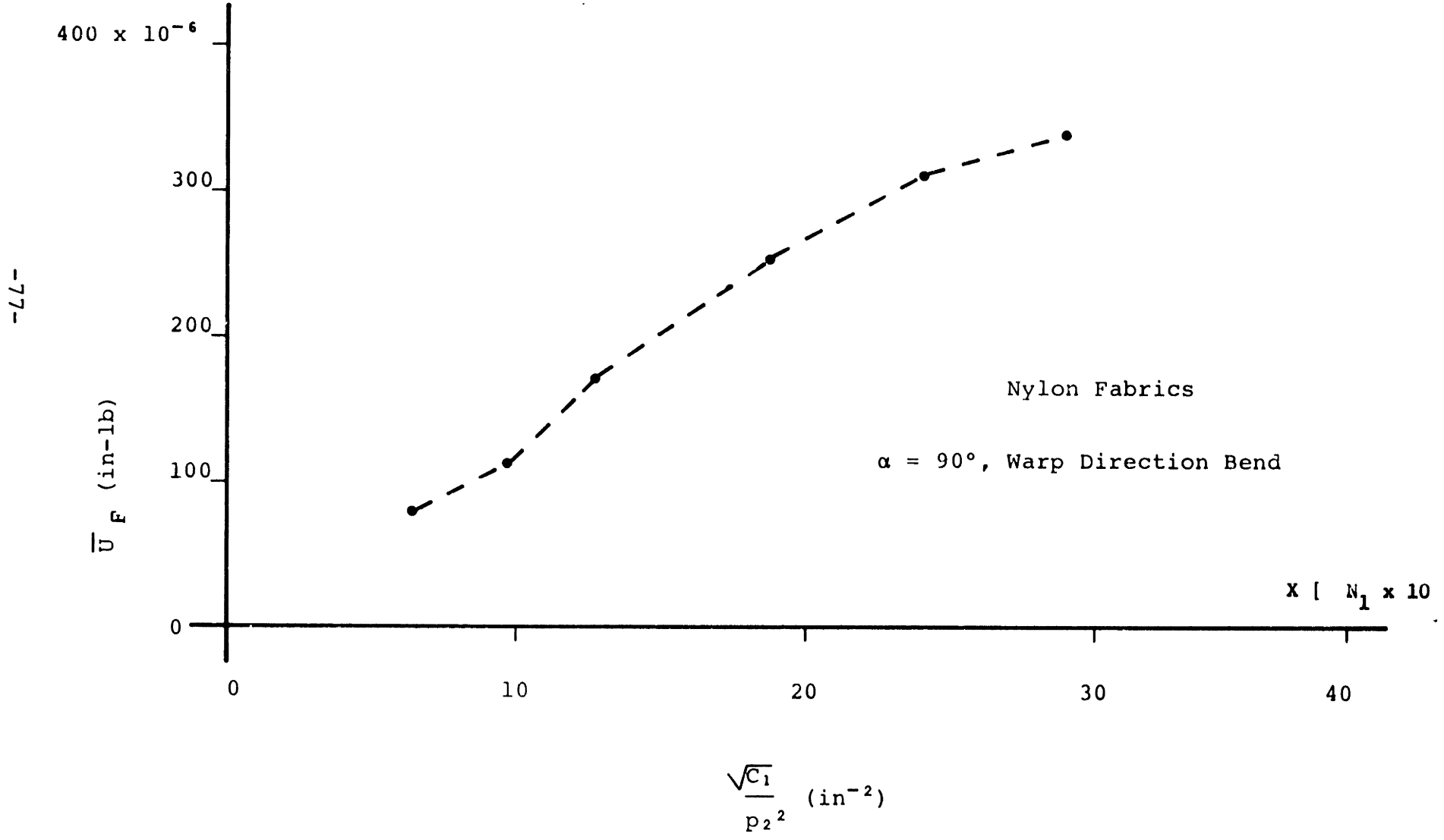

Figure 4-47

Total Frictional Work Loss vs. Structural Parameter

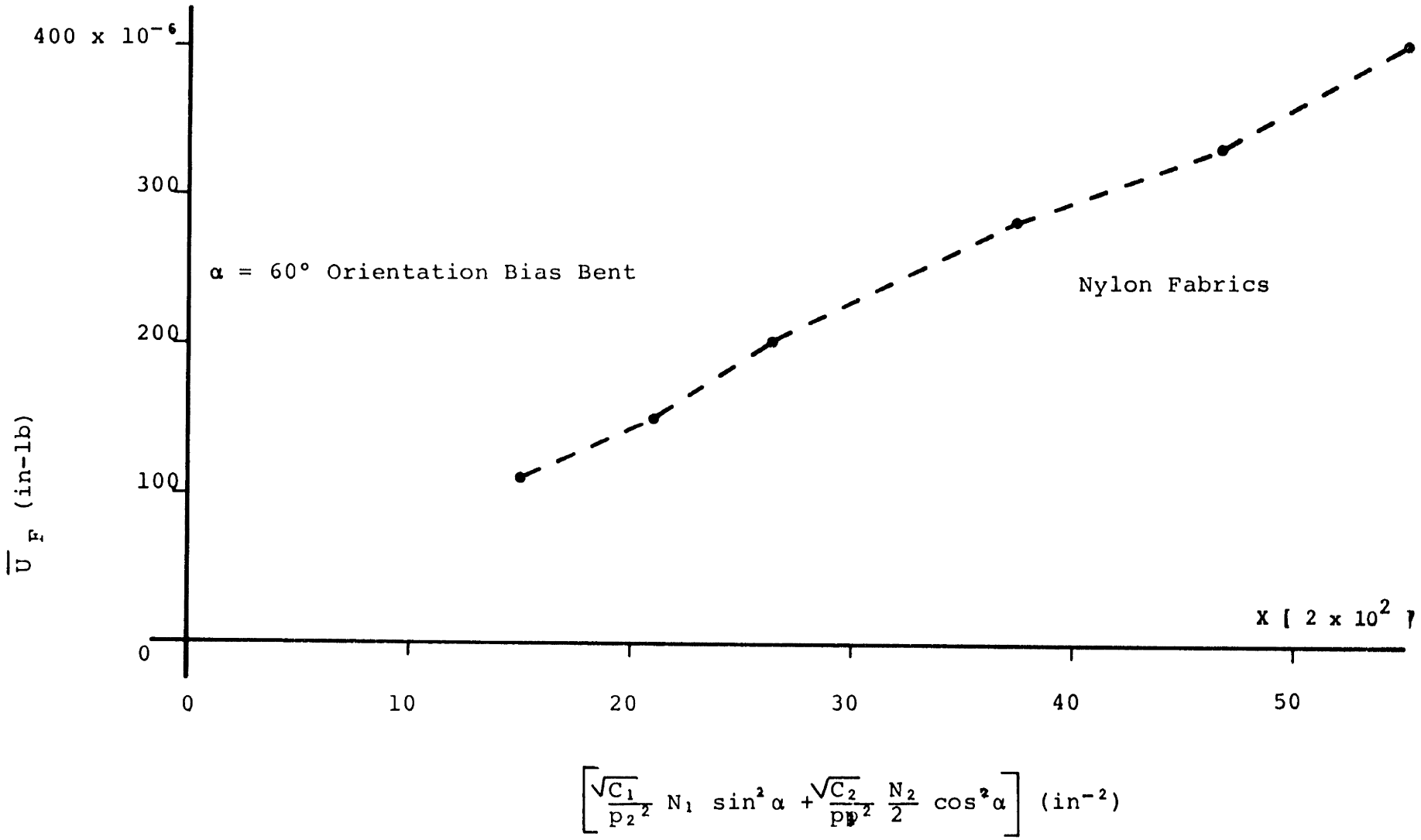

Figure 4-48

Total Frictional Work Loss vs. Structural Parameter

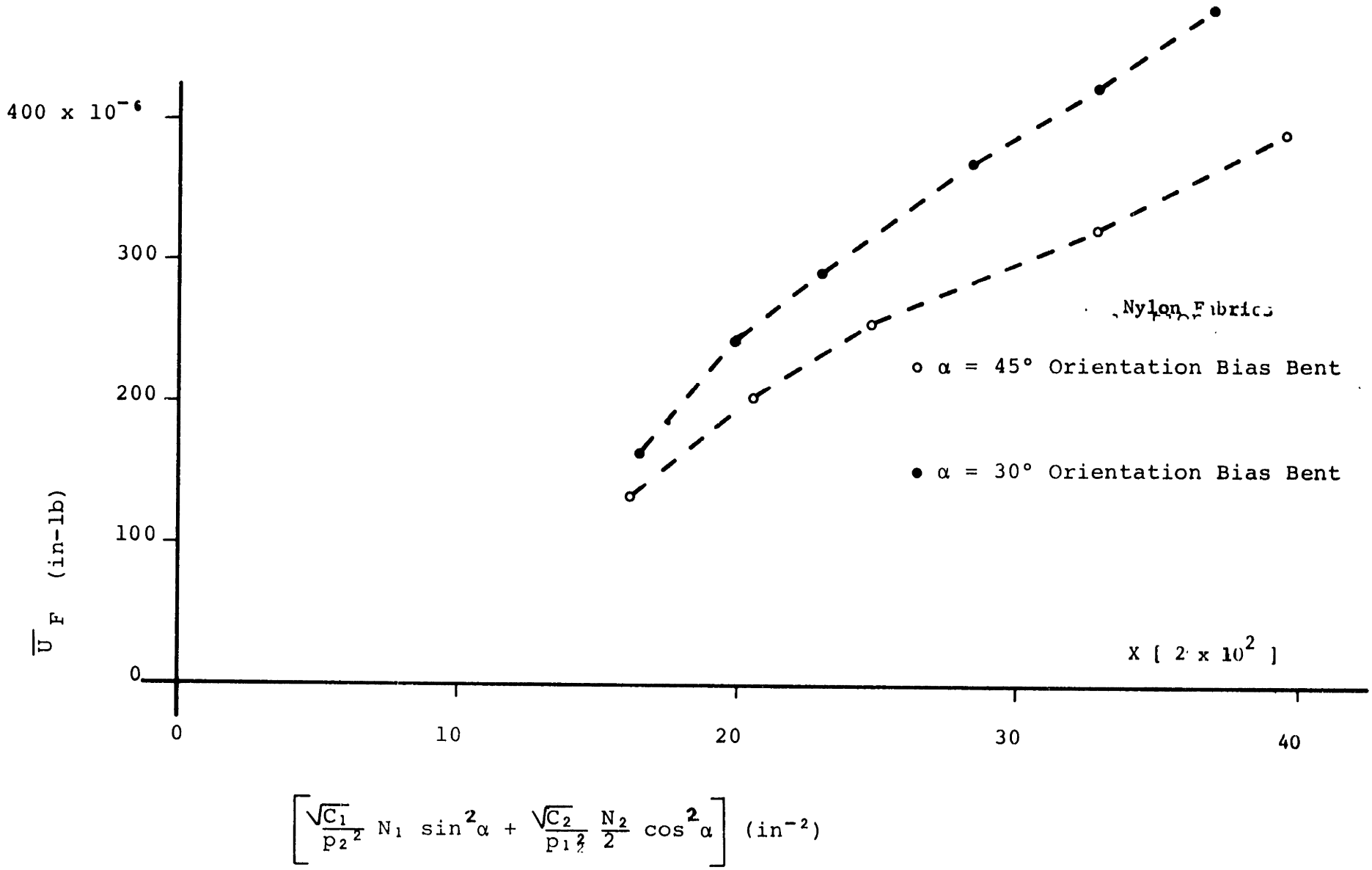

Figure 4-49

Total Frictional Work Loss vs. Structural Parameter

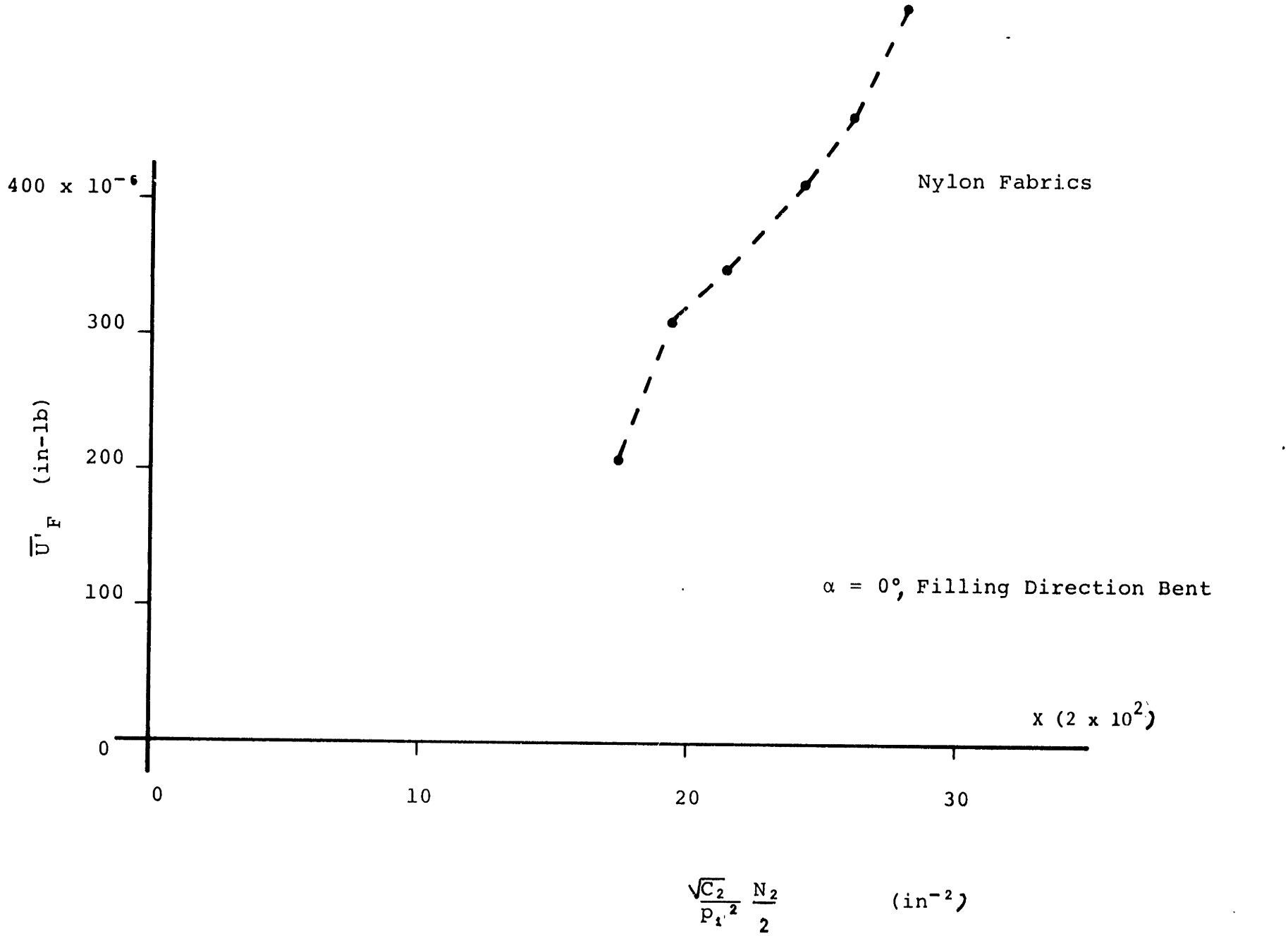

Figure 4-50
Elastic Rigidity vs. Structural Parameter

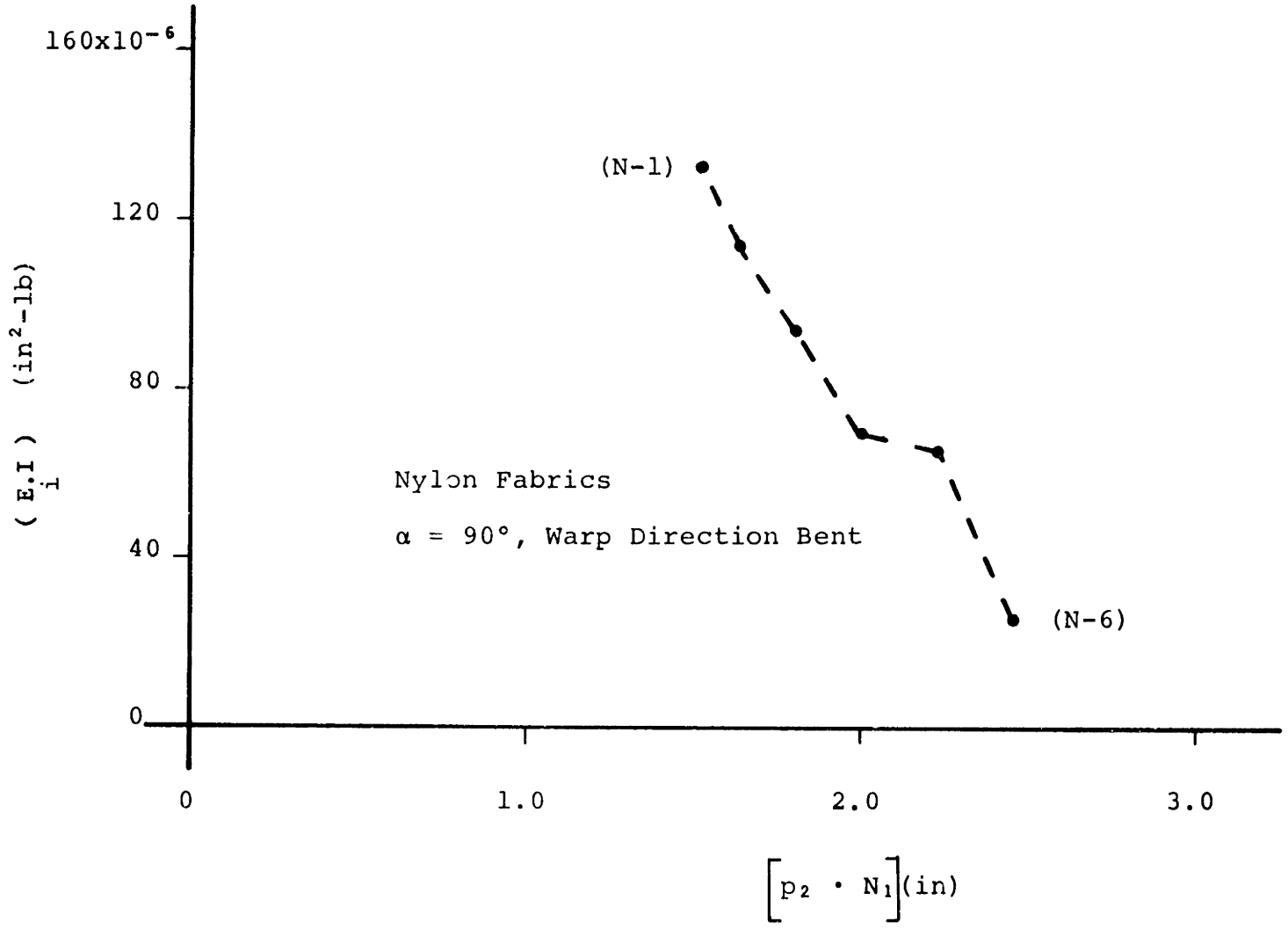

Figure 4-51

Elastic Rigidity vs. Structural Parameter

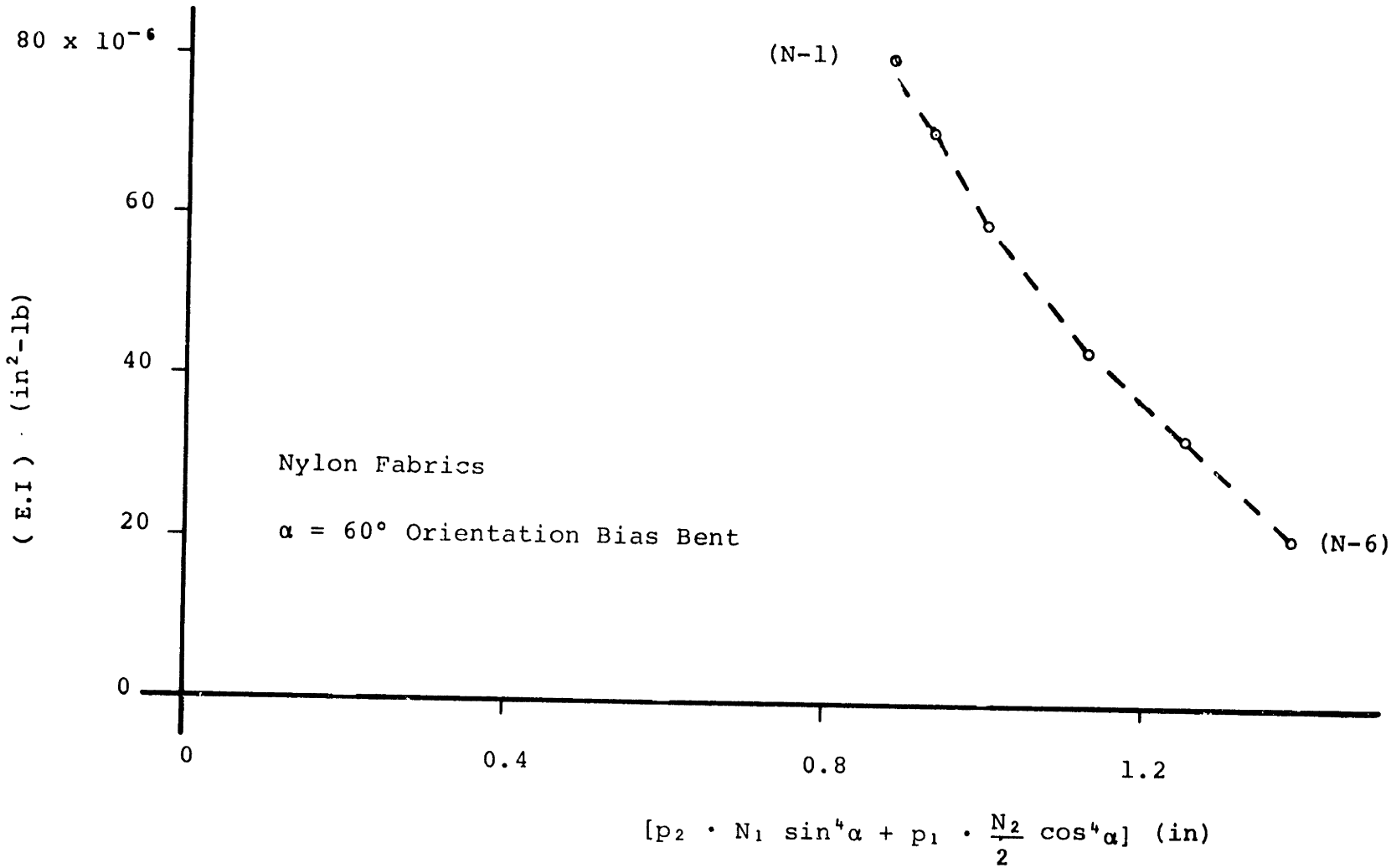

Figure 4-52

Elastic Rigidity vs. Structural Parameter

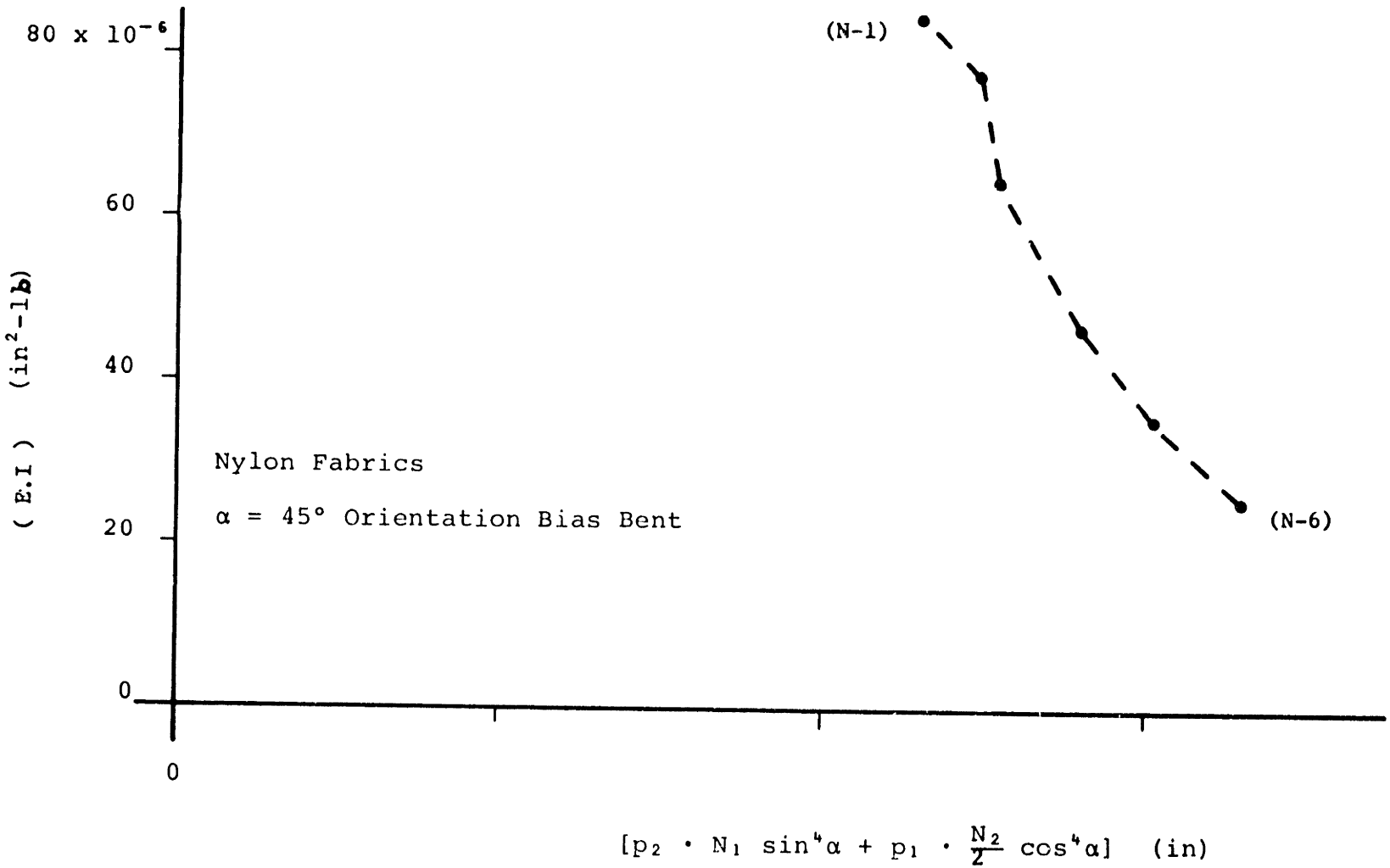

Figure 4-53

Elastic Rigidity vs. Structural Parameter

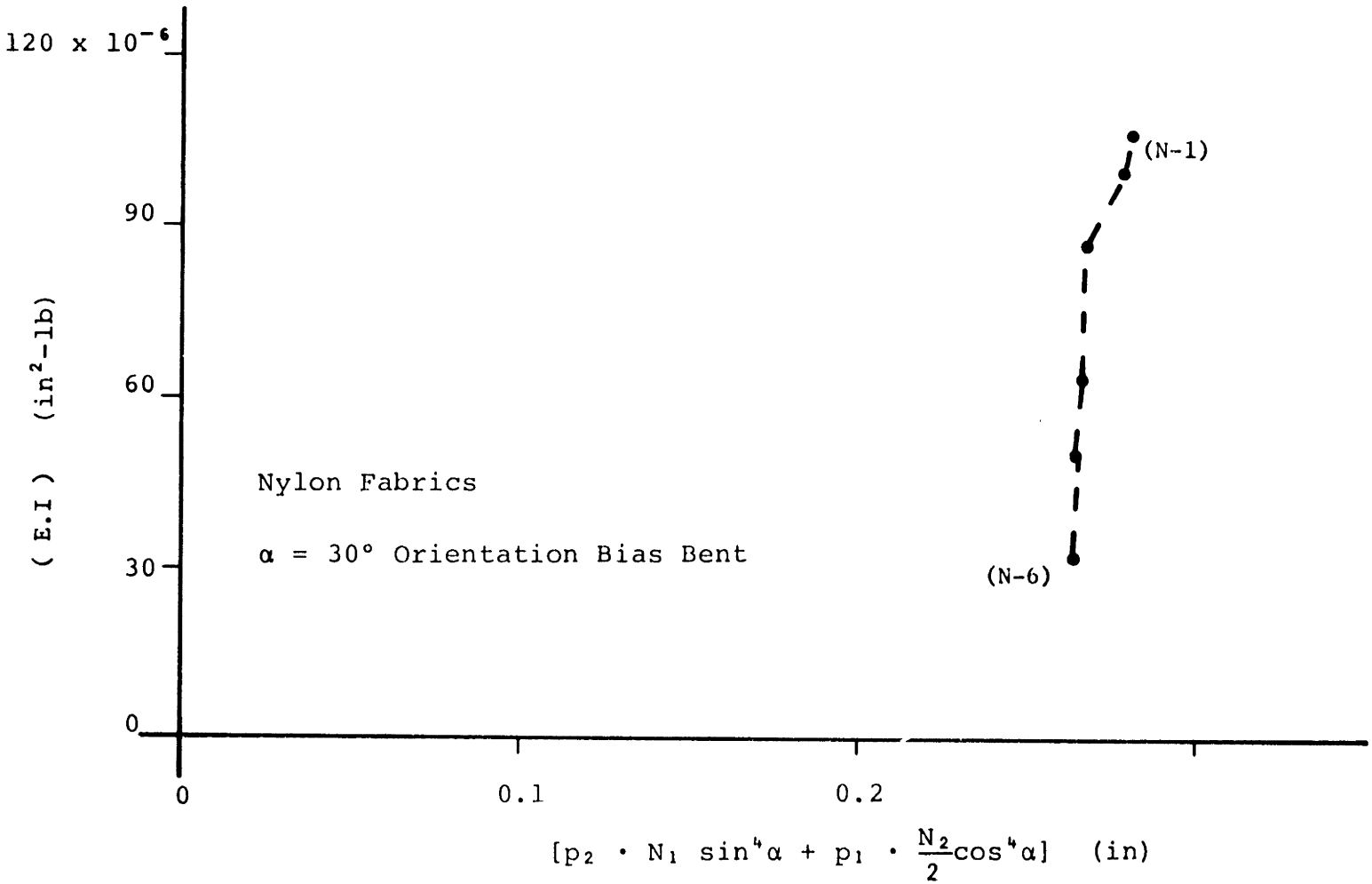

Figure 4-54

Elastic Rigidity vs. Structural Parameter

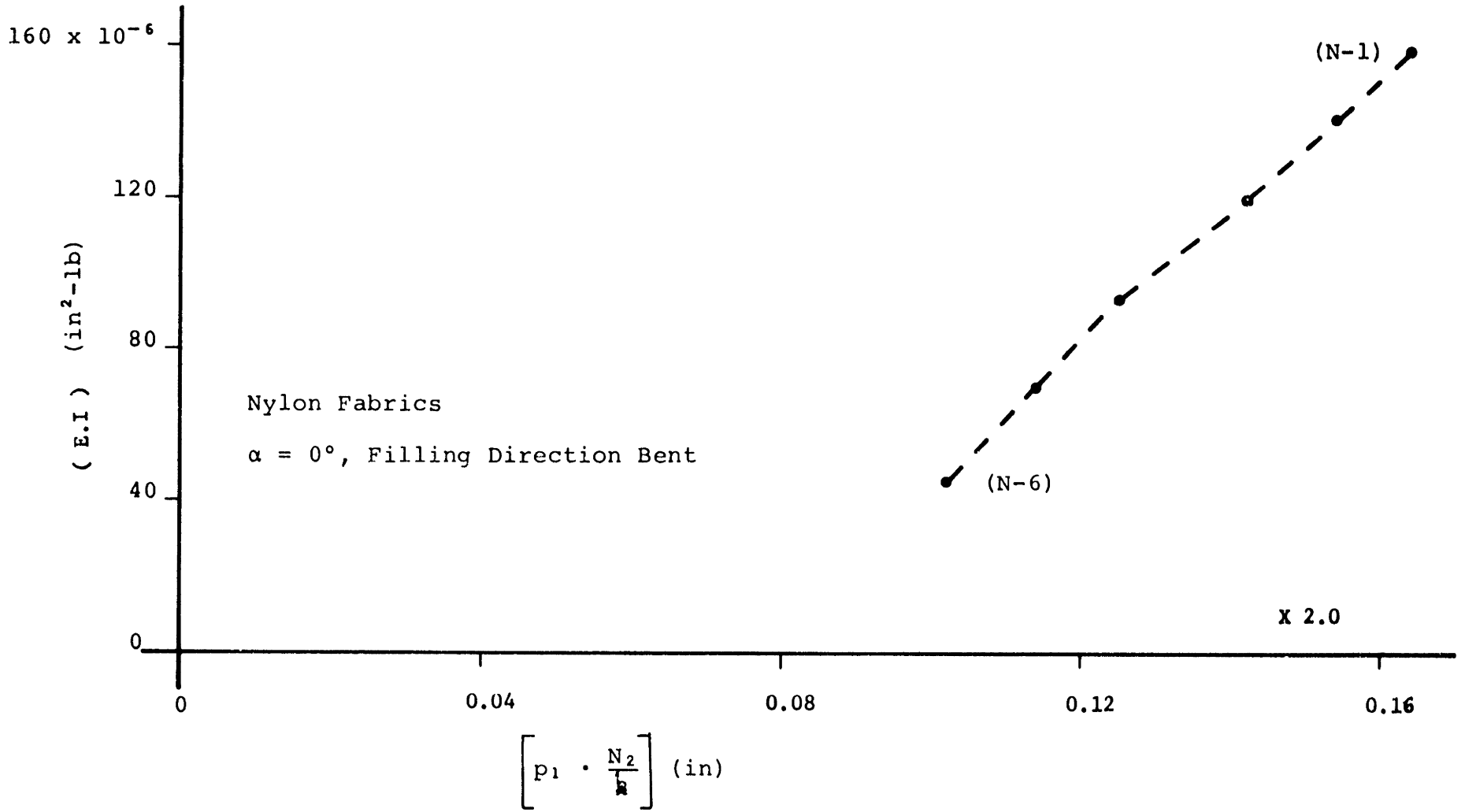

where S_t and S_r are total yarn length between crowns and the length of the restricted yarn regions respectively.

From equations (4.2) and (2.3), a relation may be established between fabric bending rigidity and looseness of the fabric which may be given by the structural variable $[p_2 \cdot N_1 \sin^4\alpha + p_1 \cdot \frac{N_2}{2} \cos^4\alpha]$. To determine the validity of the above relation, measured values of fabric bending rigidity for nylon series are plotted on Figures (4-50) to (4-54) as functions of the structural variable. A linear relation is observed at all angles of bias bends, namely increase of elastic rigidity with decreasing spacing of cross yarns.

Further, the relation between measured values of total frictional work loss and elastic rigidity is plotted on Figure (4-55) for the nylon series. The relation is linear at all angles of bends, namely increase of friction losses with fabrics of increasing elastic rigidity. Also, the relation between the measured values of residual elastic energy and bending recovery is plotted on Figure (4-56) for the nylon series. The relation is linear at all angles of bends, namely bending recovery improves as residual elastic energy decreases. For an additional representation of the recovery results, the bending recovery, measured in terms of residual elastic energy, is plotted as a function of friction, measured in terms of fabric elastic rigidity for various angles of bending on Figures (4-57) to (4-60). This curve illustrates the definite relation that as elastic rigidity of fabric increases due to structural tightness, residual elastic energy increases and the recovery is poor. The above conclusion is further represented by plotting residual elastic energy on Figures (4-61) to (4-65) as functions of the structural variable used for elastic rigidity which is a measure of looseness of fabric.

Figure 4-55

Total Frictional Work Loss vs. Elastic Rigidity

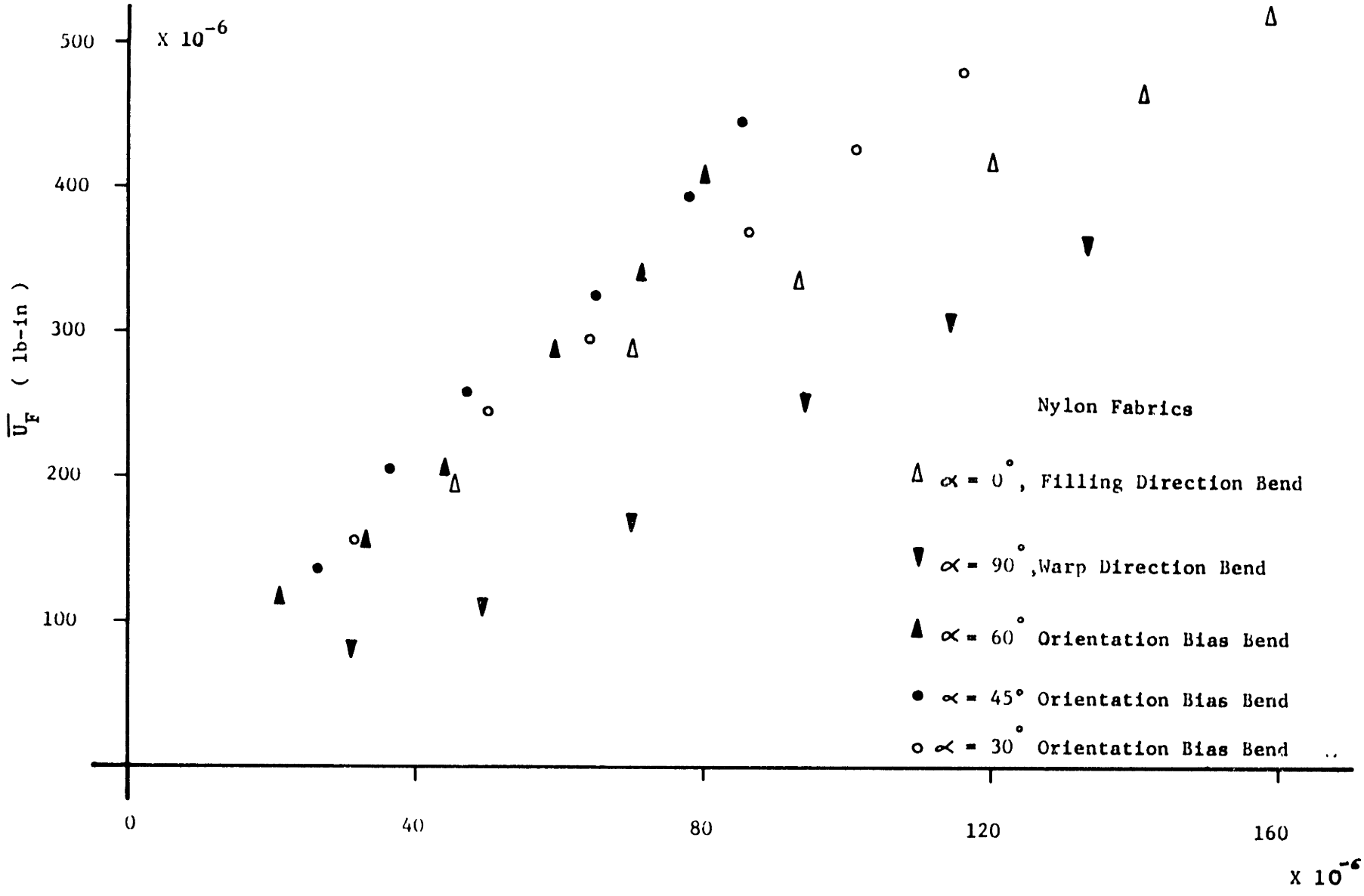

Figure 4-56

Residual Elastic Energy vs. Bending Recovery

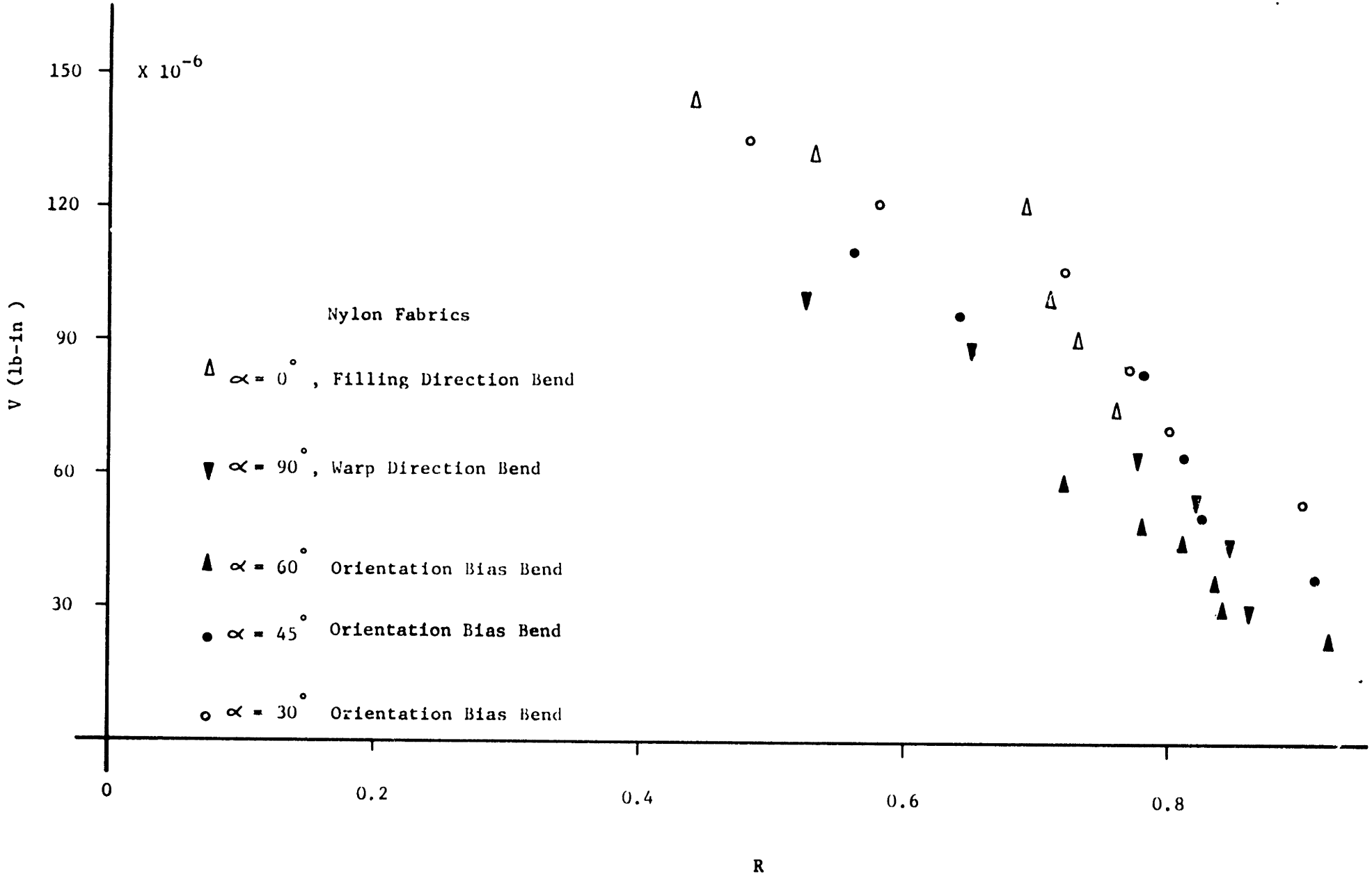

Figure 4-57

Residual Elastic Energy vs. Elastic Rigidity

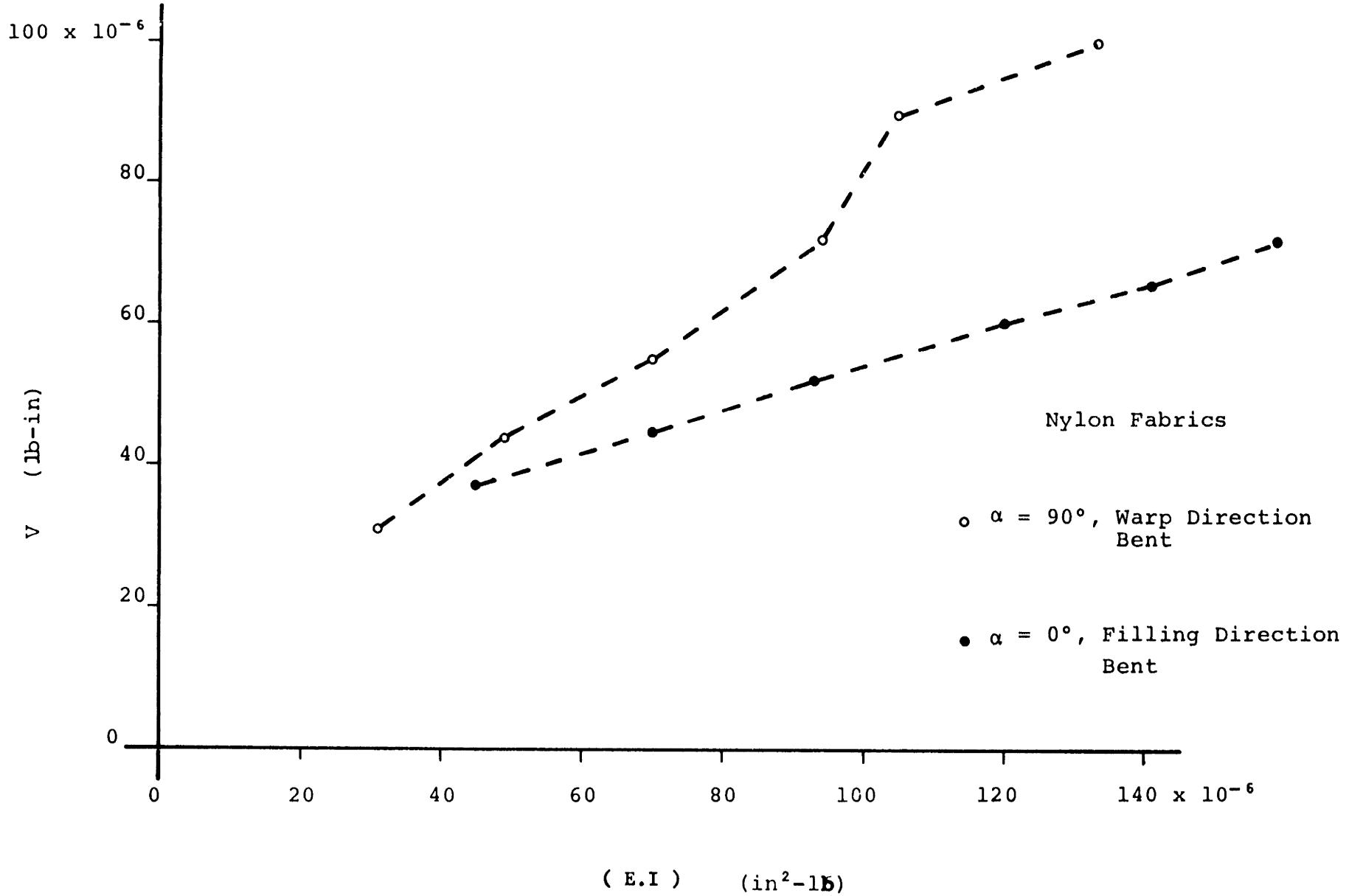

Figure 4-58

Residual Elastic Energy vs. Elastic Rigidity

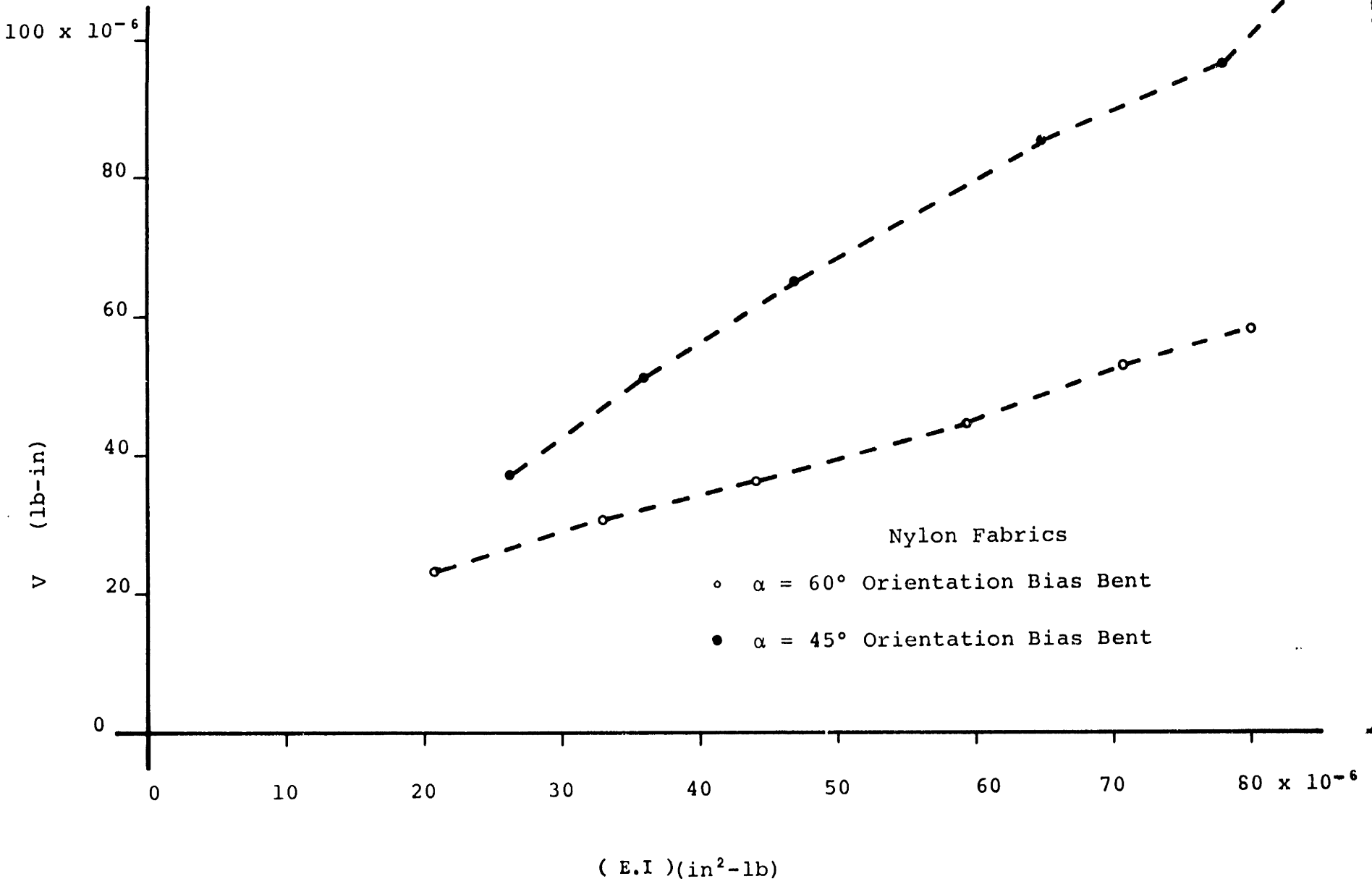

Figure 4-59

Residual Elastic Energy vs. Elastic Rigidity

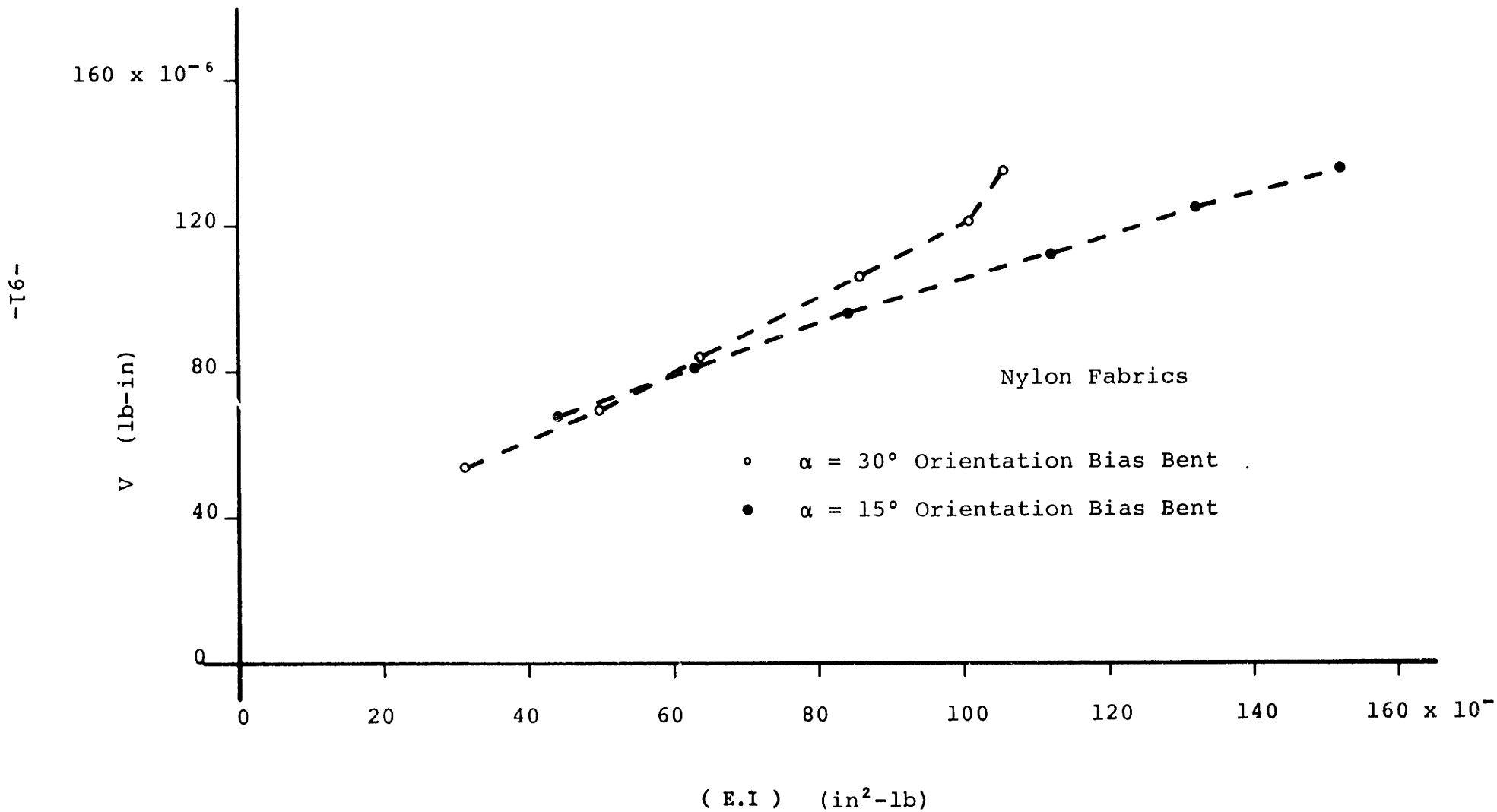

Figure 4-60

Residual Elastic Energy vs. Elastic Rigidity

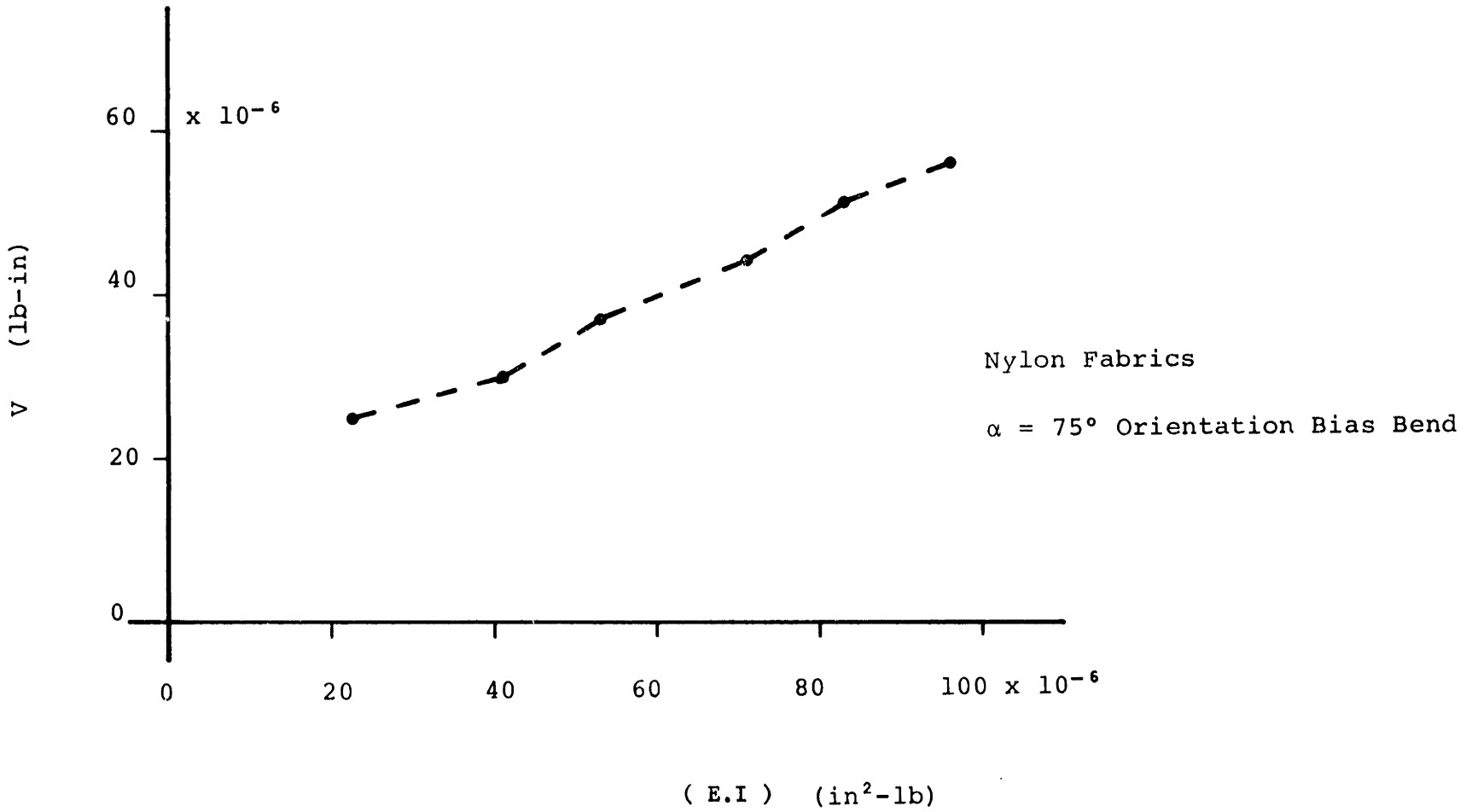

Figure 4-61

Residual Elastic Energy vs. Structural Parameter

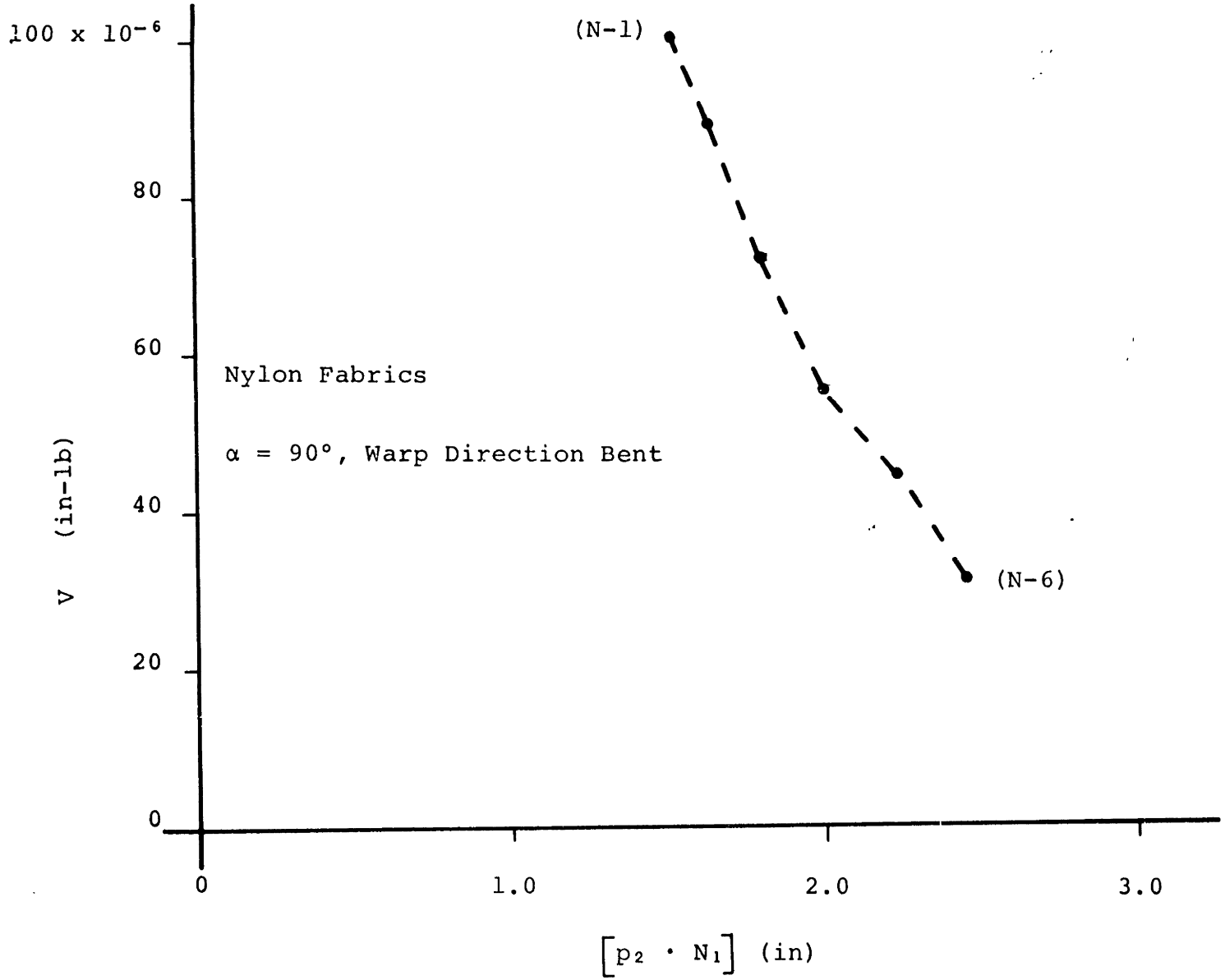

Figure 4-62

Residual Elastic Energy vs. Structural Parameter

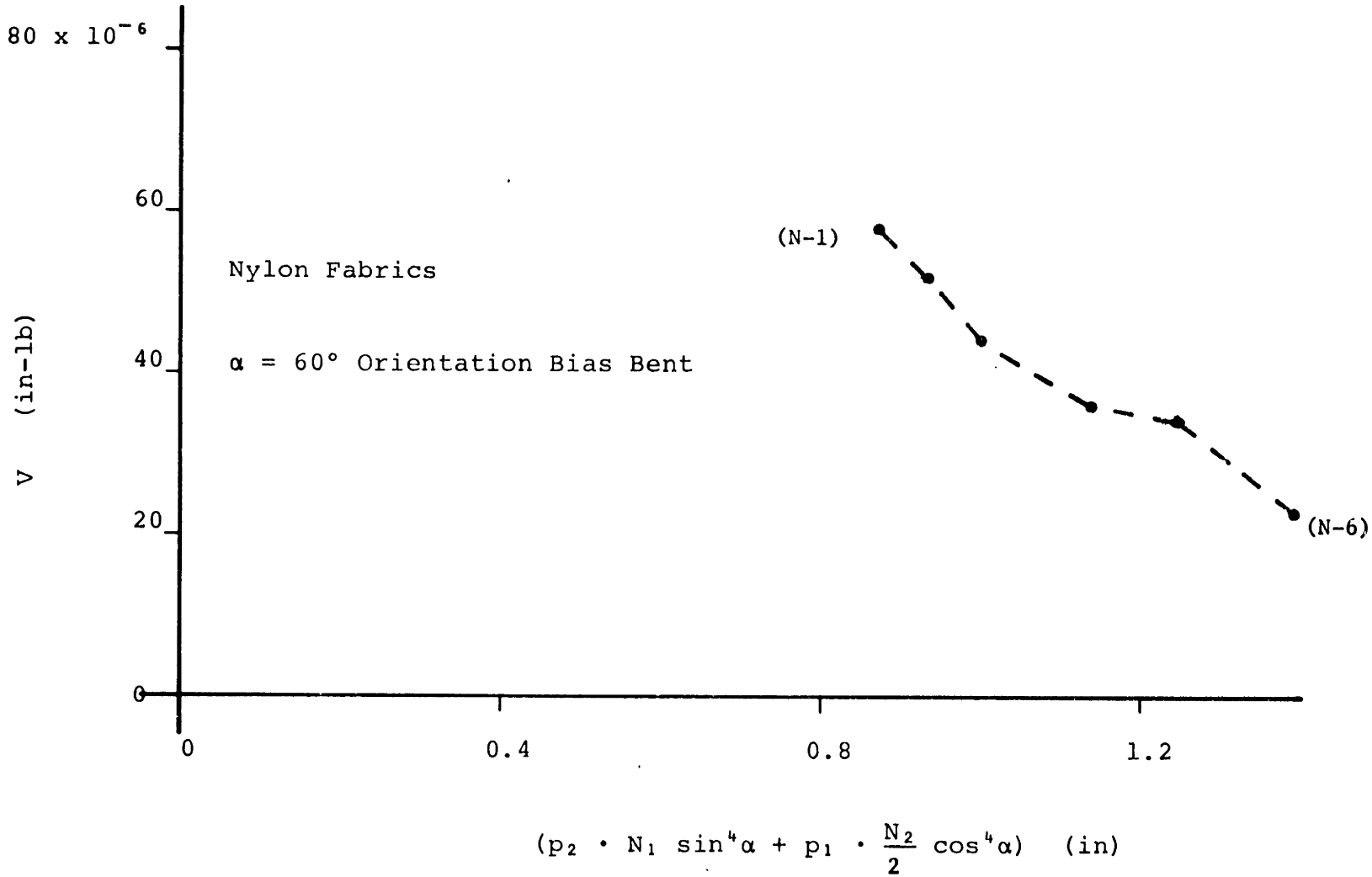

Figure 4-63

Residual Elastic Energy vs. Structural Parameter

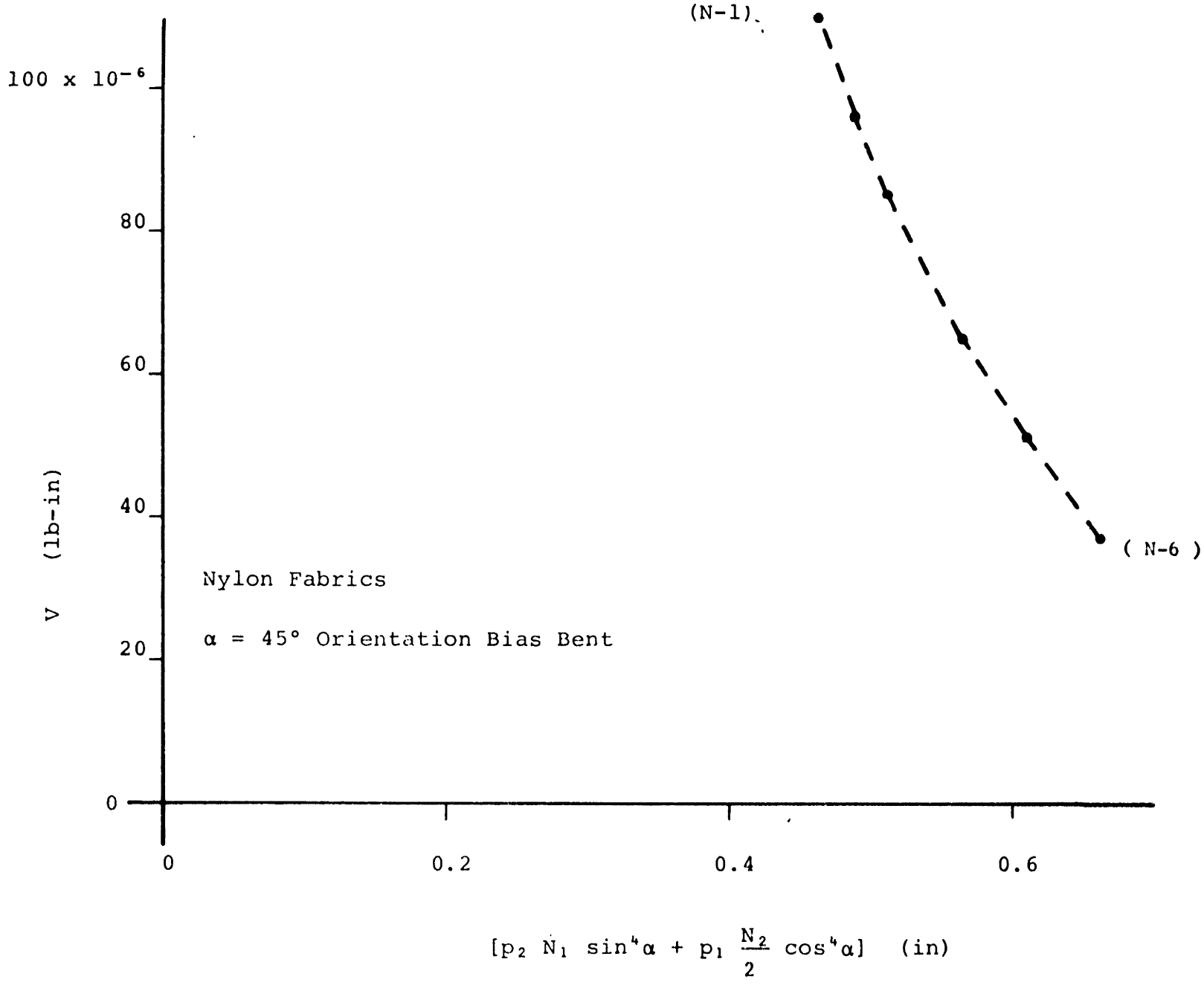

Figure 4- 64

Residual Elastic Energy vs. Structural Parameter

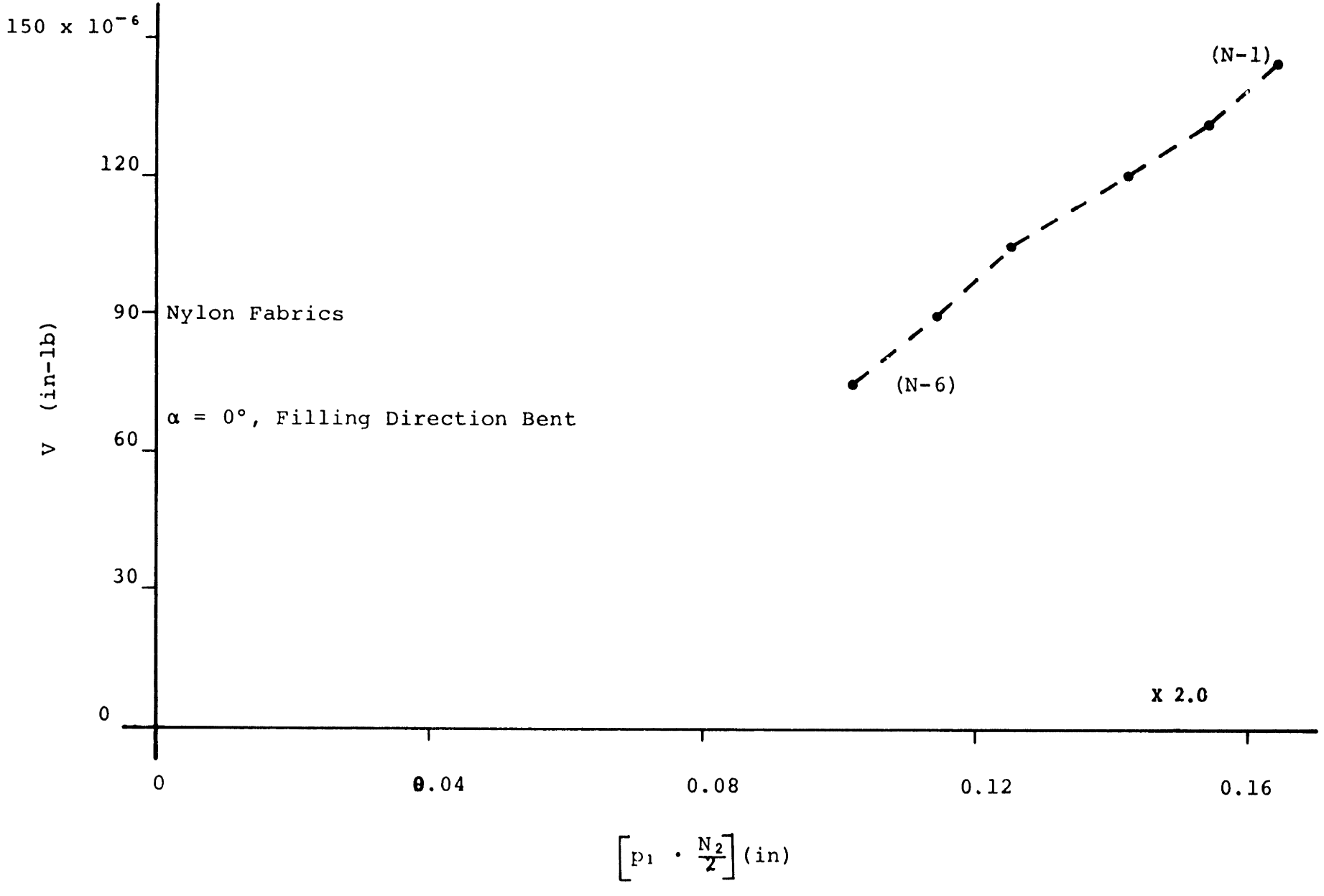

Figure 4- 65

Residual Elastic Energy vs. Structural Parameter

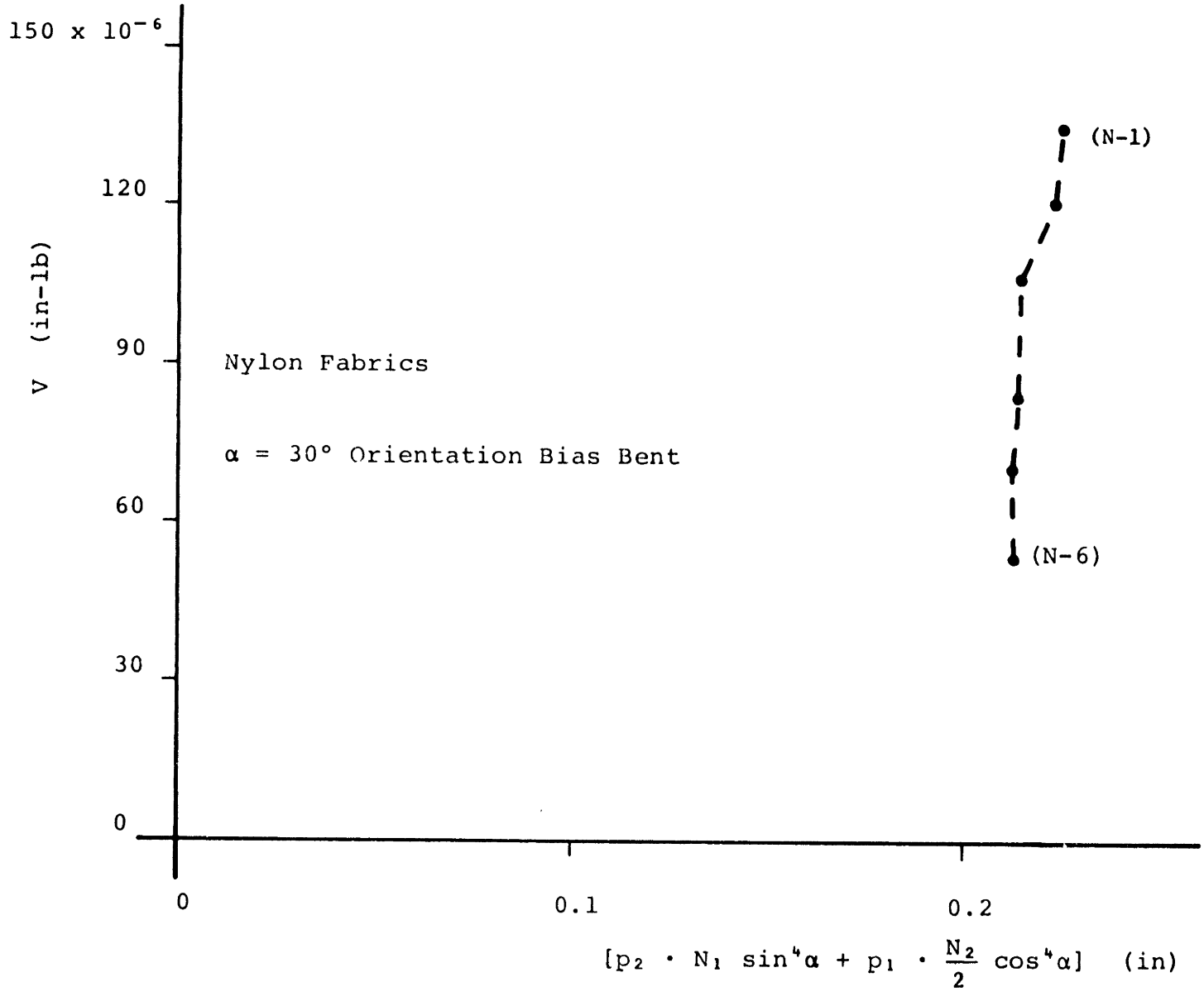

Conclusions and Recommendations

The following observations have been made in the study of the bending behavior of plain-weave multi-filament non-heatset nylon fabrics and unfinished cotton fabrics when bent on the bias.

1. In the present report we have employed the expression derived by Cooper for predicting the fabric bending rigidity. A good agreement has been observed with the measured values. It is desirable to test whether a similar or identical relation holds after the material is mechanically conditioned by repeated loading.

2. During bending, a woven fabric loses energy due to frictional interactions such as relative fiber motions. To a first approximation the magnitude of this energy loss has been observed to depend on fiber properties, structural geometry, and effective curvature of component yarns.

For given fiber properties and structural geometry, this energy loss was found to be a function of the effective curvature of component yarns; and for a dimensionally balanced fabric it was found to be constant at any orientation of bias bending.

For given fiber properties and orientation of bias bending, this energy loss increases linearly as structural tightness increases.

Further work is necessary to clarify the influence on fabric properties of additional frictional effects for bias bends such as yarn rotation at crossing points due to angular change between yarns, particularly for fabrics with relatively high interyarn pressure such as fiberglass fabrics.

3. The fundamental usefulness of the present analysis employing the assumptions of the mathematical model of frictional effect used in Popper's analysis, was exhibited by relating one set of ensemble measurements, namely total elastic energy input in bending, energy losses due to frictional restraints, and unrecoverable residual elastic energy to another set of ensemble measurements, namely fabric elastic rigidity, friction moment and imposed curvature. Further, it has been shown that hysteresis loop of a bending-unbending cycle represents the sum of the total frictional energy loss and unrecoverable residual elastic energy.

4. A definite relation has been observed between this residual

elastic energy and bending recovery. As the fabric elastic rigidity increases with increasing structural tightness, residual elastic energy increases and recovery is poor.

5. The study of the time dependent effect, relaxation of bending moment when a sample is held at a constant curvature bend can be utilized to shed light on the bending behavior at bias bends. For nylon and cotton fabrics investigated it was observed that for a given fabric the relaxation varies with orientation of bias bending and was observed to be a minimum at that angle of bias bend when the elastic rigidity was minimum.

Appendix A
SAMPLE DESCRIPTIONS

Nylon Series N	Picks/Inch	% Warp Crimp
N-1	29	12
N-2	27	11
N-3	25	9
N-4	22	7
N-5	20	6
N-6	18	4

Ends/Inch: 44
Warp Yarns: Nylon 400/68/.75 Z
Filling Yarns: Nylon 400/136/4 Z
% Filling Crimp: 4

All fabrics are non-heatset.

Appendix A
SAMPLE DESCRIPTIONS

Cotton Series C	Ends/Inch	Picks/Inch	% Warp Crimp	% Filling
C-1	45	45	10	10
C-2	45	41	4	9
C-3	44	36	5	8

Warp Yarns: 2/22's
Filling Yarns: 2/22's

All Fabrics are unfinished.

A P P E N D I X - B

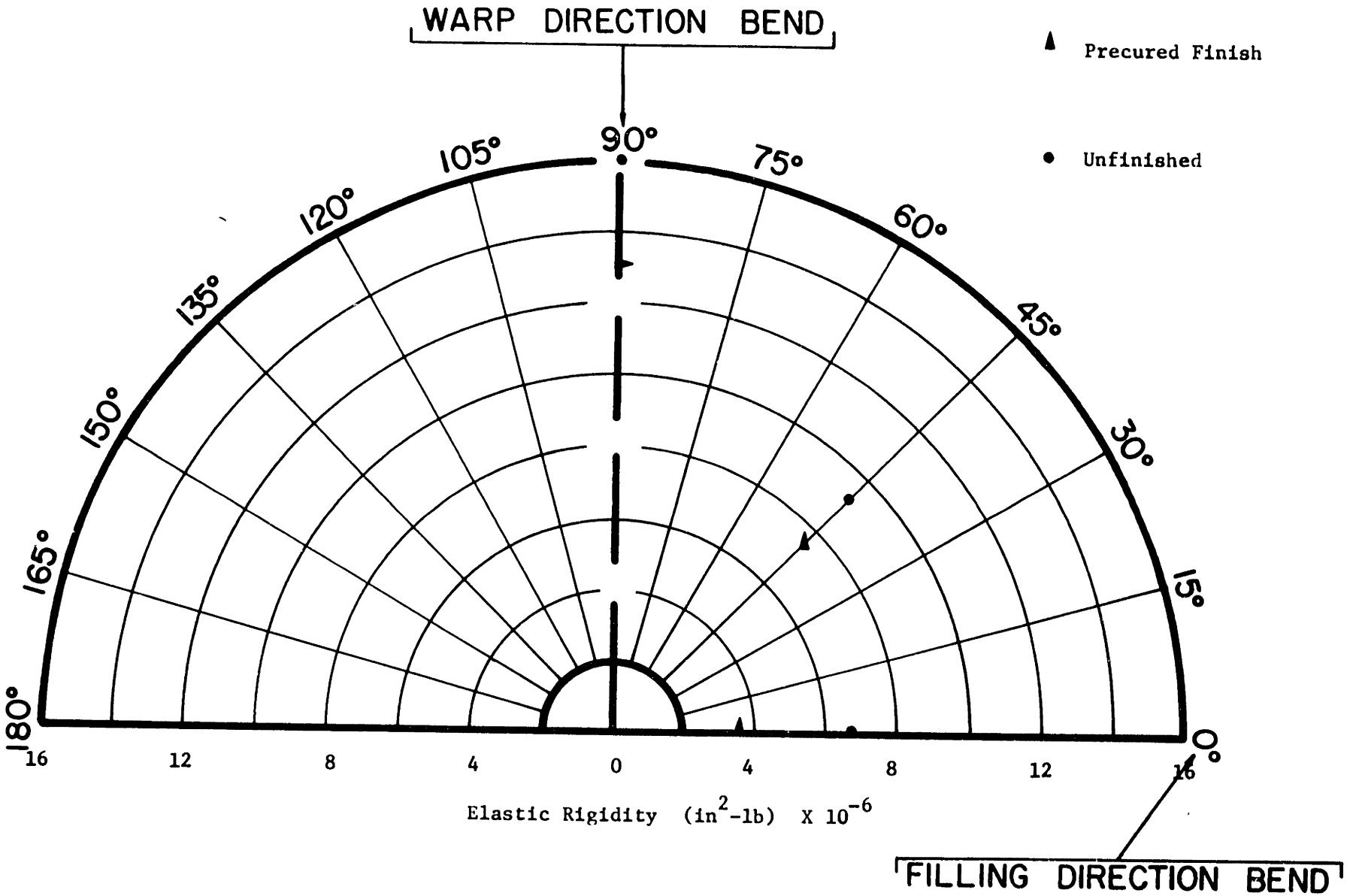

FIGURE B - 1

Directional Properties in Elastic Rigidity of Shirting Fabric
(65/35: Polyester/Cotton)

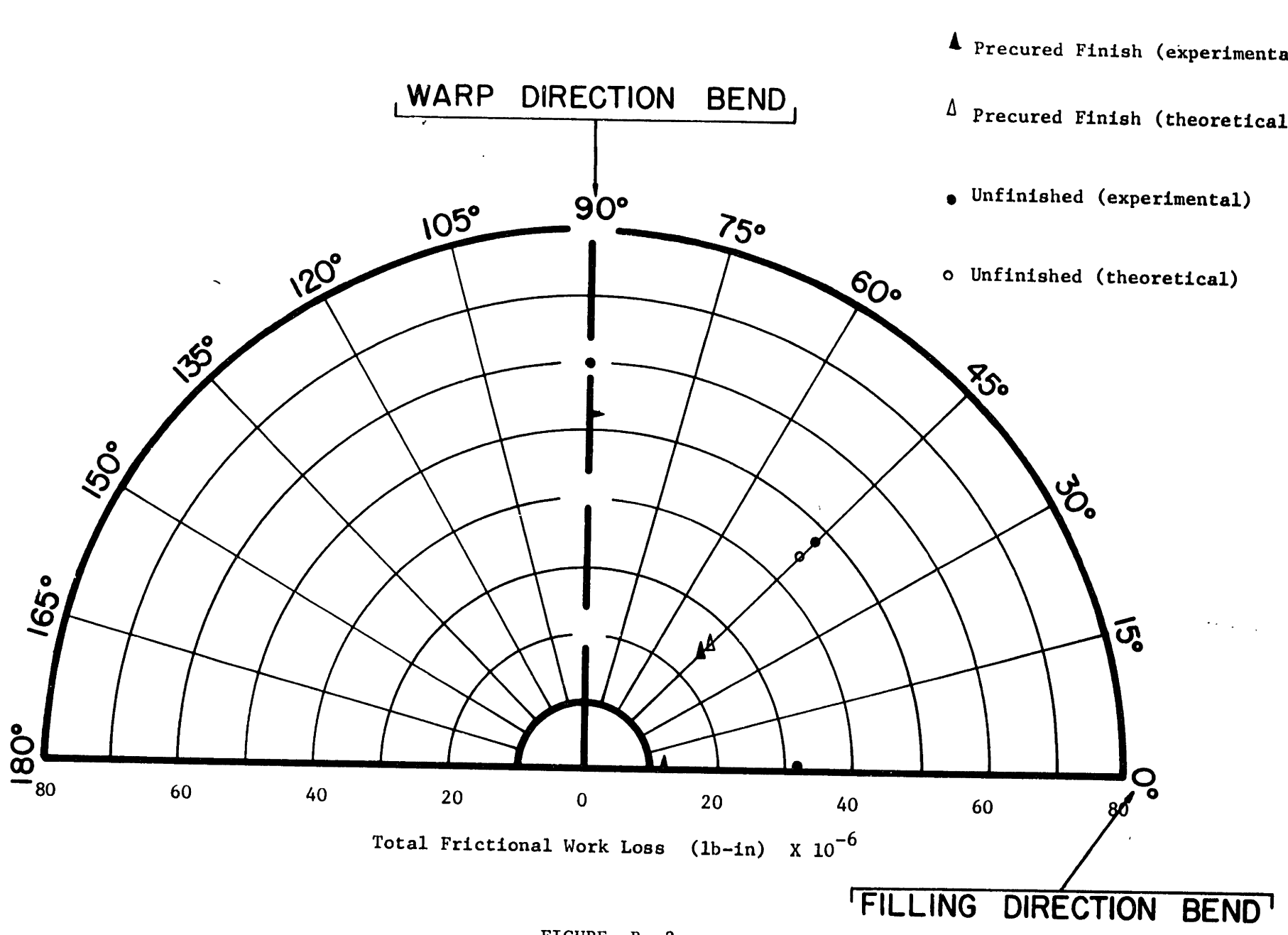

FIGURE B -2

Directional Properties in Total Frictional Work Loss of Shirting Fabric
(65/35: Polyester/Cotton)

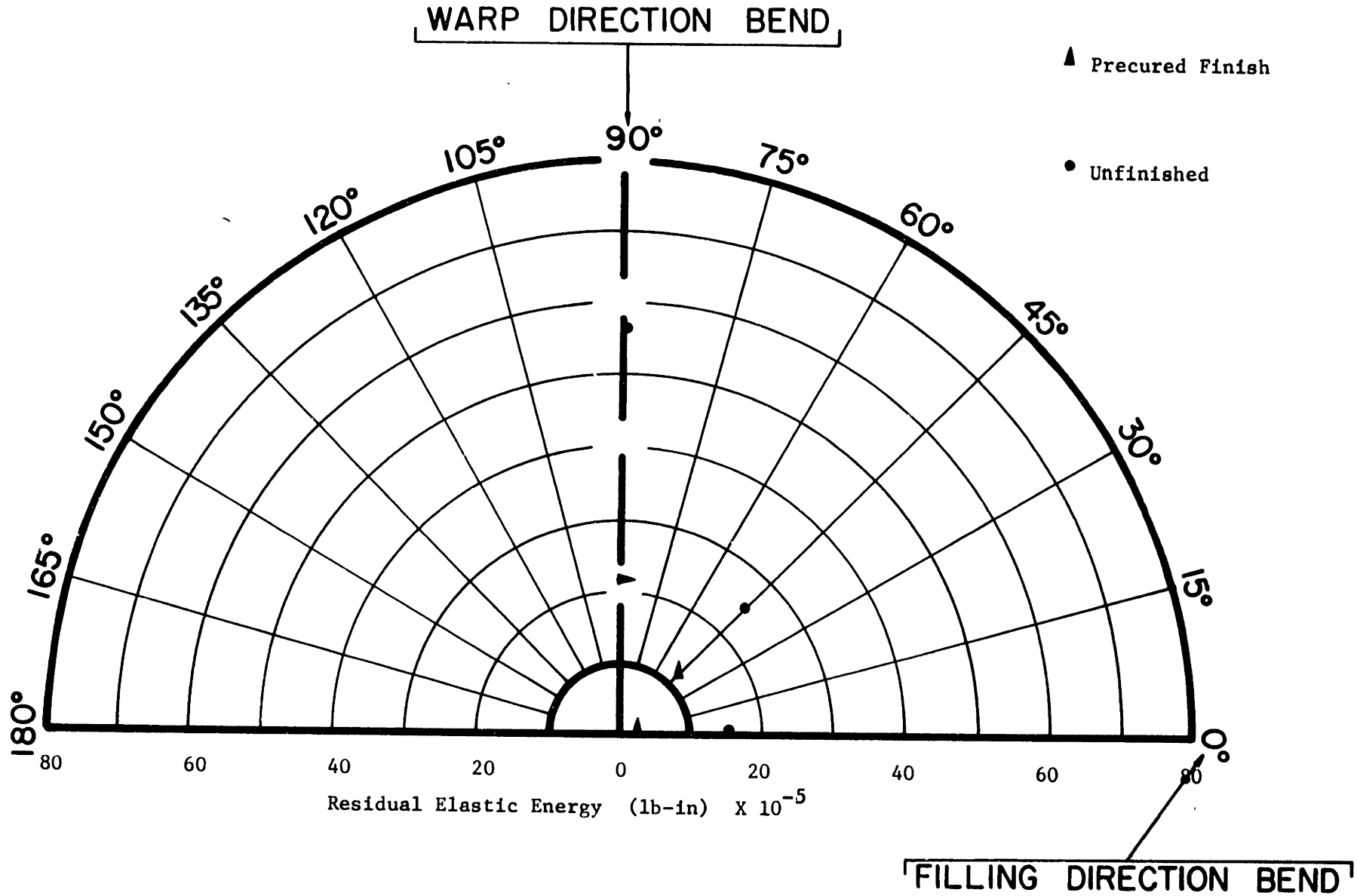

FIGURE B - 3

Directional Properties in Residual Elastic Energy of Shirting Fabric

(65/35: Polyester/Cotton)

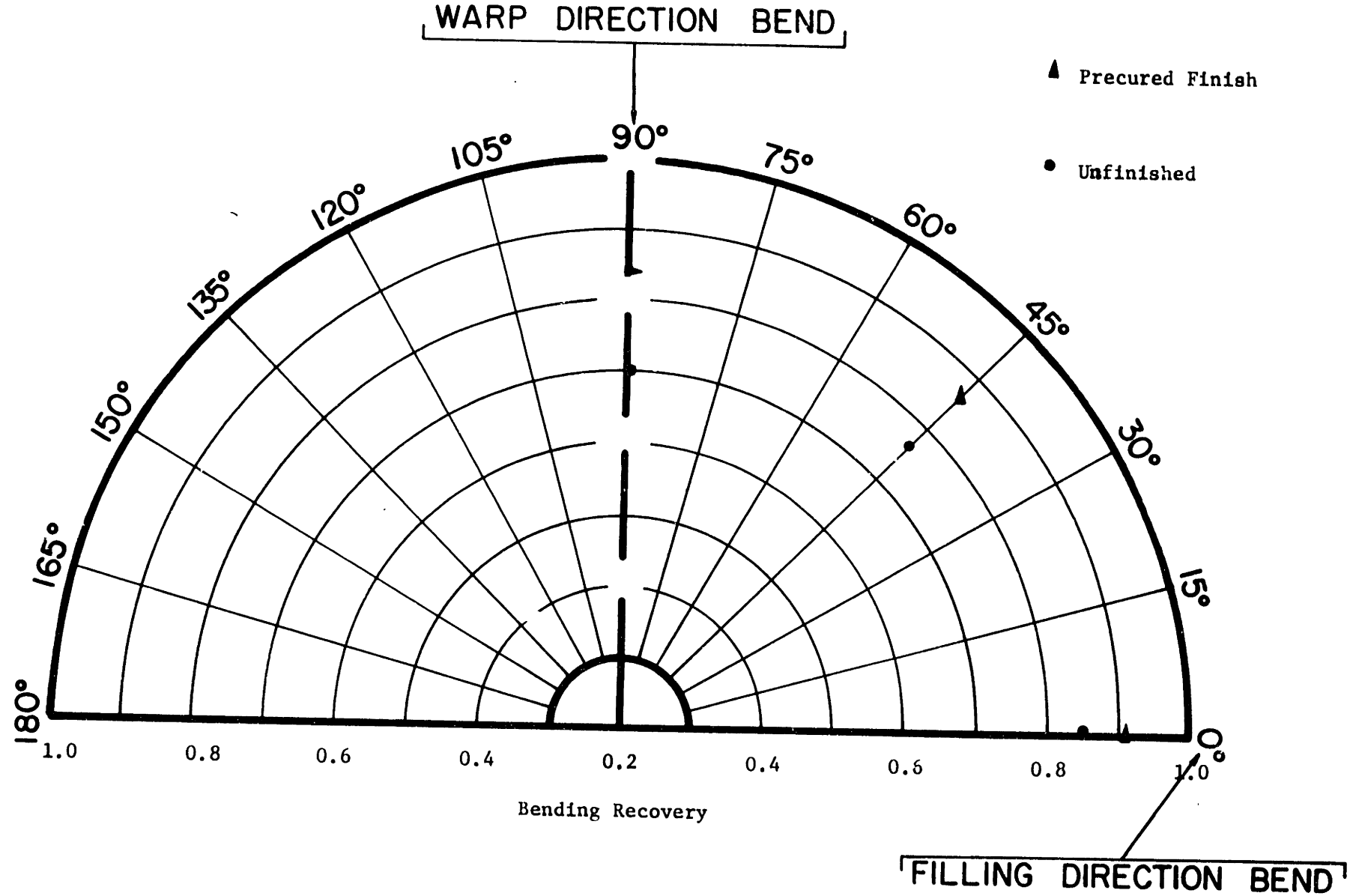

FIGURE B - 4

Directional Properties in Bending Recovery of Shirting Fabric

(65/35: Polyester/Cotton)

Appendix C

CHI-SQUARE TEST FOR TOTAL FRICTIONAL WORK LOSS

Sample: (N-1)

α	E (in-lb) x10^{-6}	T (in-lb) x10^{-6}	$\frac{(E-T)^2}{T}$
0°	517	517	0.0
15°	510	506.4	0.0257
30°	480	473.3	0.0975
45°	448	440	0.146
60°	407	399.8	0.13
75°	378	374.6	0.031
90°	363	363	0.0

$X^2 = \Sigma \frac{(E-T)^2}{T} = 0.4302$

at $\nu = 4$ degrees of freedom

(Sample: (N-2)

α	E (in-lb) x10^{-6}	T (in-lb) x10^{-6}	$\frac{(E-T)^2}{T}$
0°	462	462	0.0
15°	455	451.8	0.039
30°	426	416.5	0.217
45°	393	386	0.127
60°	340	345.5	0.083
75°	325	321	0.05
90°	310	310	0.0

$X^2 = 0.519$

at $\nu = 4$ degrees of freedom

Sample: (N-3)

α	E (in-lb) x10^{-6}	T (in-lb) x10^{-6}	$\frac{(E-T)^2}{T}$
0°	400	400	0.0
15°	380	370	0.27
30°	370	374.5	0.054
45°	330	326.5	0.038
60°	286	293.4	0.187
75°	264	262	0.015
90°	253	253	0.0

$X^2 = 0.584$

at $\nu = 4$ degrees of freedom

(Sample: (N-4)

α	E (in-lb) x10^{-6}	T (in-lb) x10^{-6}	$\frac{(E-T)^2}{T}$
0°	333	333	0.0
15°	320	323	0.028
30°	298	292.25	0.124
45°	258	251.5	0.168
60°	205	210.75	0.158
75°	175	180.75	0.178
90°	170	170	0.0

$X^2 = 0.656$

at $\nu = 4$ degrees of freedom

E: experimental value

T: theoretical value

α: orientation to filling direction of specimen

Appendix C

CHI-SQUARE TEST FOR TOTAL FRICTIONAL WORK LOSS

	Sample: (N-5)			Sample: (N-6)		
α	E (in-lb) $\times 10^{-6}$	T (in-lb) $\times 10^{-6}$	$\frac{(E-T)^2}{T}$	E (in-lb) $\times 10^{-6}$	T (in-lb) $\times 10^{-6}$	$\frac{(E-T)^2}{T}$
0°	286	286	0.0	194.8	194.8	0.0
15°	275	274.7	0.003	186.7	186.48	0.001
30°	245	240.85	0.072	156.1	166.49	0.664
45°	199	199.75	0.001	135.2	138.18	0.065
60°	154	165	0.74	116.4	109.82	0.248
75°	126	135.2	0.715	88	89.05	0.001
90°	113.5	113.5	0.0	81.55	81.55	0.0

$X^2 = 1.531$ at $\nu = 4$ degrees of freedom

$X^2 = 0.988$ at $\nu = 4$ degrees of freedom.

	Sample: (C-1)			Sample: (C-2)		
α	E (in-lb) $\times 10^{-6}$	T (in-lb) $\times 10^{-6}$	$\frac{(E-T)^2}{T}$	E (in-lb) $\times 10^{-6}$	T (in-lb) $\times 10^{-6}$	$\frac{(E-T)^2}{T}$
0°	544	544	0.0	461	461	0.0
15°	555	546	0.2	459	456.5	0.02
30°	552	543	0.15	458	455.25	0.02
45°	552	542	0.186	455	450.5	0.068
60°	548	541	0.09	452	445.25	0.11
75°	540	536.5	0.023	448	440.9	0.114
90°	540	540	0.0	440	440	0.0

$X^2 = 0.649$ at $\nu = 4$ degrees of freedom

$X^2 = 0.332$ at $\nu = 4$ degrees of freedom

Appendix C

CHI-SQUARE TEST FOR TOTAL FRICTIONAL WORK LOSS

Sample: (C-3)

α	E (in-lb) $\times 10^{-6}$	T (in-lb) $\times 10^{-6}$	$\frac{(E-T)^2}{T}$
0°	367	367	0.0
15°	368	364.6	0.06
30°	358	360.5	0.02
45°	356	352.5	0.04
60°	350	346.8	0.03
75°	348	339.6	0.274
90°	338.5	338.5	0.0

$X^2 = 0.424$

at $\nu = 4$ degrees of freedom

Appendix C

CHI-SQUARE TEST FOR ELASTIC RIGIDITY

Sample: (N-1)

α	E $(in^2\text{-}lb)\times10^{-6}$	T $(in^2\text{-}lb)\times10^{-6}$	$\frac{(E-T)^2}{T}$
0°	159	159	0.0
15°	152	158	0.102
30°	116	114	0.035
45°	85	85	0.0
60°	80	96	0.267
75°	96	92	0.018
90°	133	133	0.0

$X^2 = \Sigma \frac{(E-T)^2}{T} = 0.422$

at ν = 3 degrees of freedom

Sample: (N-2)

α	$(in^2\text{-}lb)\times10^{-6}$	$(in^2\text{-}lb)\times10^{-6}$	$\frac{(E-T)^2}{T}$
0°	141	141	0.0
15°	132	125	0.394
30°	101	100.1	0.001
45°	78	78	0.0
60°	71	82	1.48
75°	83	93	1.04
90°	114	114	0.0

$X^2 = 2.915$

at ν=3 degrees of freedom

Sample: (N-3)

α	$(in^2\text{-}lb)\times10^{-6}$	$(in^2\text{-}lb)\times10^{-6}$	$\frac{(E-T)^2}{T}$
0°	120	120	0.0
15°	112	112.46	0.002
30°	86	79.84	0.478
45°	65	65	0.0
60°	59.4	66.8	0.825
75°	71	79.56	0.925
90°	94	94	0.0

$X^2 = 2.23$

at ν = 3 degrees of freedom

Sample: (N-4)

α	$(in^2\text{-}lb)\times10^{-6}$	$(in^2\text{-}lb)\times10^{-6}$	$\frac{(E-T)^2}{T}$
0°	93	93	0.0
15°	84	82	0.049
30°	64	65.5	0.035
45°	47	47	0.0
60°	44	54	1.85
75°	53	59	0.61
90°	70	70	0.0

$X^2 = 2.544$

at ν = 3 degrees of freedom

E: experimental value

T: theoretical value

α: specimen orientation to filling direction

Appendix C

CHI-SQUARE TEST FOR ELASTIC RIGIDITY

Sample: (N-5)

α	E $(in^2\text{-}lb)x10^{-6}$	T $(in^2\text{-}lb)x10^{-6}$	$\frac{(E-T)^2}{T}$
0°	70	70	0.0
15°	63	66	0.137
30°	50	55	0.455
45°	36	36	0.0
60°	33	37	0.433
75°	41	45	0.356
90°	49	49	0.0

$X^2 = 1.374$

at $\nu = 3$ degrees of freedom

Sample: (N-6)

E $(in^2\text{-}lb)x10^{-6}$	T $(in^2\text{-}lb)x10^{-6}$	$\frac{(E-T)^2}{T}$
45.25	45.25	0.0
43.9	45.1	0.212
31.5	32.5	0.07
26.2	26.2	0.0
20.69	25.1	0.775
22.8	28.6	1.1
31.4	31.4	0.0

$X^2 = 2.157$

at $\nu = 3$ degrees of freedom

Sample: (C-1)

α	E $(in^2\text{-}lb)x10^{-6}$	T $(in^2\text{-}lb)x10^{-6}$	$\frac{(E-T)^2}{T}$
0°	134	134	0.0
15°	122	123	0.08
30°	102	101.4	0.036
45°	90.6	90.6	0.0
60°	101	88.18	1.92
75°	123.5	129.1	0.124
90°	134	134	0.0

$X^2 = 2.160$

at $\nu=3$ degrees of freedom

Sample: (C-2)

E $(in^2\text{-}lb)x10^{-6}$	T $(in^2\text{-}lb)x10^{-6}$	$\frac{(E-T)^2}{T}$
115	115	0.0
106	110	0.33
86	87	0.02
79	79	0.0
85	88.18	0.102
102.2	112.5	0.895
113	113	0.0

$X^2 = 1.347$

at $\nu = 3$ degrees of freedom

A P P E N D I X - D

Appendix C

CHI-SQUARE TEST FOR ELASTIC RIGIDITY

Sample: (C-3)

α	E $(in^2\text{-}lb)x10^{-6}$	T $(in^2\text{-}lb)x10^{-6}$	$\frac{(E-T)^2}{T}$
0°	96	96	0.0
15°	83	84	0.012
30°	70.3	71.5	0.02
45°	66	66	0.0
60°	71	69	0.06
75°	81	86	0.292
90°	91.25	91.25	0.0

$X^2 = 0.384$

at $\nu = 3$ degrees of freedom

FIGURE D-1

STRESS RELAXATION OF NYLON FABRIC (N-3)

$\alpha = 0^{\circ}$, Filling Direction Bend

$k_1 = 3.141 \ (in^{-1})$

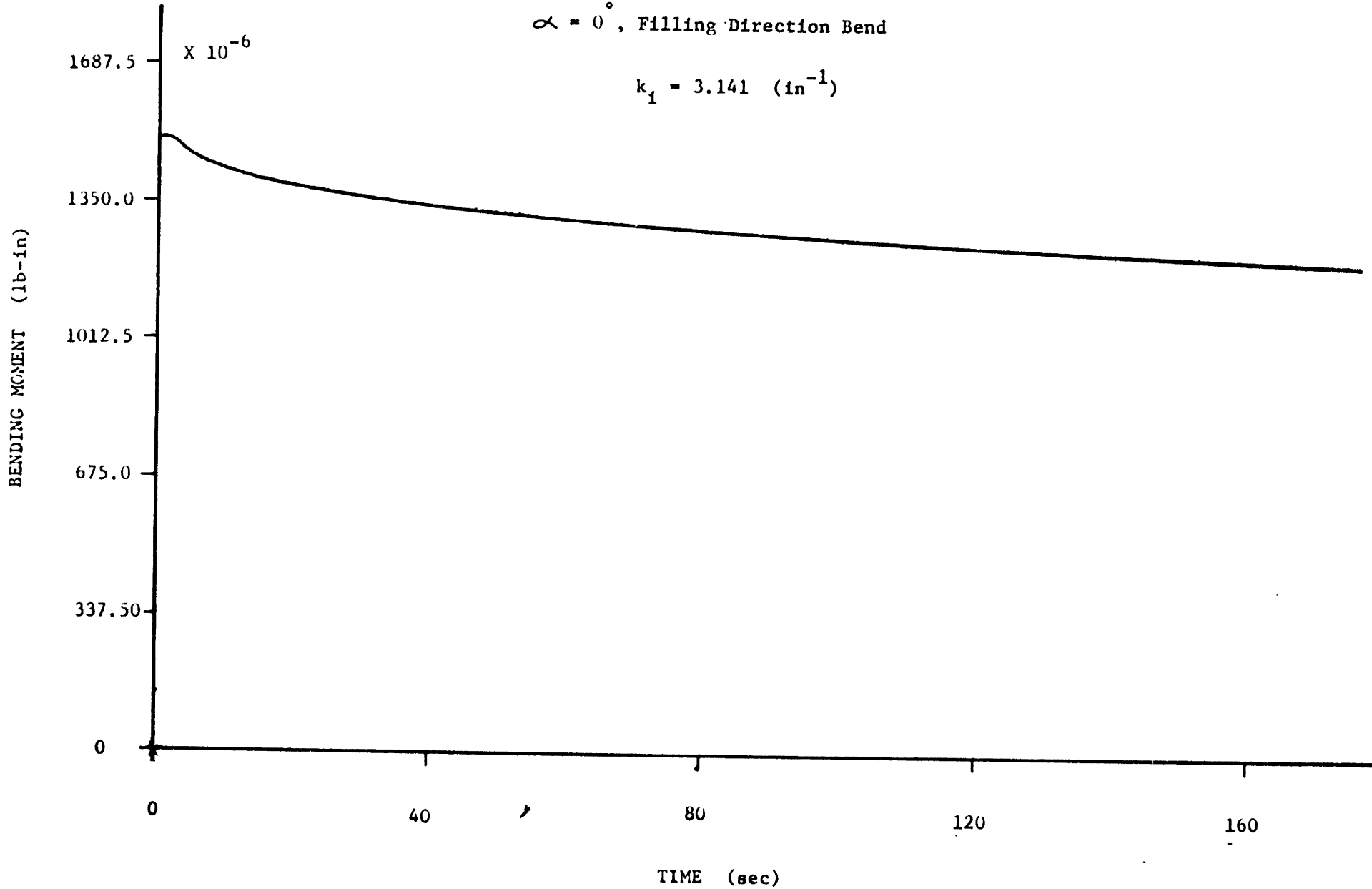

FIGURE D-2

STRESS RELAXATION OF NYLON FABRIC (N-3)

α = 45° Orientation Bias Bend

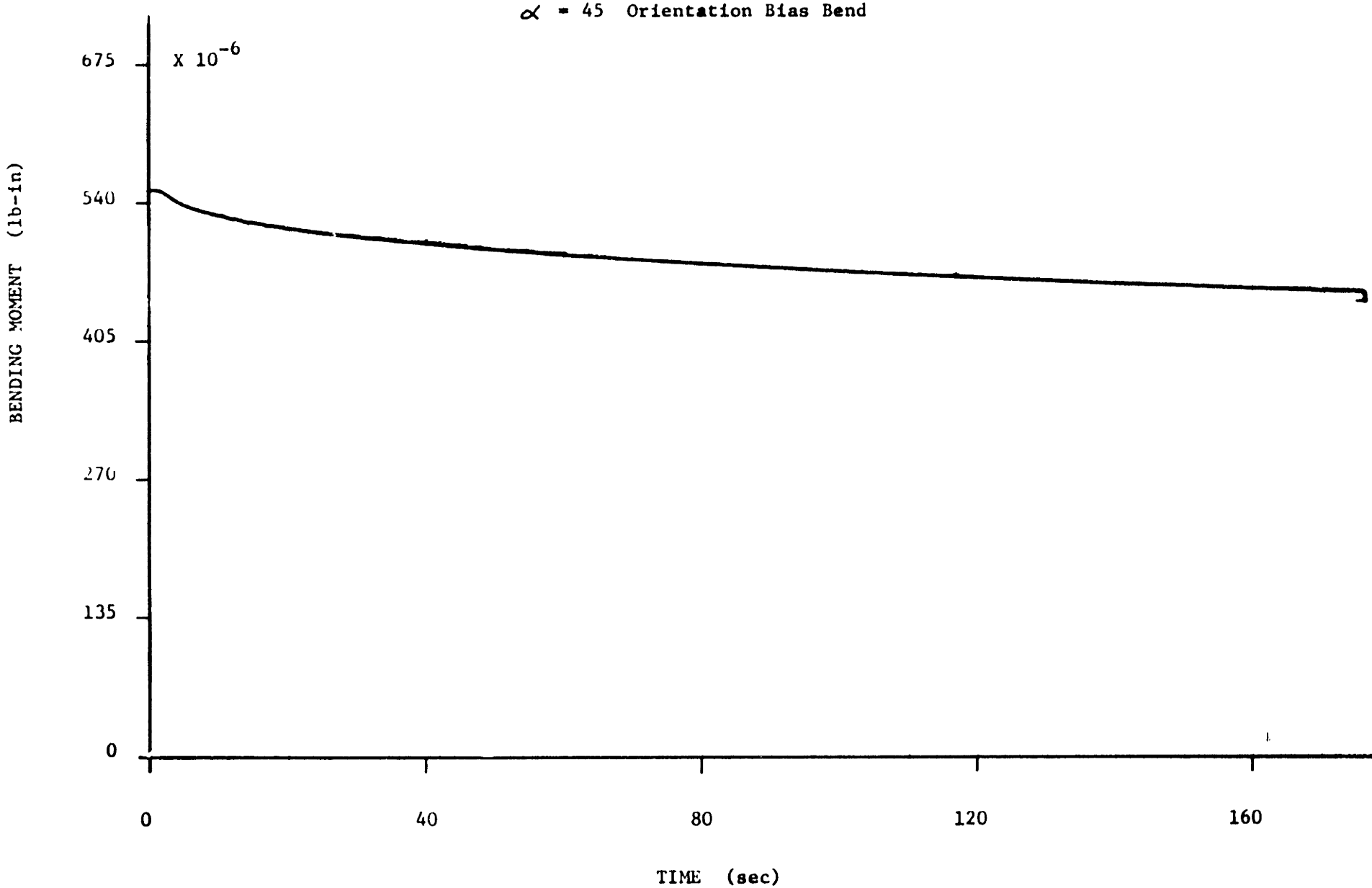

FIGURE D-3

STRESS RELAXATION OF NYLON FABRIC (N-3)

$\alpha = 60^{\circ}$ Orientation Bias Bend

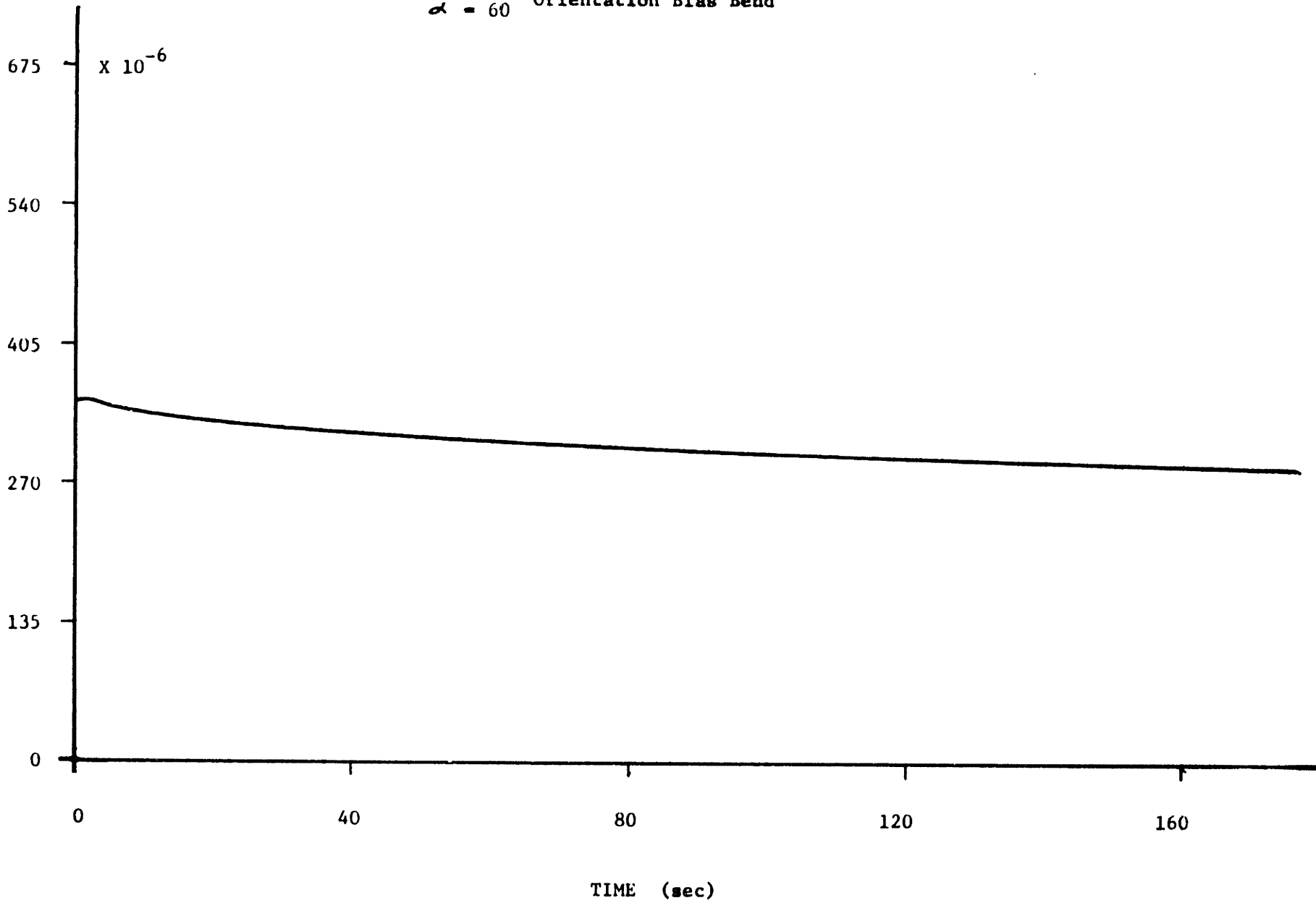

FIGURE D-4

STRESS RELAXATION OF NYLON FABRIC (N-3)

$\alpha = 90^{\circ}$, Warp Direction Bend

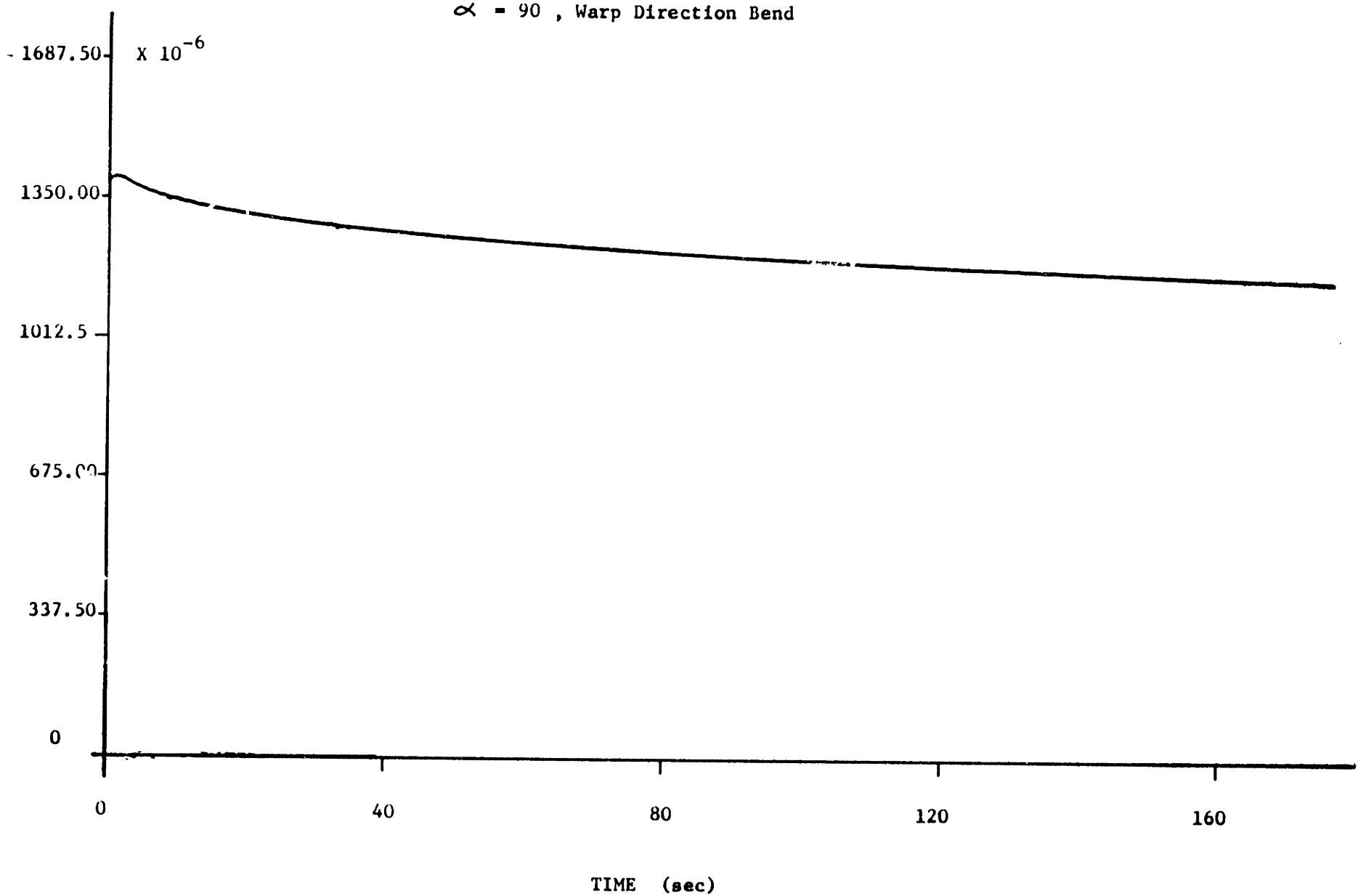

FIGURE D-5

STRESS RELAXATION OF NYLON FABRIC (N-5)

$\alpha = 0^{\circ}$, Filling Direction Bend

$k_1 = 3.141 \ (in^{-1})$

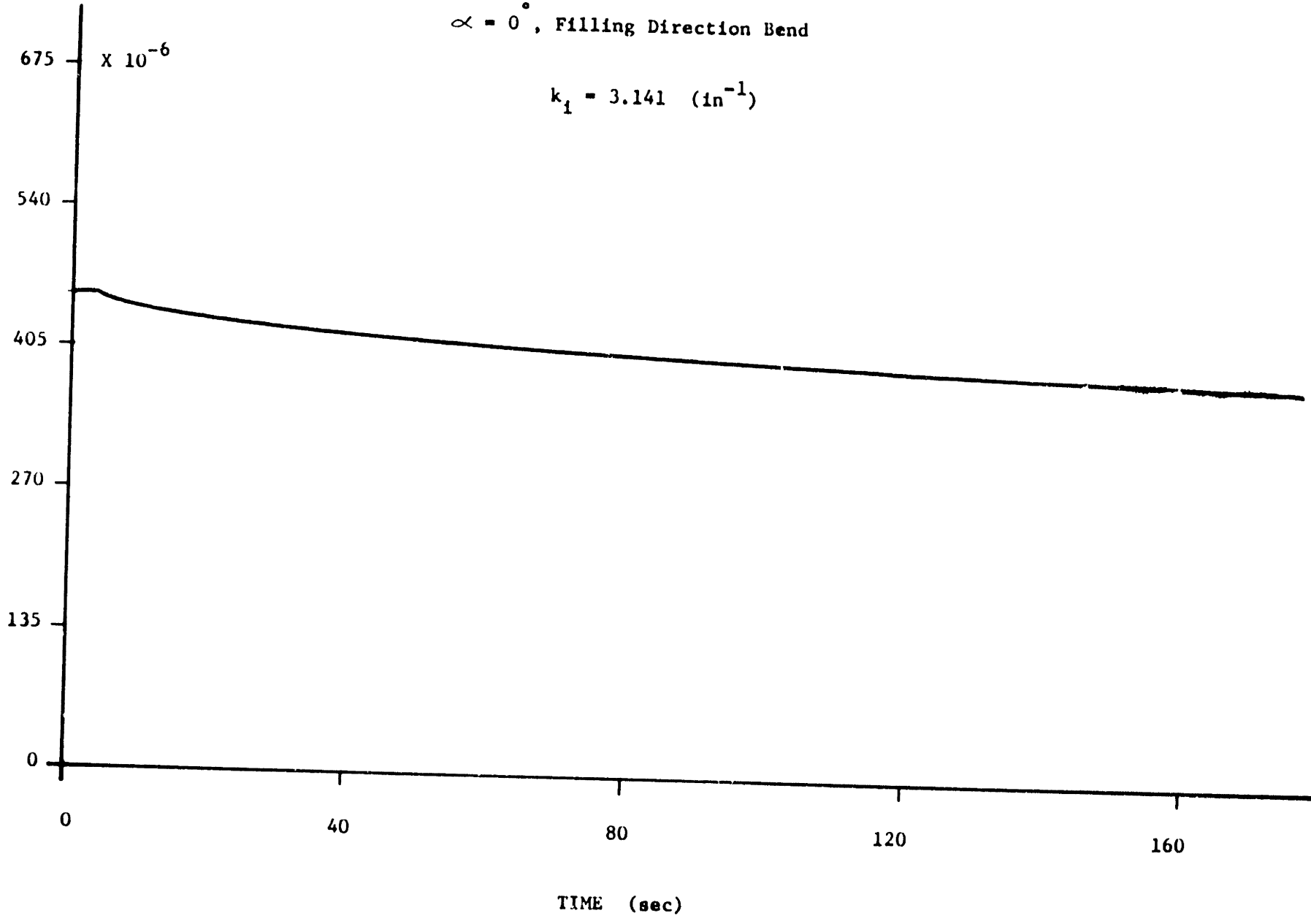

FIGURE D-6

STRESS RELAXATION OF NYLON FABRIC (N-5)

α = 45° Orientation Bias Bend

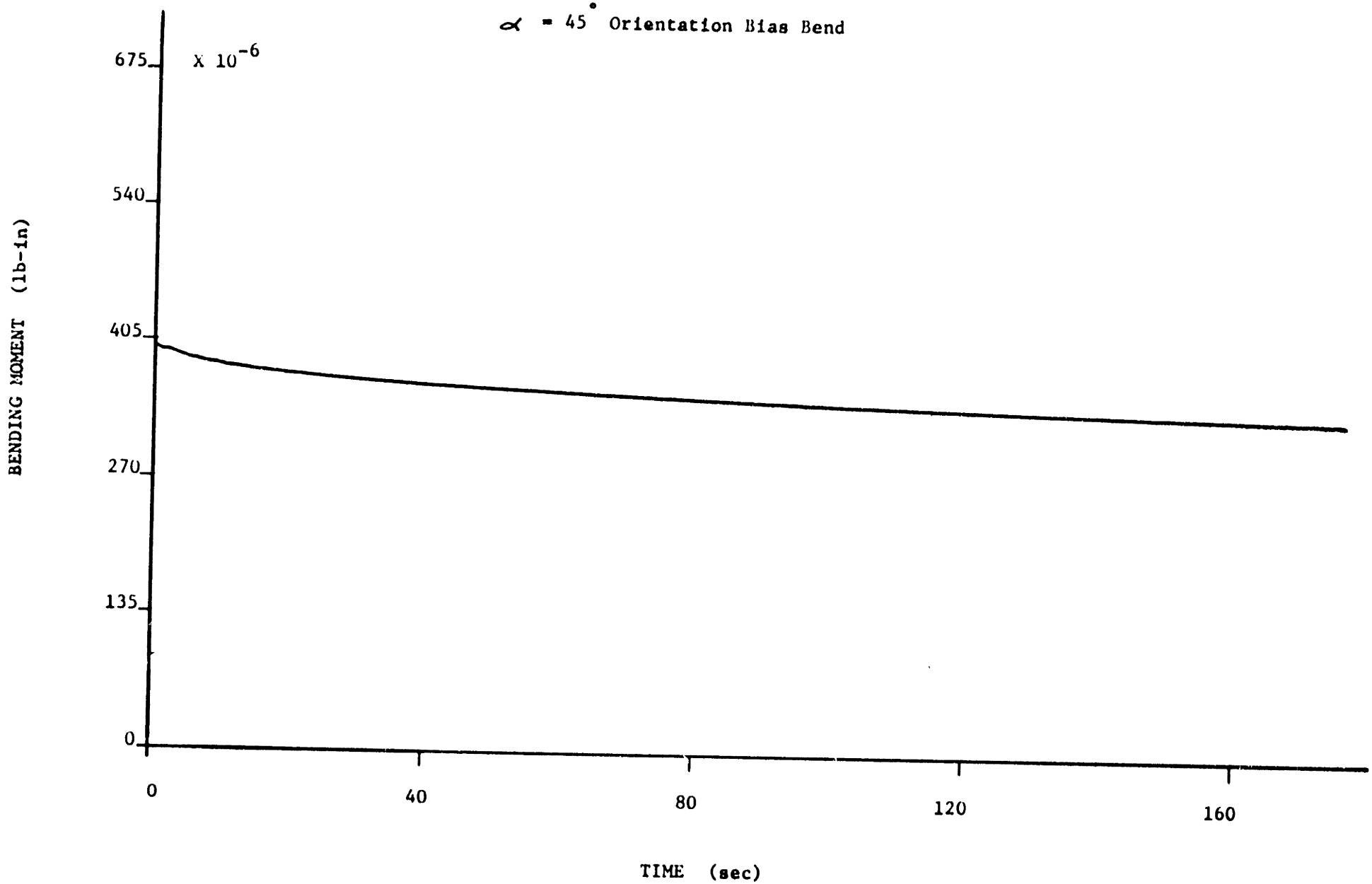

FIGURE D-7

STRESS RELAXATION OF NYLON FABRIC (N-5)

α = 60° Orientation Bias Bend

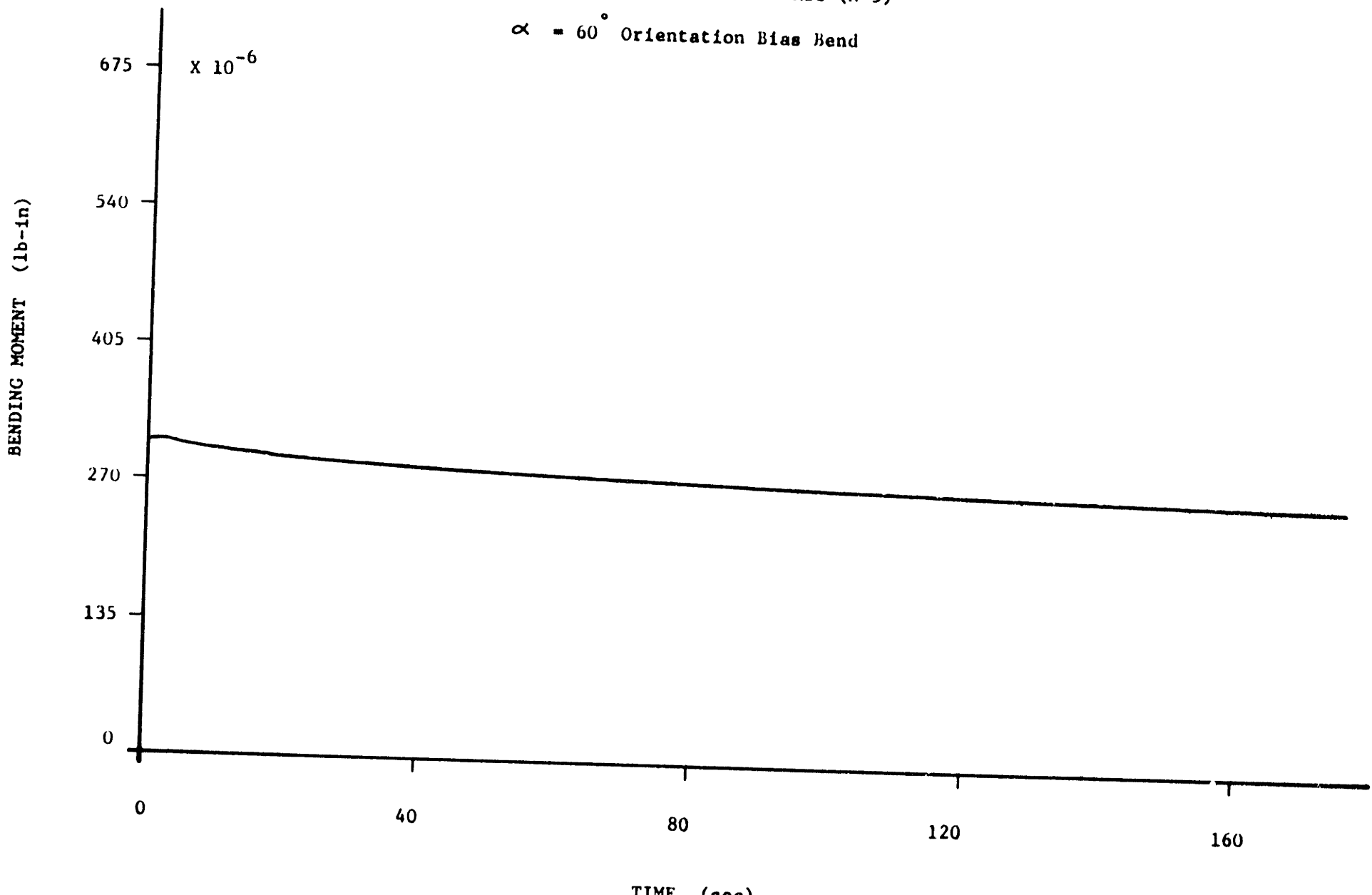

FIGURE D-8

STRESS RELAXATION OF NYLON FABRIC (N-5)

$\alpha = 90^{\circ}$, Warp Direction Bend

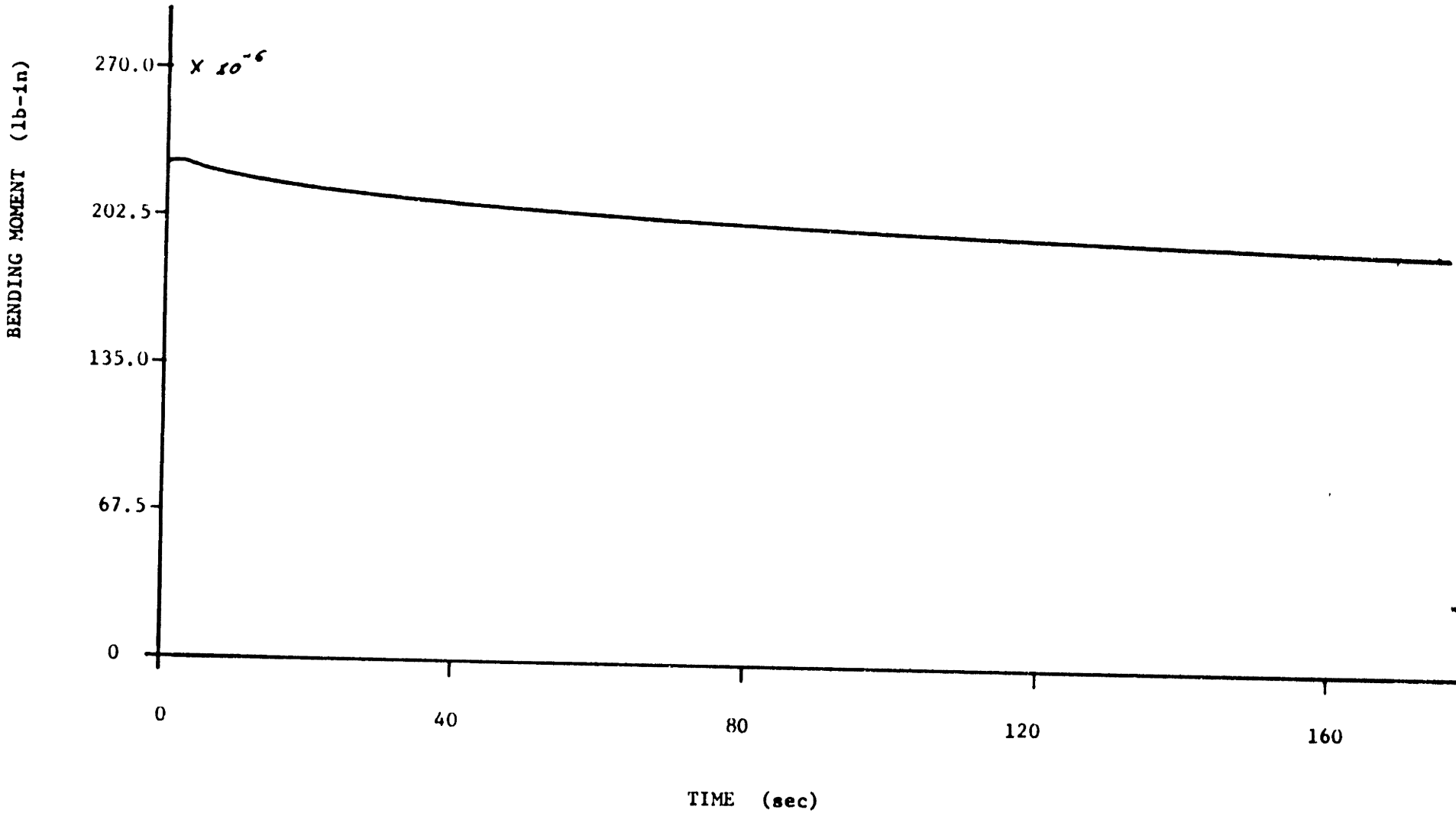

FIGURE D-9

STRESS RELAXATION OF COTTON FABRIC (C-1)

$\alpha = 0^{\circ}$, Filling Direction Bend

$k_1 = 3.141 \ (in^{-1})$

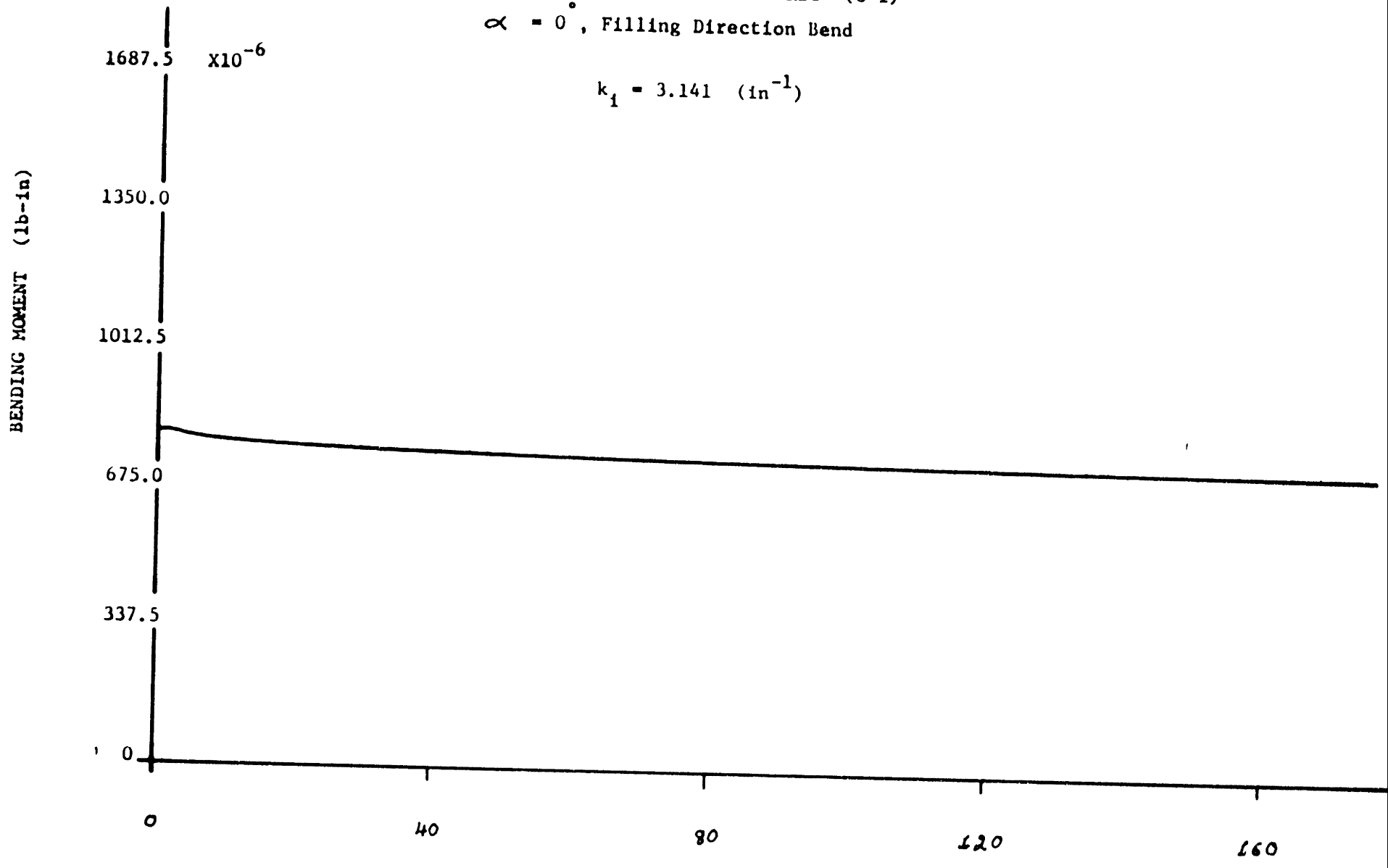

FIGURE D-10

STRESS RELAXATION OF COTTON FABRIC (C-1)

α = 45° Orientation Bias Bend

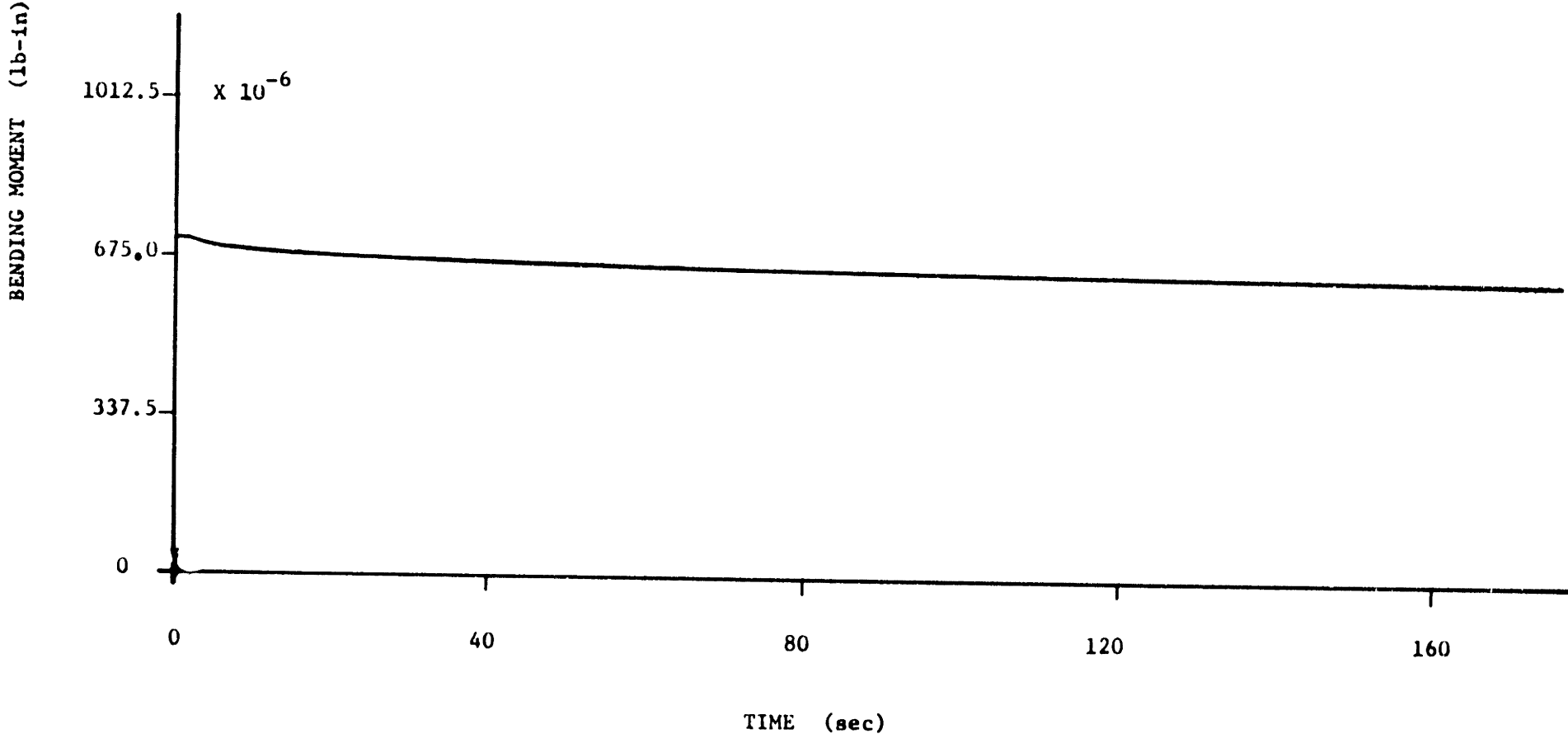

FIGURE D-11

STRESS RELAXATION OF COTTON FABRIC (C-1)

$\alpha = 90^{\circ}$, Warp Direction Bend

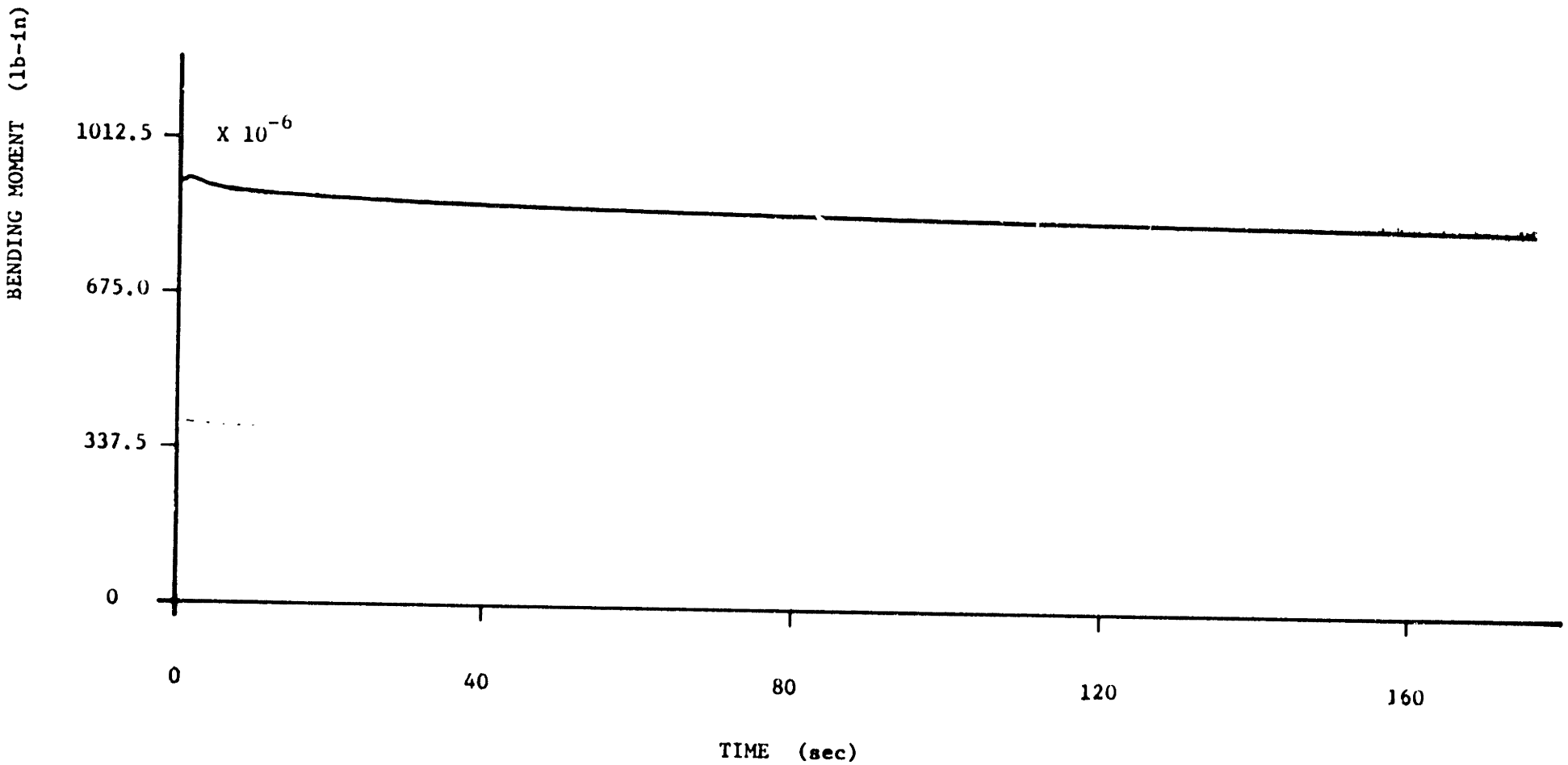

FIGURE D-12

STRESS RELAXATION OF COTTON FABRIC (C-3)

$\alpha = 0^{\circ}$, Filling Direction Bend

$k_i = 3.141 \ (in^{-1})$

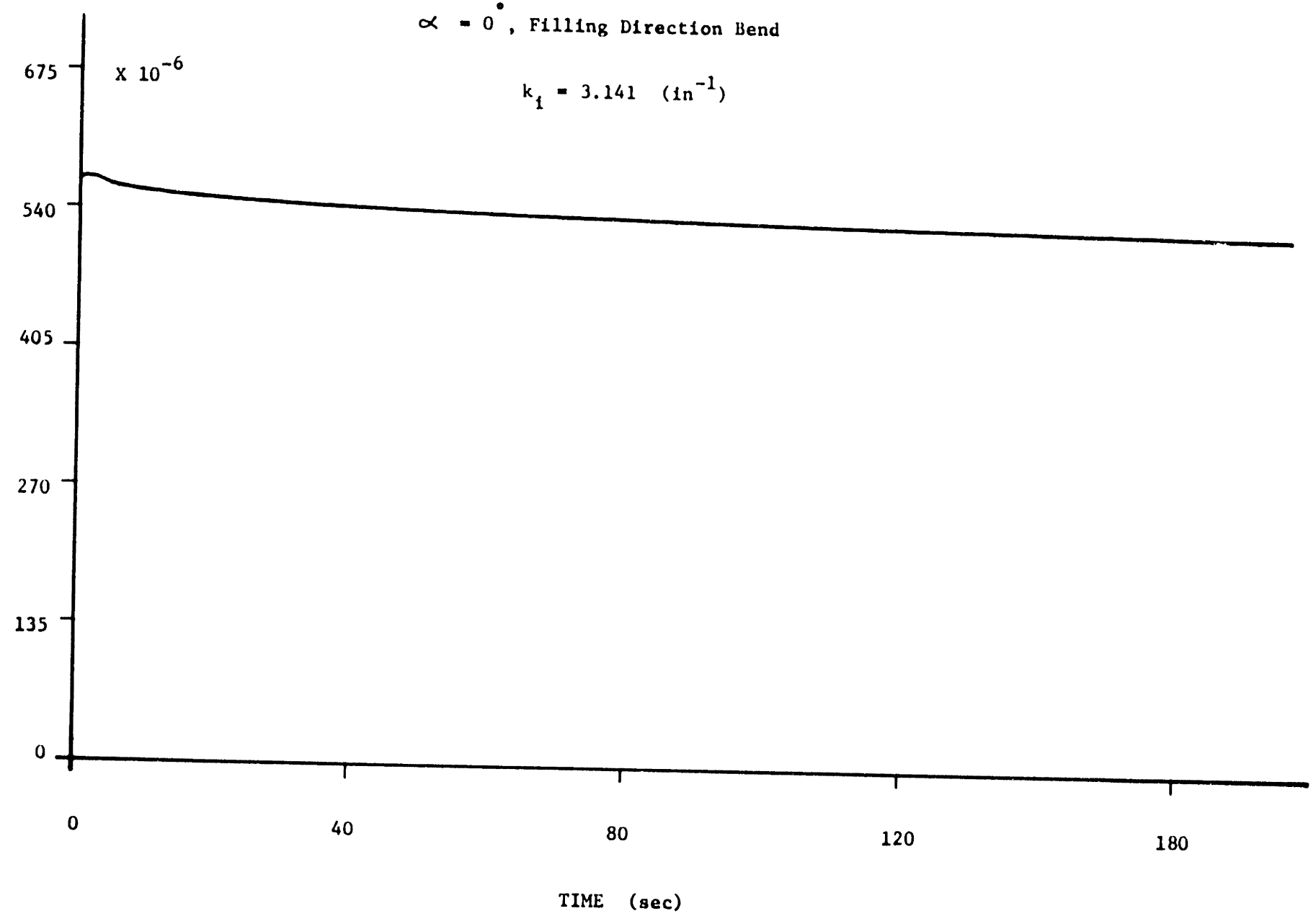

FIGURE D-13

STRESS RELAXATION OF COTTON FABRIC (C-3)

α = 45° Orientation Bias Bend

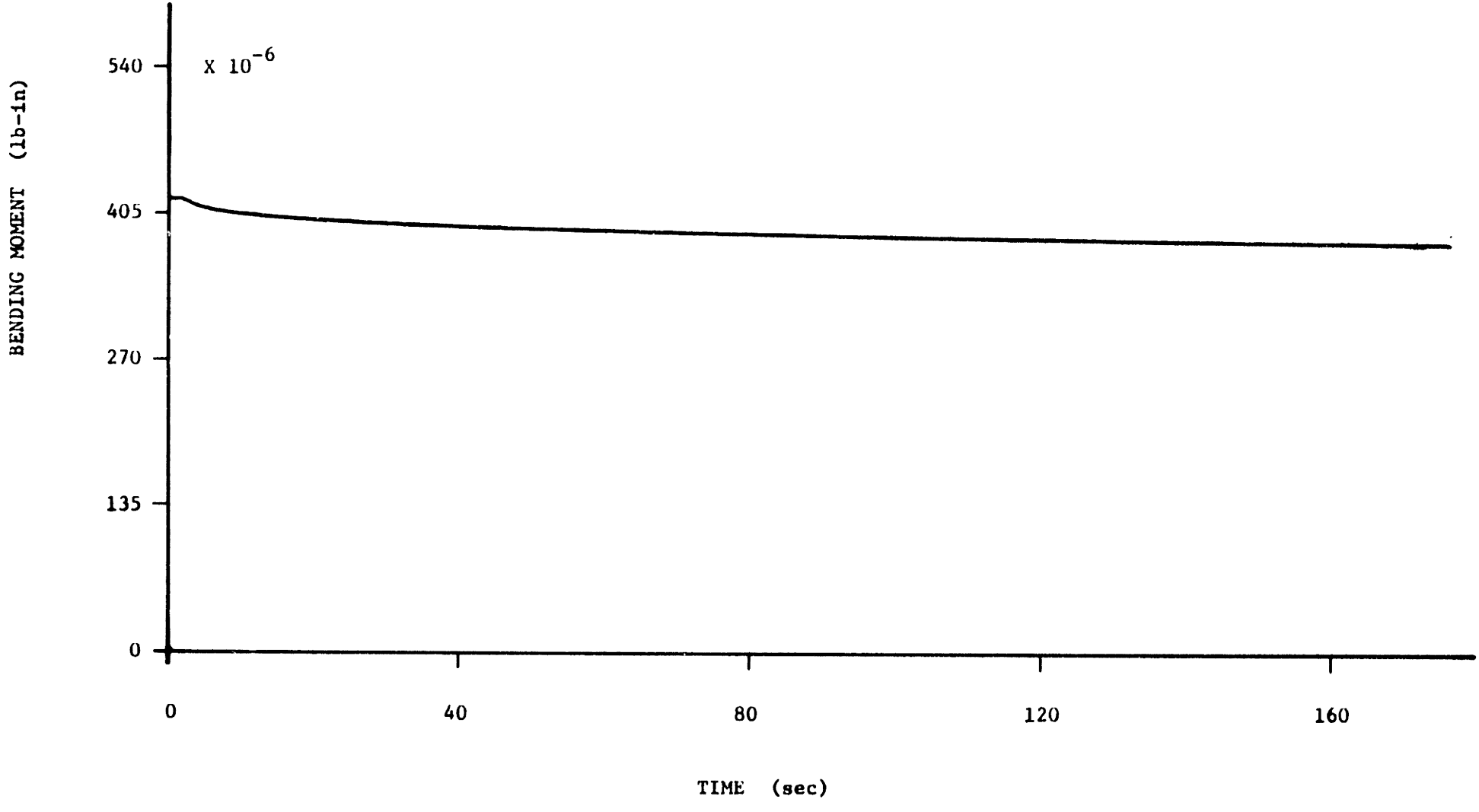

FIGURE D-14

STRESS RELAXATION OF COTTON FABRIC (C-3)

$\alpha = 90^{\circ}$, Orientation Bias Bend

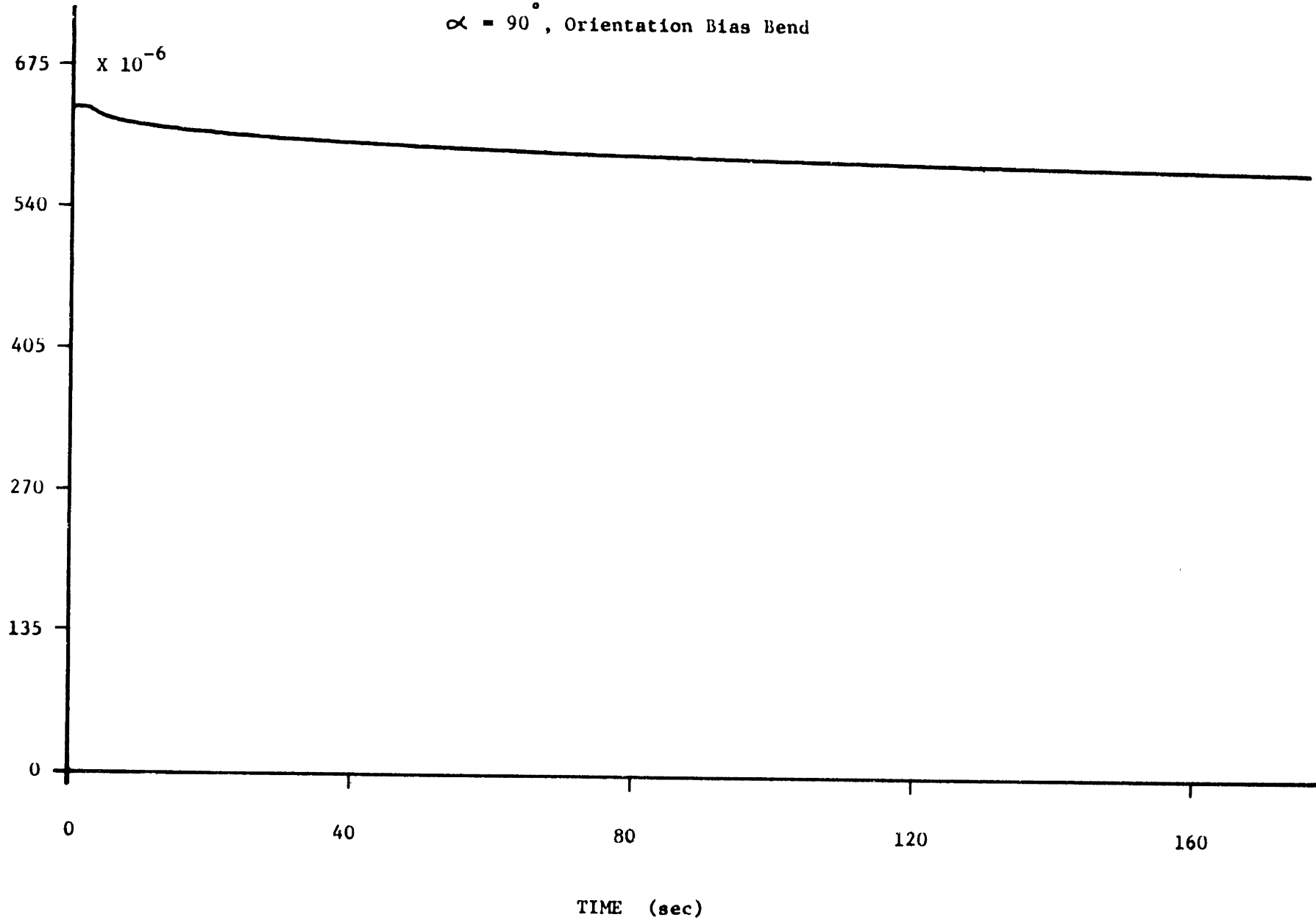

FIGURE D-15

STRESS RELAXATION OF POPLIN(POLYESTER/COTTON), UNFINISHED FABRIC

$\alpha = 0^{\circ}$, Filling Direction Bend

$k_1 = 3.141 \ (in^{-1})$

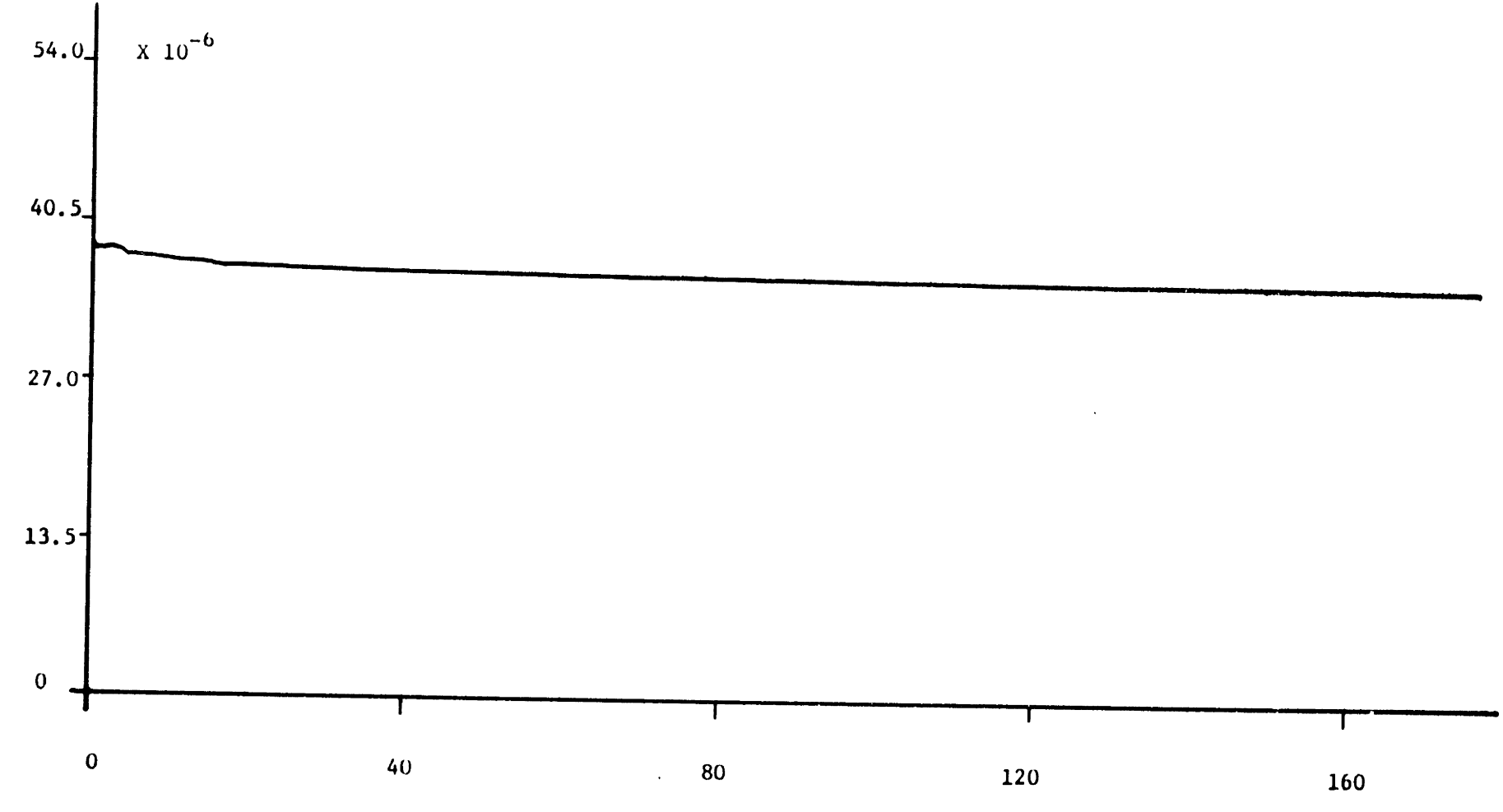

FIGURE D-16

STRESS RELAXATION OF POPLIN(POLYESTER/COTTON), UNFINISHED FABRIC

$\alpha = 45^{\circ}$ Orientation Bias Bend

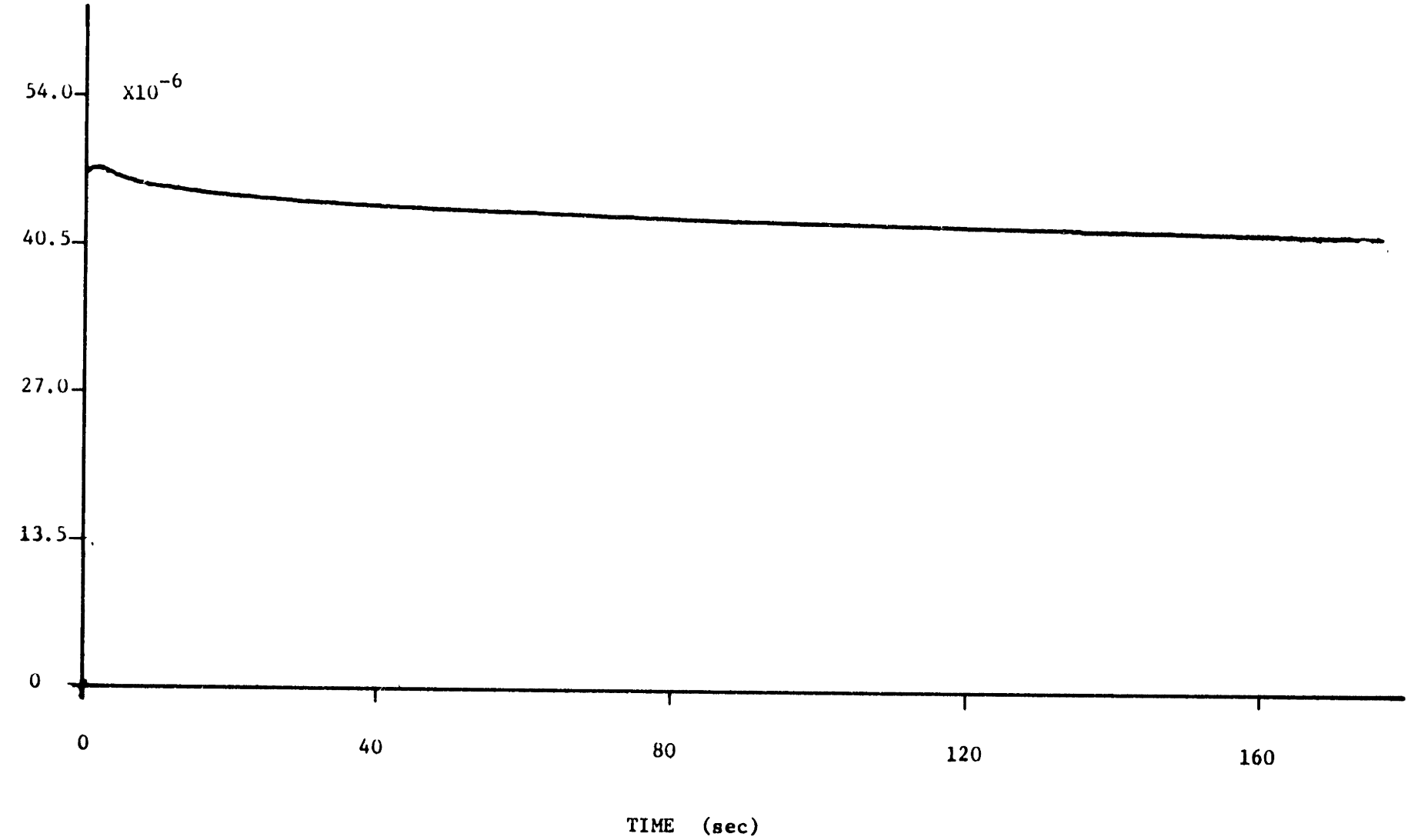

FIGURE D-17

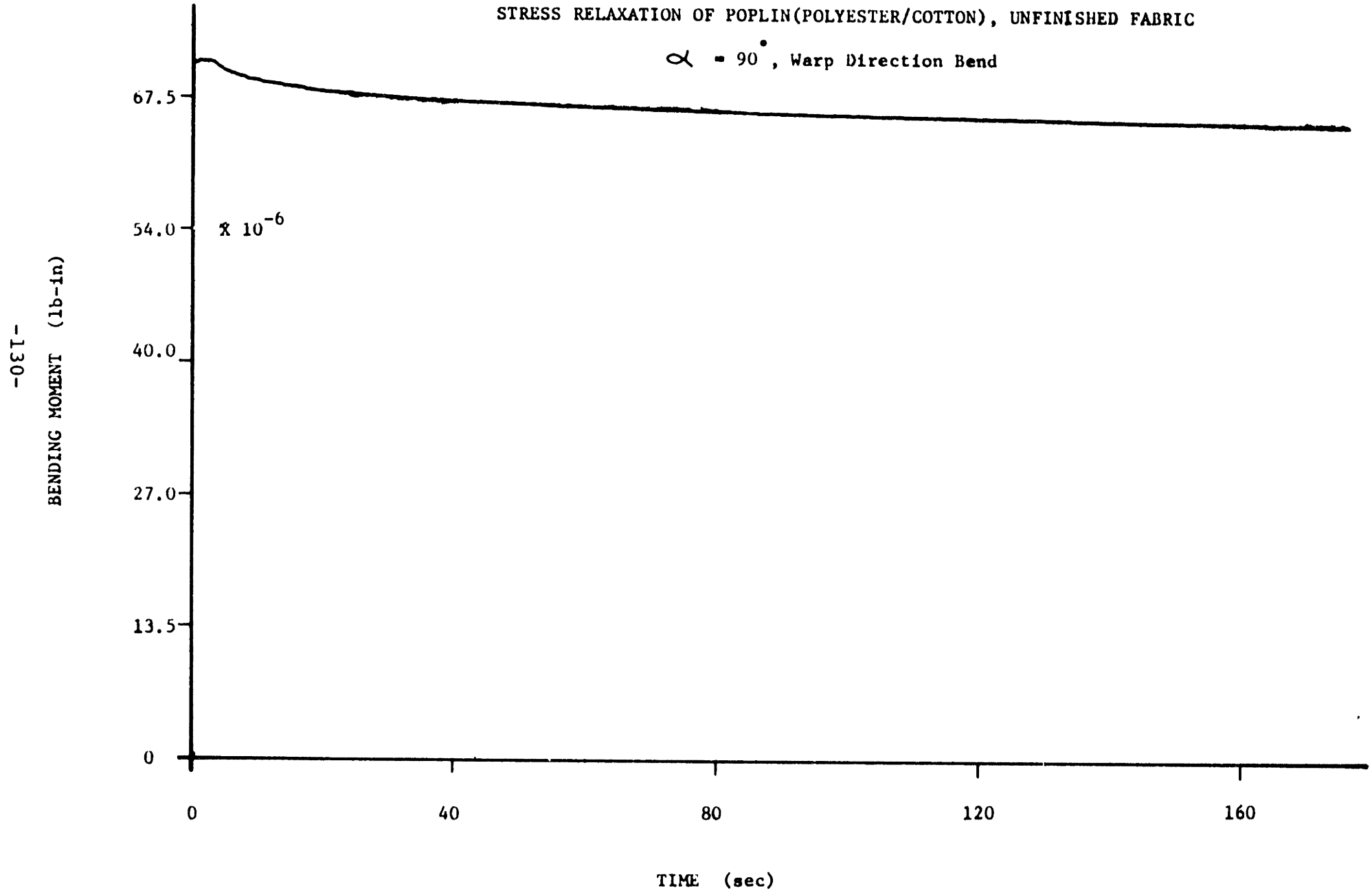
STRESS RELAXATION OF POPLIN(POLYESTER/COTTON), UNFINISHED FABRIC
α = 90°, Warp Direction Bend
67.5
54.0
40.0
27.0
13.5
0
X 10^-6
BENDING MOMENT (lb-in)
0
40
80
120
160
TIME (sec)

FIGURE D-18

STRESS RELAXATION OF POPLIN(POLYESTER/COTTON), PRECURED FINISH FABRIC

$\alpha = 0^{\circ}$, Filling Direction Bend

$k_1 = 3.141 \ (in^{-1})$

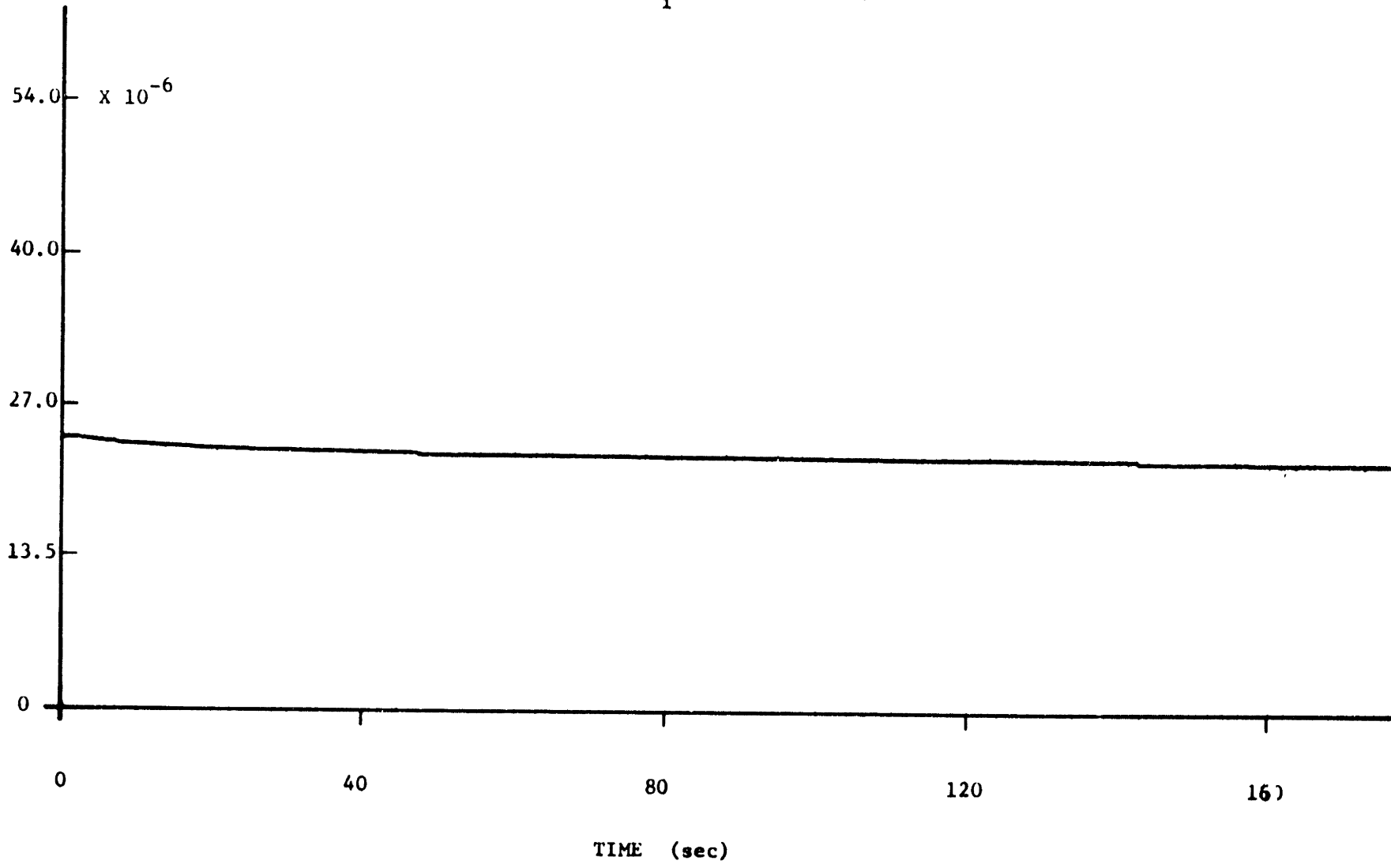

FIGURE D-19

STRESS RELAXATION OF POPLIN(POLYESTER/COTTON), PRECURED FINISH FABRIC

α = 45° Orientation Bias Bend

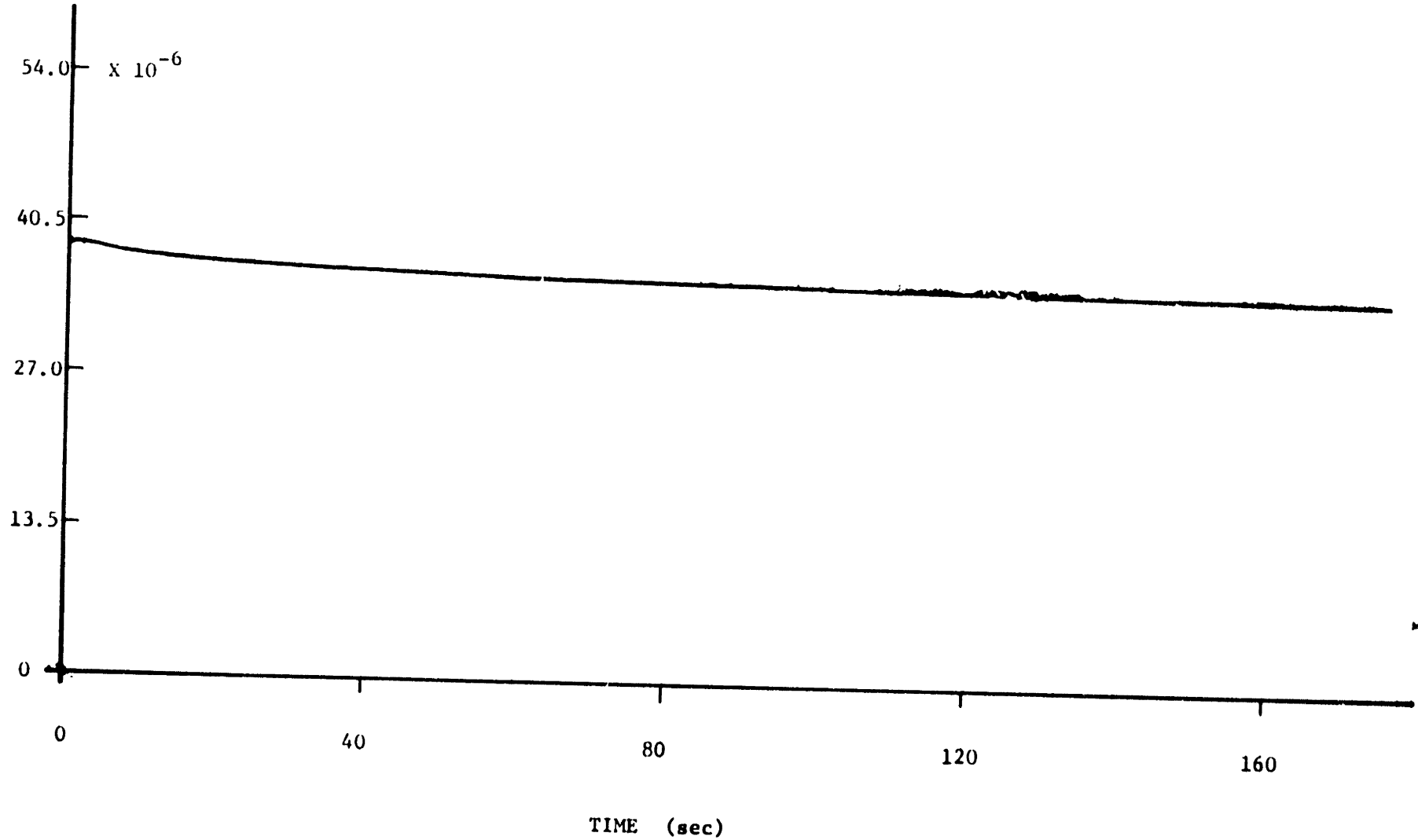

FIGURE D-20

STRESS RELAXATION OF POPLIN(POLYESTER/COTTON), PRECURED FINISH FABRIC

α = 90°, Warp Direction Bend

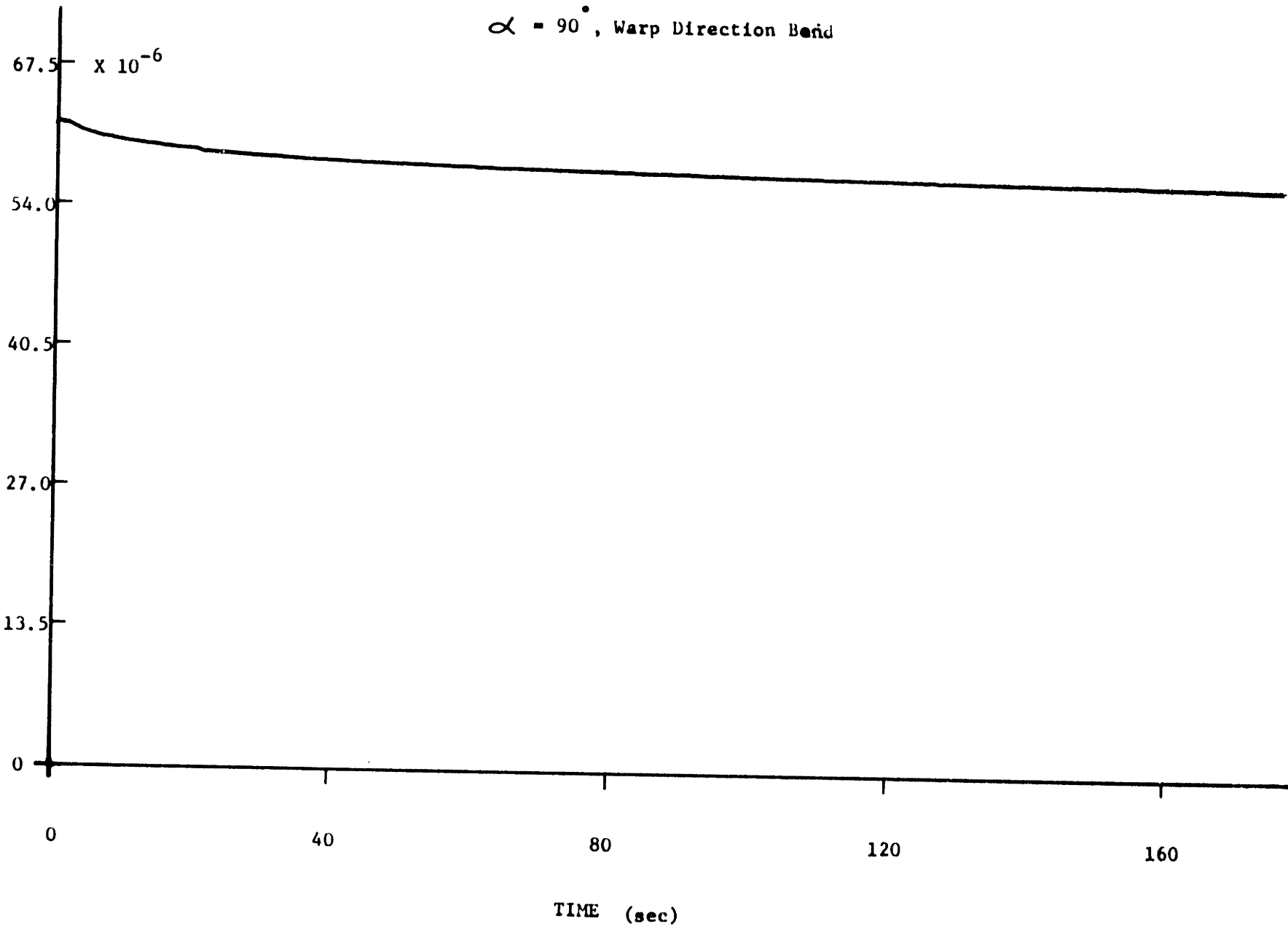

FIGURE D-21

STRESS RELAXATION OF WORSTED(ALL WOOL) FABRIC

$\alpha = 0^{\circ}$, Filling Direction Bend

$k_i = 3.141 \quad (in^{-1})$

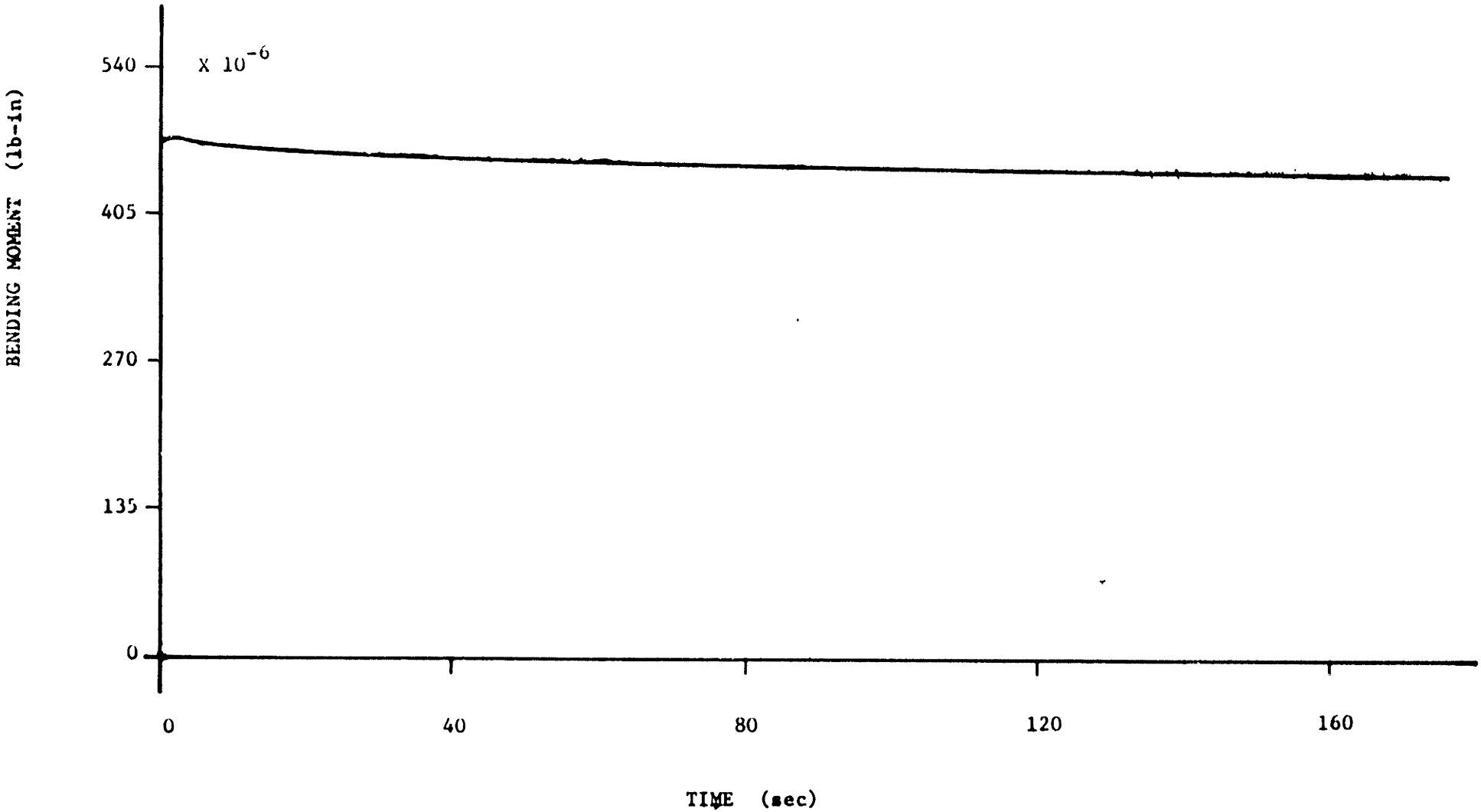

FIGURE D-22

STRESS RELAXATION OF WORSTED(ALL Wool) FABRIC

α = 45° Orientation Bias Bend

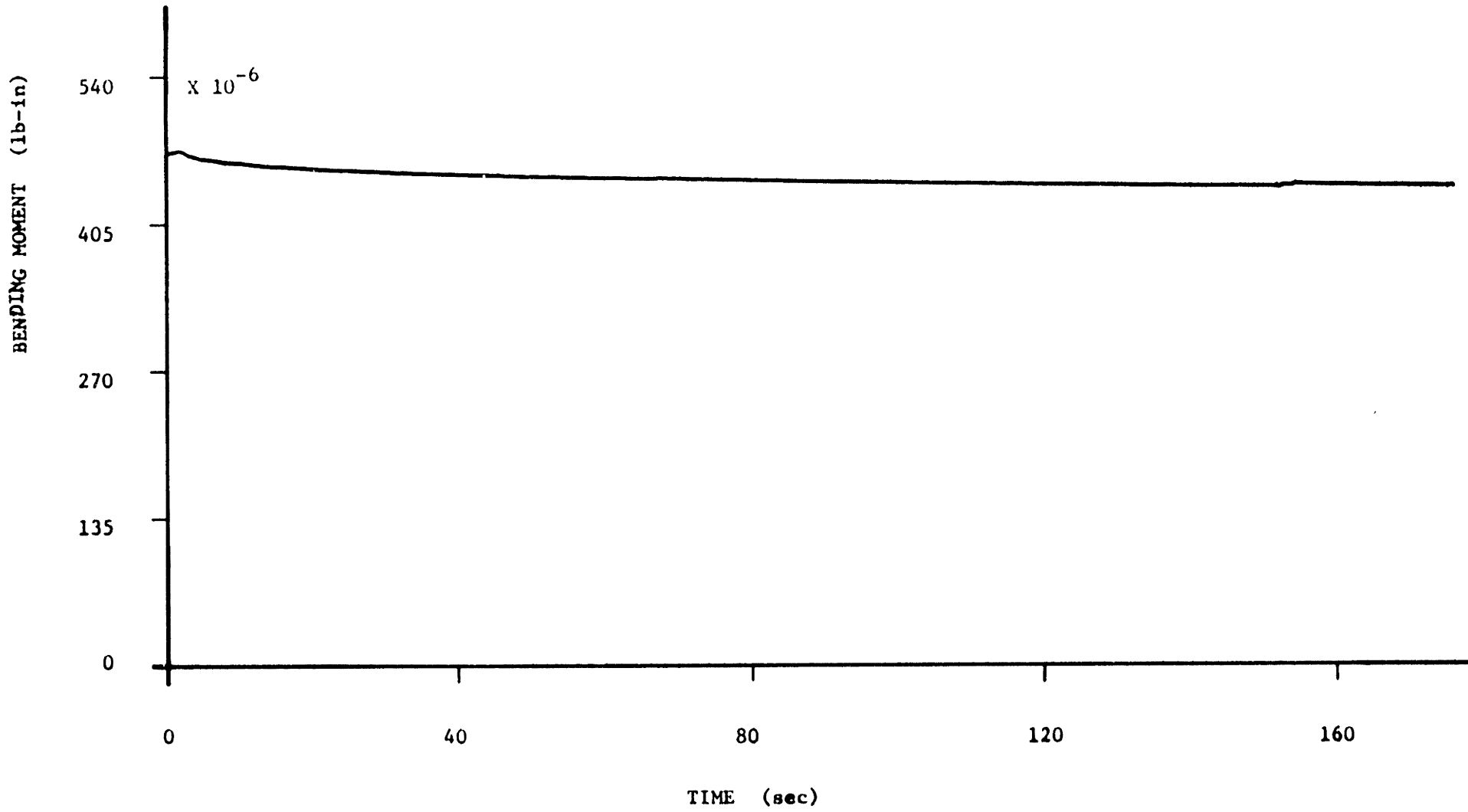

FIGURE D-23

STRESS RELAXATION OF WORSTED(ALL WOOL) FABRIC

$\alpha = 90^{\circ}$, Filling Direction Bend

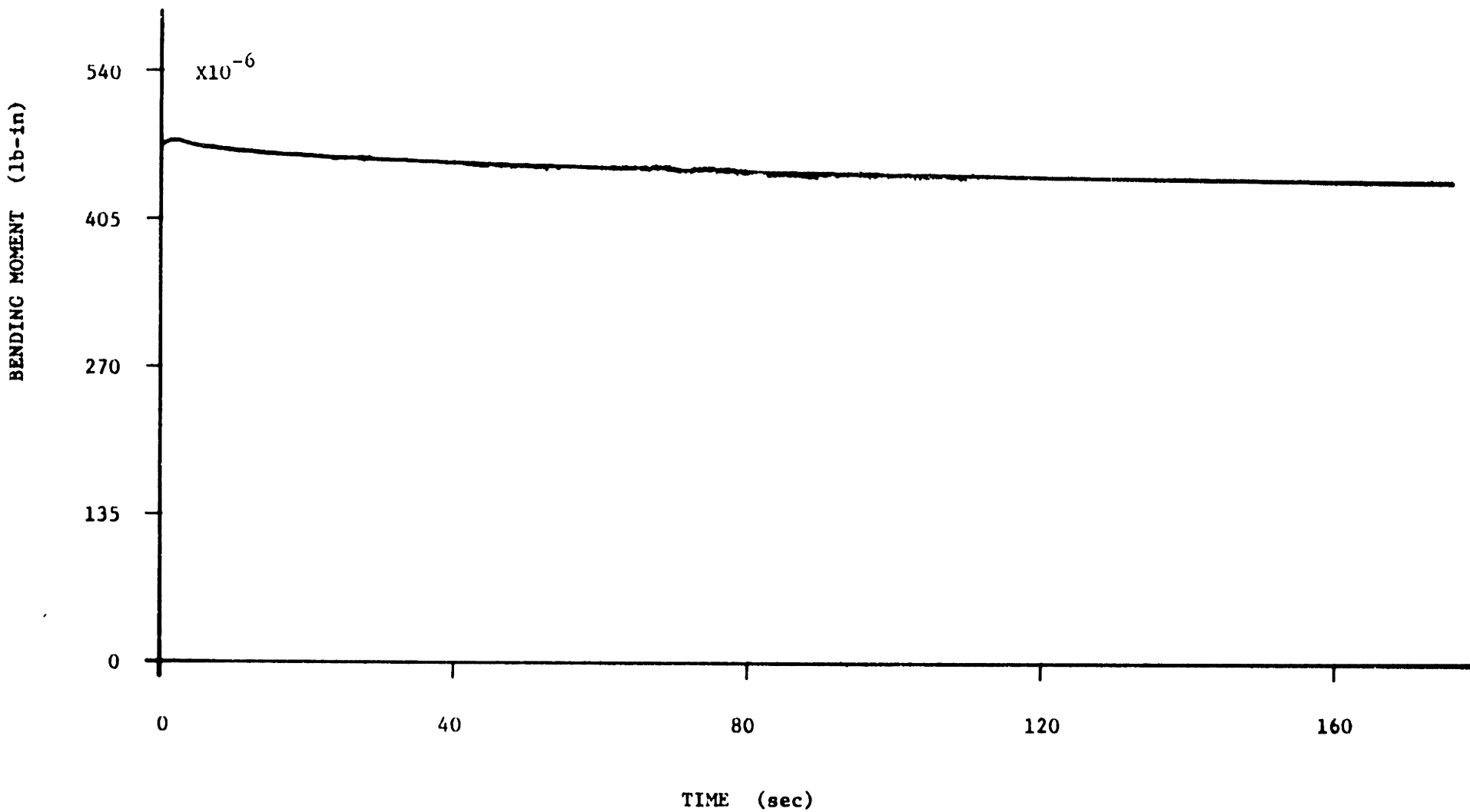

Figure D-24
Typical Cyclic Bending Plot (at Constant Moment Levels)
of Nylon-Fabric (N-3)

$\alpha = 0°$, Filling Direction Bend

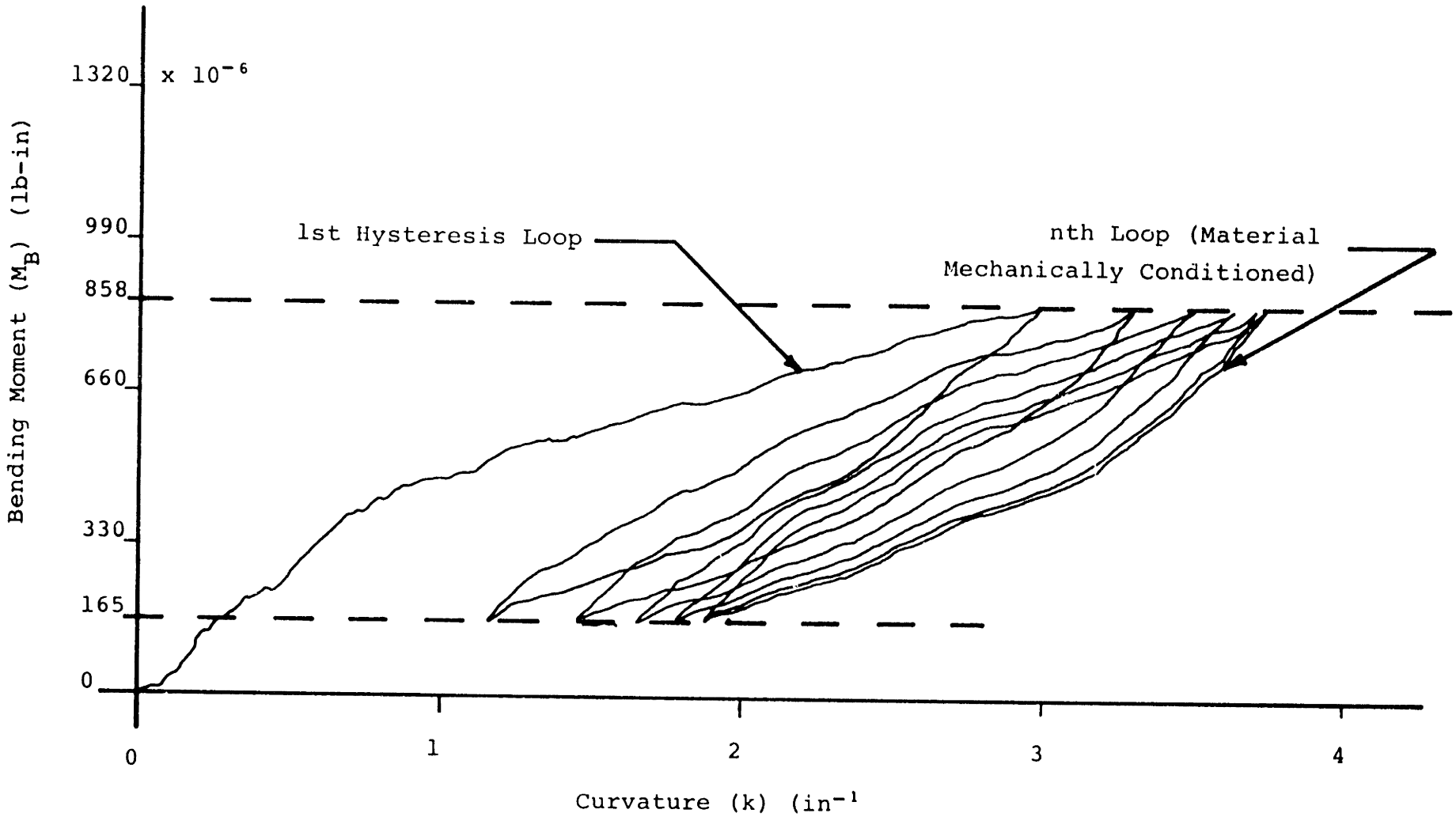

Bibliography

1. Bostwick, C., Behre, B., Karrholm, M., "Some Fundamental, Theoretical, and Experimental Aspects of Fabric Creasing", JTI 53, 1962, p. P116.

2. Cooper, D.N.E., "The Stiffness of Woven Textiles", JTI 51, 1960, p. 317.

3. Grosberg, P., "The Mechanical Properties of Woven Fabrics - Part II. The Bending of Woven Fabrics", TRJ 36, 1966, p. 205.

4. Grosberg, P., Swani, N.M., "The Mechanical Properties of Woven Fabrics - Part IV. The Determination of Bending Rigidity and Frictional Restraint in Woven Fabrics", TRJ 36, 1966, p. 338.

5. Isshi, T., "Bending Tester for Fiber, Yarns, and Fabrics", Textile Machinery Society of Japan Journal 1, 1957.

6. Livesey, R.G., Owen, J.D., "Cloth Stiffness and Hysteresis in Bending", JTI 55, 1964, P. 516.

7. Olofsson, B., "A Study of Inelastic Deformations of Textile Fabrics", JTI 58, 1967, p. 221.

8. Popper, P., "The Effect of Friction and Fiber Mobility on the Bending and Unbending Behavior of Cotton Structures", Doctoral Thesis, M.I.T., 1966.

9. Shinohara, A., Go,Y., "Anisotropy of Crease Recovery of Textile Fabrics", Textile Machinery Society of Japan Journal 1, 196 .

10. Skelton, J., "A Theoretical and Experimental Investigation of the Stiffness and Crease Recovery of Monofilament Fabrics", JTI 57, 1966, p. 505.

11. Steele, R., "The Effect of Yarn Twist on Fabric Crease Recovery", TRJ 26, 1956, p. 739.

12. Stuart, I.M., Hetherington, P., Baird, K., "An Investigation of Cloth Bending - Part I", TRJ 36, 1966, p. 803.

13. Stuart, I.M., Mann, R.K., "An Investigation of Cloth Bending - Part II", TRJ 37, 1967, p. 613.

14. Timoshenko, S., Woinowsky-krieger, S., "Theory of Plates and Shells", McGraw-Hill, New York, 1959.

15. Zorowski, C.F., Chen, C.S., "Cantilever Bending Behavior of Plain Weave Fabrics Constructed of Continuous Filament Cords", TRJ 36, 1966, p. 119.

16. MITEX II - Moment-Curvature Instrument, Instruction Manual, H. M. Morgan Company, Cambridge, Mass.

17. Freeston, W.D., Platt, M.M., "Mechanics of Elastic Performance of Textile Materials", TRJ 34, 1964, p. 308.

18. Daniels, W.W., "Relationship between Fiber Properties and Fabric Wrinkle Recovery", TRJ 30, 1960, p. 656.